AALBORG UNIVERSITY

DENMARK

Fault Diagnosis and Fault Tolerant Control of A Ship-mounted Satellite Tracking Antenna

N. Soltani, Mohsen

Publication date:
2008

Document Version
Publisher's PDF, also known as Version of record

[Link to publication from Aalborg University](#)

Citation for published version (APA):
Soltani, M. (2008). Fault Diagnosis and Fault Tolerant Control of A Ship-mounted Satellite Tracking Antenna. Aalborg: Department of Control Engineering, Aalborg University.

Fault Diagnosis and Fault Tolerant Control of A Ship-mounted Satellite Tracking Antenna

S. Mohsen N. Soltani

Aalborg University
Department of Electronic Systems
Automation and Control Section
Fredrik Bajers Vej 7C . DK 9220 Aalborg Ø . Denmark

Fault Diagnosis and Fault Tolerant Control of A Ship-mounted
Satellite Tracking Antenna

Ph.D. Thesis

This thesis was typeset using LaTeX2e in `iesreport` document class- standard Institute of Electronic Systems `report` class.

Preface

This thesis is submitted in partial fulfillment of the requirements for the Doctor of Philosophy at the Department of Electronic Systems, Aalborg University, Denmark. The work has been carried out in the period February 2005 to June 2008 under the supervision of Professor Rafael Wisniewski and Associate Professor Roozbeh Izadi-Zamanabadi.

The main subject of this thesis is fault diagnosis and fault tolerant control of ship-mounted satellite tracking antenna. Although the main focus is on the application, a number of theoretical contributions are also obtained and presented.

<div style="text-align: right">

June 2008, Aalborg, Denmark
S. Mohsen N. Soltani

</div>

Abstract

The main subject of this thesis is Fault Diagnosis and Fault Tolerant Control (FTC) of A Ship-mounted Satellite Tracking Antenna system. The task of the control system in the satellite telecommunication is to direct the on-board antenna toward a chosen satellite regardless of the actual position on the earth. The challenge arises when the antenna is used for the purpose of marine communication where the wind and the waves disturb the antenna system.

The need for a fault tolerant control system is motivated by demand for marine satellite tracking antenna which is capable of handling the control task during a faulty period. Certain faults (communication system malfunction or signal blocking) cause interruption in the overseas satellite connection resulting in the loss of functionality. The Fault Detection system, which is required to estimate these faults, must be robust to the uncertainties and disturbances on the system. In order to meet these requirements, an optimization-based FDI for a class of nonlinear systems is developed. Robust Fault Detection and Identification (FDI) method is combined with a reconfiguration control strategy to accommodate the fault. Both FDI technique and control method are based on the nonlinear approaches as the analysis of the model has shown that the nonlinear model of the satellite tracking antenna is fitting well to the real system.

This thesis makes four major contributions. The first one is to model the antenna system. Having a complete model which includes all the elements of the satellite tracking antenna is a prerequisite to design control and FDI systems. This model includes dynamics and kinematics of the antenna and tracking system as well as the model of the disturbances and ship motions.

The second contribution is to propose a Nonlinear Internal Model Controller (NIMC) in addition to the conventional robust controller which is designed for linearized version of the antenna model. The problem of controlling the output of the system so as to achieve asymptotic tracking of prescribed trajectories and asymptotic rejection of disturbances is solved by internal model control. There is, in fact, a big benefit to switch to the internal model control when the FDI system has estimated a fault in the antenna system.

The third contribution is to improve an optimization based fault detection system which

focuses on fault estimation for systems with parametric faults on the nonlinear model of the satellite tracking antenna. The employed method is inspired by or derived from the area of robust control theory. The system is reformulated in a so-called robust standard problem set-up. The standard set-up formulates an abstract optimization problem, that is general enough to comprise many significant control problems, and pursues a general solution to this optimization problem, independent of specific control problems. Eventually, the fault tolerant control scheme is tested on an industrial test facility showing the capabilities of the FTC scheme on a real application.

Finally, further study on the fault estimation has been conducted by the comparison of the employed method with two other optimization based fault estimation methods.

Sammenfatning

Det væsentligste emne i denne Ph.D.- afhandling omhandler metodeudvikling til fejldiagnose og fejltolerantregulering af et satellitsporingssystem for en kommunikationsantenneplatform til søfarttøjer. Regulatorens opgave i et satellit- kommunikationssystem er, at dirigere antennen hen imod en udvalgt satellit uden at tage hensyn til den aktuelle position på jorden. Men da antennen anvendes til søfarts-kommunikation, bliver udfordringen her at designe algoritmer, som kan undertrykke udefra kommende forstyrrelser. Disse forstyrrelser stammer typisk fra vind og bølgers virkning på skibet og dermed også selve antennesystemet.

Kravet for udvikling af et fejltolerant sporingssystem er motiveret af efterspørgslen efter et antennesystem, som er i stand til at opretholde kommunikationen selv i perioder, hvor der opstår bestemte fejl som for eksempel en målefejl eller en signalblokering. Forekomsten af disse fejl kan, i værste fald, resultere i kommunikationsafbrydelse med satellitten og dermed også omverden. Et krav for fejldiagnosesystemet er at være robust over for ukendte forstyrrelser og systemets ulineær dynamik. Disse krav er forsøgt imødekommet ved at udvikle en fejldiagnosealgoritme til en klasse af ulineare systemer, som er baseret på frekvensbaserede optimeringsmetoder. Robustfejldiagnose- metoder er kombineret med mulige omkonfigurerings kontrol algoritmer for at tilpasse fejlsituationen.

Denne afhandling fremsætter fire vigtige bidrag til emnet. For det første at udvikle en komplet dynamisk model til antennesystemet. Det er en forudsætning, når man designer kontrol og FDI-algoritmer, at have en fuldendt model som omfatter alle relevante elementer i antennen. Denne model inkluderer dynamisk og kinematisk beskrivelse af antennen samt sporingssystemet og forstyrrelses- og skibsbevægelsesmodellen.

Ud over en robust reguleringsalgoritme, hvis design er baseret på en linear model af antennesystemet, er der foreslået en kontrolstrategi baseret på "nonlinear internal model control (NIMC)" metode. Brug af den NIMC-baserede algoritme, bevirker at forskellen mellem retningen mod den udvalgte satellit og den faktiske retning, går asymptotisk mod nul selv under påvirkning af eksterne forstyrrelser. Når FDI-systemet har fundet en fejl i antennesystemet, er der faktisk store fordele ved at anvende NIMC-baseret kontrolalgoritme.

Det tredje bidrag er at forbedre en optimal fejldiagnosemetode i antennesystemets ulinear model. Denne metode fokuserer på fejlvurderinger i systemer, hvor fejlen er beskrevet som værende en fejl i systemparameteret. Den anvendte metode er inspireret af og udledt af ideer som er tilgængelige inden for forskningsområdet: robustregulering. Systemet er omformuleret i en såkaldt robust-standardproblemopstilling. Denne opstilling formulerer et abstrakt optimeret problem, som omfatter mange betydelige kontrolproblemer, og viderefører en generel løsning til denne optimerede problemstilling - som er uafhængig af specifikke kontrolproblemer. Yderligere kan det nævnes, at alle de udviklede algoritmer og modeller er testet og verificeret på et industrielt testsystem, hvilket bekræfter det udviklede fejltolerantsystems evne til at detektere og håndtere udvalgte fejl i virkelige situationer.

Endeligt er der foretaget yderligere komparative studier hvor den præsenterede fejldiagnosemetode er sammenlignet med to optimerings baserede alternativer.

Contents

List of Figures

Chapter 1

Introduction

This thesis considers the design and analysis of the fault diagnosis and fault tolerant control system for a ship-mounted satellite tracking antenna. The goal is to study fault diagnosis methods as well as different control techniques for the antenna system. The fault detection and control methods have special highlights on the robustness, disturbance rejection, and nonlinearity in this system. When the control system encounters some faults, those three elements create difficulties to distinguish the faults from the effects of those elements.

1.1 Background and Motivation

Communication over large distances is preserved by means of satellite communication. This can be maintained if the constellation of the communication satellite ensures that it is always possible to make contact with a satellite, regardless of the actual position on Earth. The important factor in this case is to track the satellite by directing the on-board antenna toward the satellite and sustain contact with it. For stationary antennas this is simple: once the satellite has been tracked, the communication antenna on the ground will remain fixed on it. The challenge arises when the antenna is used in a non-stationary case, e.g. marine communication. Once the ship-mounted antenna has tracked a communication satellite, movements of the ship, partly due to waves, will force the antenna to point away from the satellite and thereby break the communication. If the antenna system is not capable of compensating for the disturbances in an appropriate way, the antenna system will not be able to maintain contact with the satellite. In this case, it is of great importance that the antenna has a control system, which ensures the antenna to compensate for these disturbances and to remain locked on the satellite.

Besides, some number of faults result in incorrect data to the control system and consequently the interruption of the communication via wrong control actuation provided by the control system. The need for a fault tolerant control system is according to the demand for more reliable satellite tracking antenna system with improved overall performance. Control reconfiguration is an active approach to achieve fault-tolerant control for dynamic systems (Blanke, Staroswiecki, and Wu, 2001). It is used when severe faults, such as actuator or sensor outages, cause a break-up of the control loop, which must be restructured to prevent failure at the system level. Control reconfiguration is a building block toward increasing the dependability of systems under feedback control. Prior to control reconfiguration, it must be at least determined whether a fault has occurred (fault detection) and if so, which components are affected (fault isolation). Preferably, a model of the faulty plant should be provided (fault identification). These questions are addressed by fault diagnosis methods. In this thesis, the proposed method is implemented and verified on the antenna application. Background of this case study is explained in the following section.

Figure 1.1: F77, SpaceCom's satellite tracking antenna.

1.1.1   Ship-mounted Satellite Tracking Antenna

SpaceCom A/S is a Danish company that, as a sub-supplier, specializes in the development and production of satellite tracking antenna for mobile system applications, mainly

marine vehicles. The production assortment spans from small size two axes land-based mobile antennas to large three axes antennas used for overseas applications. Fleet 77 (F77) antenna is developed at SpaceCom A/S for use on ships. Its task is to maintain communication with satellite at all times, regardless of sea and bad weather conditions where it is also considered as *Emergency Call System* on the ship.

The manufactured products by SpaceCom A/S are mainly intended for use with the satellite communication provider- Inmarsat. This company have multiple GEO-stationary satellites and can provide satellite communication to nearly all parts of the earth surface except close to the poles. Inmarsat, as the owner and operator of these communication satellites, provides a list of standards including the precision of the tracking regarding the specified assessment of ship movements. This requires a dedicated control system which is not only tries to regulate the tracking error, but also rejects the disturbances. In addition, the reliability of the products is highly important since, as mentioned above, they are used in harsh and severe environmental situations.

The F77 is a motor-controlled antenna system with features for tracking and communicating with a satellite. The F77 antenna prototype is illustrated in figure 1.1. The physical antenna system is composed by a number of actuators/sensors including motors, beam sensor, and gyros which are explained in the following.

Actuators

The system contains a mechanical three axes antenna (3-DOF), with a stepper motor attached to each axes of rotation. These axes have to make a final rotation to the plate of the antenna so that the plate can cover every position of the satellite on the entire of the hemisphere.

- The *Azimuth* axis allows the antenna to operate in the horizontal plane. The physical construction of the antenna pedestal allows the antenna to move freely around the azimuth axis.

- The *Elevation* axis allows the antenna to operate in the vertical plane. The motor is mounted behind the plate of the antenna. The physical construction of the antenna restricts the full rotation of the plate around this axis.

- The *Cross-elevation* axis grants the capability to the antenna to operate in a plane perpendicular to the elevation axis. In this thesis, the main focus is on under-actuated antenna system. Consequently, this is done by keeping the cross-elevation motor locked[1].

---

[1]Locking the cross-elevation motor results in some constraints when the satellite is just above the antenna. These constraints are shortly explained in Appendix B. This topic is also proposed for future work since it is out of the scope of this thesis

Sensors

There are two types of sensors that are used for both control schemes and FDI system: beam sensor and gyros. Besides, the angels of the joints are calculated in the motor driver.

- *Beam sensor* is developed by SpaceCom A/S and is used to measure the angle between the antenna Line Of Sight (LOS) and Satellite directional vector (SAT) by two angular values (in the same way as two angles of the polar coordinates in 3-D space). In fact, they can be interpreted as Elevation and Cross-elevation error measurements.

- *Rate gyros* are used to measure the angular velocity by positioning them on a cube which is attached to the base of the antenna. Three rate gyros are fixed to the cube aligned with three rotational axes, roll, pitch, and yaw.

The external effects on the tracking system are primarily the disturbances and faults. Disturbances are due to the waves and wind and affect the antenna trough ship motions and the faults are mostly blocking of the signal and temporal satellite shutdown. In the following these two external effects are introduced in more details.

Motions at Sea

The ship motion, in general, is a specific field of science. A conclusion that has been attained here is an abstract version of (Fossen, 2002; Perez and Blanke, 2002) where from the wave spectrum it has been concluded that a significant harmonic exists along with other frequencies within a small band of frequencies. In other words, the common way to describe the ship motions at sea, which caused by waves, wind, etc, is with multiple sinusoids that have random initial phases (Perez and Blanke, 2002). Furthermore, vessel motions can be seen as a low-pass filter of the wave disturbance e.g., with an approximated second order filter with a resonance frequency. In this thesis, it has been considered to apply the maximum frequency and amplitude of the sinusoidal wave to each DOF of the ship as it has been extracted from Inmarsat standards (Inmarsat, 2003).

Faults

A Failure Mode, Effect, and, Analysis (FMEA) (Izadi-Zamanabadi, 1999) is used to identify the severity and occurrence of each fault considered in the state of the art analysis of F77 antenna. FMEA is normally used to find the weak spots of the design in early

and later stages of the development. However, it can also be used to analyze a running system for possible faults, which is the case for F77 antenna. FMEA provides a classification of all possible faults based on the severity-occurrence index. It also provides the priority of the faults to be detected.

Making such analysis on sensors and actuators, the major faults, which have the higher severity-occurrence index compared to the others, are to be detected in the beam sensor. These faults occur due to appearance of a hurdle between the antenna and satellite (Animals, airplanes, bridges, etc), temporary satellite shutdown, and sudden changes of temperature and pressure in the higher levels of atmosphere.

The other possible scenarios such as wire breakage of beam sensor, motors windup, and loss of physical mounting comparatively have much lower severity-occurrence index and thus do not attract our attention here.

1.2 Overview of The Techniques

A typical FTC system includes a FDI system and an on-line control reconfiguration system. This section briefly reviews literature on FDI and control reconfiguration.

1.2.1 Fault Detection and Identification

Historically, the FDI problem has attracted the attention of the researchers in early 70's. In 1971 the problem of residual generation has been studied by both stochastic and deterministic schemes, almost, at the same time. Those two schemes lead to two essential approaches in model-based fault diagnosis.

The stochastic approach has been studied by Merha and Peschon in (Mehra and Peschon, 1971). In those works, residual generation design was done in the basis of some well-known filters like Kalman filter and with statistical analysis of the residuals which were, in fact, the Innovations of Kalman filter the faults have been detected. Those works generally were based on the fact that the Innovations of the Kalman filter, in absence of fault, are white Gaussian process with zero mean and known variance. The problem that they were encountered was the lack of robustness to the unknown inputs. This problem was due to the fact that if they could not define the unknow inputs as a stochastic process then it was not possible to consider them in Kalman filter design. On the other hand, if the disturbances affect the residual, they can destroy the residual information and cause false fault detection in the decision part. This problem initiated several researches where their goal was to disconnect the relation of unknown inputs

from residuals. Recent works such as (Nikoukhah, 1994) has suggested the idea of Innovation Generation which solves the problem entirely in the state space. The efforts by (Willsky and Jones, 1976) are noticeable in this track.

In the second approach, Beard in (Beard, 1971), with a deterministic consideration and based on the geometric perception, proposed a special full order observer called Fault Detection Filter. The gains of the observer was adjusted such that each fault could generate a residual in a unique vector. This approach, which was more flourished in 70's than the Kalman Filters, has been used extensively in many fault diagnosis problems. The problem that researchers were met in this approach was that, in general, the choice of the gain for design of fault detection filters, particularly in presence of noise, needs special concerns. Subsequently, in 1973, Jones proposed a method, which in the first step, the observer gain was chosen such that different faults were generating linear independent vectors and in the next step the remaining degrees of freedom in gain design was determined according to $\mathcal{H}_2$-norm minimization of the estimation error covariance matrix (Jones, 1973). Indeed, with the efforts by Beard and Jones the model-based fault diagnosis has been founded. However, there were still lack of more research on the fault detection filters which were also known as Beard-Jones filters. These filters were structured as full order observers, but the post researches showed that forcing such a structure to the residual not only will force the set of the faults to be diagnosed in a relatively specific situation and restricts the class of the problems, but also force the user to use a very complicated method to design the filter gain.

The attempts to come over the above limitations lead to the number of outstanding results in 80's (Massoumnia, 1986; Massoumnia, Verghese, and Willsky, 1989; Frank and Keller, 1981; Frank and Wunnenberg, 1989; Viswanadham and Srichander, 1987; Patton and Kangethe, 1989; White and Speyer, 1987). (Massoumnia, 1986) analyzed the fault detection filters in an absolutely geometric manner and its relation to the Completely Decoupling Problem has been studied in (Wonham, 1985). This work considered other filter gain design methods under simpler conditions for applications. Furthermore, in (White and Speyer, 1987), the gain filter computation has been done by the assignment of the Eigenvectors. The structural restrictions of the fault detection filters was eliminated in (Massoumnia et al., 1989) and the necessary and sufficient conditions for designing the reduced order filters have been provided. In the same track, the efforts by (Chung and Speyer, 1998; Douglas and Speyer, 1995; Park and Rizzoni, 1994) are noticeable in the area of fault detection filter design. In fact, they tried to solve a so-called Fundamental Problem in Residual Generation in absence of noise but in presence of unknown inputs. Moreover, in (Patton and Chen, 1992) a method based on the Eigenstructure Assignment and in (Wunnenberg, 1990) another method based on computing the Kronecker Forms are proposed. In general, the above works tried to annihilate the transfer matrices from the unknown inputs.

In the above problems, there is no information about the nature of the unknown inputs,

which affect the residuals, and unsurprisingly they should be decoupled from the residuals completely. Consequently, the conditions under which those problems are solvable are not completely satisfied. In contrast, it is usually possible to assume that the unknown inputs have limited energy. These considerations caused substituting the logic of annihilating the transfer matrices by minimizing a proper norm of those matrices in early 90's. This new phenomenon opened the doors of the $\mathcal{H}_2$ or $\mathcal{H}_\infty$ optimization approaches to the field of fault diagnosis.

In fact, the efforts in (Edelmayer, Bokor, and Keviczky, 1996; Edelmayer and Bokor, 2000; Frank and Ding, 1994; Mangoubi, Appleby, Verghese, and Vander Velde, 1995; Mangoubi and Edelmayer, 2000; Mangoubi, 1998; Sauter and Hamelin, 1999) tried to define the fault diagnosis problem on an optimization problem basis, mainly $\mathcal{H}_2$ and $\mathcal{H}_\infty$ optimization. However, those works cannot be defined in a so-called standard set-up for robust control based on LFT (Zhou, Glover, Bodenheimer, and Doyle, 1994; Zhou, Doyle, and Glover, 1996). The attempts to conquer this problem resulted in another field of fault diagnosis which the residual was indeed an estimation of the fault. The methods in (Frisk and Nielsen, 1999; Niemann and Stoustrup, 1997; Tyler and Morari, 1994; Stoustrup, Grimble, and Niemann, 1997) have tried to define the fault diagnosis (and sometimes control compensation) problem in a standard set-up for robust control.

Many of the above methods are based on the linear system dynamics. Obviously, a linearized model is an approximation of the nonlinear system dynamics around an operating point. For a system which is highly nonlinear it would involve a large number of fault diagnosis systems if one consider a FDI system for each operating point and therefore would not be practical. Many researchers tried to extend the fault diagnosis problem directly into the nonlinear models in 90's. (Hengy and Frank, 1986) used a nonlinear identity observer, (Frank, 1987; Adjallah, Maquin, and Ragot, 1994) continued this work; however, it did not result in development of gain matrix ensuring the stability. (Frank and Ding, 1994) proposed an adaptive observer based fault diagnosis for time-varying class of nonlinear systems which were highly difficult as it was purely mathematical approach. Several studies has been done on bilinear systems fault diagnosis as a specific class of nonlinear systems by (Yu, Shields, and Mahtani, 1994a,b; Yu and Shields, 1997; Yang and Saif, 1995). (Edwards, Spurgeon, and Patton, 2000) applied a sliding mode observer and (Krishnaswami and Rozzoni, 1994; Krishnaswami, Luh, and Rizzoni, 1995) extended the parity relation to the nonlinear FDI problem. (De Persis and Isidori, 2001) extended the geometric residual generation in (Massoumnia, 1986) to the nonlinear systems class. Neural Networks have been extensively used for nonlinear fault diagnosis (Watanabe, Matsuura, Abe, Kubota, and Himmelblau, 1989; Willis, Di Massimo, Montague, Tham, and Morris, 1991; Napolitano, Neppach, Casdorf, Naylor, Innocenti, and Silvestri, 1995; Patton, Chen, and Siew, 1994; Patton and Chen, 1996). Beside the linear optimization based FDI methods(Stoustrup and Niemann, 1999) has proposed an optimization based fault estimation for a class of nonlinear systems which

has sector bounded nonlinearity.

1.2.2   Fault Tolerant Control

During the last two decades, extensive research activities have focused on developing fault-tolerant control (FTC) to maintain the system stability and to avoid losses under various failure scenarios. Fault Tolerant Control is basically developed in three approaches in 90's (Blanke, Kinnaert, Lunze, and Staroswieski, 2006). These approaches are in the framework of adaptive, robust control, or switching of the on/off-line designed controllers. (Patton, 1997; Rauch, 1995) survey these approaches. Most of the existing fault accommodation schemes are mainly designed either based on the powerful and well-developed linear design methodology or based on the assumption of a certain type of nonlinear systems under simple failure conditions to obtain the desired objectives. The representative approaches are shortly described here. Model-matching is proposed in (Huang and Stangel, 1990) for controller reconfiguration and (Gao and Antsaklis, 1989) ensures the stability by some improvements. (Maciejowski, 2002) used a model predictive control and (Yang and Blanke, 2000) proposed a control mixer approach for fault accommodation. (Blanke, 1996) suggested a systematic fault analysis and (Bøgh, 1997; Bøgh, Izadi-Zamanabadi, and Blanke, 1995) used a predetermined design of accommodation on a satellite application. (Lunze, 1994; Lunze and Schiller, 1992) employed logic inference on qualitative models.

1.2.3   Internal Model Control

Obtaining asymptotic tracking of demanded trajectories while asymptotic attenuating of disturbances is one of the most essential problems in control theory. There are generally three possibilities. Tracking by dynamic inversion is used in (Hunt, Meyer, and Su, 1994; Devasia, Chen, and Paden, 1996; De Cuyper and Verhaegen, 2002) requires the complete knowledge of the trajectory and the model of the system. The problem in using this method was that in the non-minimum-phase system case the resulting inverse trajectory will not, in general, have an initial condition that corresponds to the initial condition of the control system. Adaptive tracking used in (Cheah, Liu, and Slotine, 2006a,b) tries to adjust the control input parameters so that the tracking error converges to zero. Internal Model Based tracking is able to handle simultaneously uncertainties in plant parameters. It has been proved that, if the trajectory belongs to the set of all trajectories generated by some fixed dynamical systems, a controller which incorporates an internal model of such a system is able to secure asymptotic decay to zero of the tracking error for every possible trajectory in this set and does it robustly with respect to parameter uncertainties (Isidori, Marconi, and Serrani, 2003b).

1.3 Objectives and Contributions

The aim of this thesis is to analysis and design of a *fault diagnosis and fault tolerant control system for ship-mounted satellite tracking antenna*. There are several important factors to be considered when looking at the subject.

- A fault tolerant control system needs an FDI system to detect if a fault has occurred.

- A fault tolerant control system as a multi-model switching needs more control scenario possibilities.

- The control system should be able to reject disturbances as the antenna system is disturbed by the ship motions.

- The control system should be able to perform the asymptotic convergence of the tracking error to zero.

- The FDI system should not be sensitive to the disturbances.

- Both controller and FDI system should be designed for the nonlinear model of the satellite tracking antenna, since the nature of this system is highly nonlinear.

The set of the above objectives gave us a contribution framework as follows.

- The satellite tracking antenna F77 has been analyzed regarding the sensors, actuators, and mechanical model. The combination of all dynamics and kinematics of the system together with sensors and actuators resulted in a mathematical model of the system, which can be used for the design of the fault tolerant control system. The obtained model has been verified in (Soltani, 2006) trough real-time tests and the results of the measurements have confirmed the model.

- The design of an internal-model-based controller for the satellite tracking antenna, capable of rejecting the most effective disturbances, is addressed in this thesis. A new type of antenna that utilizes only two actuators to deliver the same functionalities as the existing three-axis actuated antenna is considered.

- A particular focus is on designing a FDI system for the satellite tracking antenna which is robust to the uncertainties and disturbances in the system. Employing methods for fault diagnosis, which have been inspired by and derived from the area of robust control theory or in wider generality of optimization based control synthesis methods, is emphasized. Such an approach was presented in (Stoustrup and Niemann, 1999).

- The fault estimation system proposed in (Stoustrup and Niemann, 2002) is implemented on a nonlinear antenna system. However, to the best of our knowledge, no application of this method for the nonlinear fault estimation has been reported before.

- Additional improvements to the method proposed by (Stoustrup and Niemann, 2002) is achieved; a solution for the problem of distinguishing faults from the disturbances for nonlinear system's case is proposed. The results of the proposed method is implemented and demonstrated on the satellite tracking antenna.

- A design factor for $\mathcal{H}_\infty$ optimization and a practical algorithm for estimating the uncertain fault parameter is proposed. The main results of this improvement is applied to the "Hopper" launch vehicle simulator (provided by SNECMA) to be evaluated for the next generation of ESA's (European Space Agency) satellite launch vehicle.

- When the FDI system recognizes the presence of fault, the control system has to switch automatically to the second control strategy which is not affected by the fault. A fault tolerant scheme based on switching between different controllers is proposed.

- An alternative optimization method is considered to solve the optimization problem i.e., numerical algorithms for μ optimization. The method is compared with some other optimization-based approaches and the capabilities of the proposed technique is evaluated. The comparison is implemented on a linearized plant application(Hopper propulsion system) which is more suitable for the purpose of comparing different methods.

1.4 Outline of The Thesis

The organization of the thesis, shown in figure 1.2, is as follows:

- **Chapter 1: Introduction**

- **Chapter 2: Satellite Tracking Antenna System**

  This chapter describes the model of the satellite tracking antenna. This model includes the dynamic and kinematic model of the antenna, actuators, sensors, the effect of the ship motion, and the fault analysis. The proposed model especially suggests a format which fits to the model-based FDI. It also describes which assumptions is taken into account. The presented model is verified by the ship
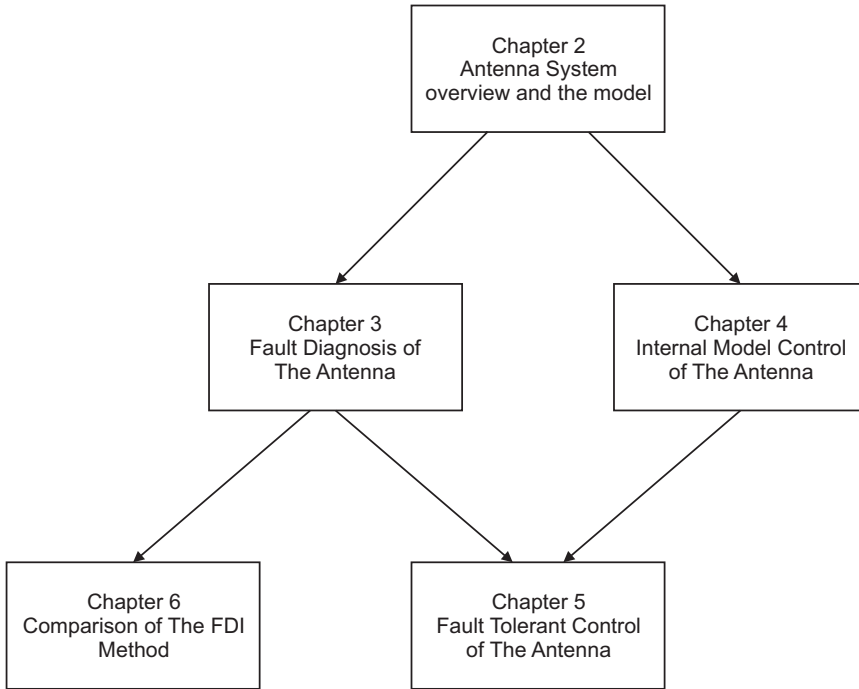
Figure 1.2: The structure of the thesis.

simulator, which is an industrial test device. The results of the verification can be found in (Soltani, 2006).

- **Chapter 3: Robust FDI for A Ship-mounted Satellite Tracking Antenna**, (Soltani, Izadi-Zamanabadi, and Wisniewski, 2008b). In the Proceeding of IEEE Multi-conference on Systems and Control, the IEEE International Conference on Control Applications (CCA), San Antonio, Texas, USA, 2008.

As it has been expressed in the literature, one of the most important steps toward constructing a fault tolerant control structure is to develop a fault diagnosis system. This essential requirement has attracted our attention as a key element toward our goal. Consequently, the FDI problem has been studied in this chapter as the major requirements and contributions of the thesis are achieved in FDI area.

The design of a residual is the main goal in Fault detection. The challenge is how to deal with the disturbances, noise, and nonlinearity in the dynamics of the system. Those difficulties are interpreted as unknown inputs and uncertainties which can affect the residual and make trouble for FTC system. As it has been discussed, the biggest challenge for the researchers was to design a FDI system

which has higher sensitivity to the fault and less sensitivity to the unknown inputs. This problem lead the designers to totally decouple the effect of the fault from the effect of the unknown inputs without considering any property or the nature for the fault and/or the unknown input. The resulting suggested FDI methods could hence be applied in special constructions, which compared to the general case, provides less satisfactory results.

The other type of approaches, which recently have attracted the attention, are optimization-based approaches. These approaches adhere to the philosophy that a suitable norm of the residual to unknown input sensitivity function is reduced. This requires assuming some special properties for the unknown inputs such as limited or constant Spectral Density or limited Power or Energy.

The method, which is proposed in this chapter, is a developed format of the (Stoustrup and Niemann, 2002). In fact, we encounter the nonlinearity as well as the disturbances. This method is useful when the nonlinear portion of the system can be separated so that it remains bounded. Indeed, in a class of nonlinear systems, it is possible to split the linear and nonlinear dynamics. The other requirement for the FDI system is to separate the frequency range of the fault from the disturbances. When the system has been modeled with those requirements, it is helpful to set-up the system into the robust standard form. The design of the $\mathcal{H}_\infty$ filter for the standard format is done using **Robust Control Toolbox** in **MATLAB**.

This chapter begins with a short discussion on the model of closed loop control system of the satellite tracking antenna. This model presents the operating model of the antenna under the normal working conditions. The model is followed by a discussion on the effect of the fault and then the robust FDI method in a standard set-up for a class of nonlinear systems is explained. The conditions, under which this method can be used, are described and followed by the design procedure of the FDI for the antenna system. Finally, the results of the detection method on the practical set-up is illustrated and conclusions are made.

The main contribution of this chapter to the thesis is to develop the FDI method so that it can be used for the antenna system. The results of this chapter are very necessary for the topic of the thesis. In fact, the FDI part, as it has been discussed, plays the most important role in a fault tolerant control system. By the aid of this results, it is possible to say that the next step toward FTC is the design of the alternative control system which is discussed in the next chapter.

- **Chapter 4: High Precision Control of Ship-mounted Satellite Tracking Antenna**, (Soltani, Izadi-Zamanabadi, and Wisniewski, 2007) In Proceedings of the European Control Conference (ECC), Kos, Greece, 2007.

The Internal Model Control philosophy relies on the Internal Model Principle, which states that *control can be achieved only if the control system encapsulates, either implicitly or explicitly, some representation of the process to be controlled* (Tham, 2002). Specially if the control scheme is developed based on an exact model of the process, then perfect control is theoretically possible. By this representation, the internal model control is also used in fault tolerant control system as an alternative controller.

The alternative control system is designed so that the faults could not affect the control task. By this consideration, the measurements of the alternative control system are different from the one used in normal operation. This is due to the fact that the faults, we concern about, are mainly on the beam sensor.

This chapter first describes the nonlinear model of the satellite tracking antenna. It formulates the problem in a way to be suitable for designing an internal model control. Then the internal model theory and generalized tracking problem is defined shortly. The internal model controller is designed next and followed by the practical results from the tests on the evaluation set-up of the antenna system.

The results of this chapter are used in the fault tolerant control as the other control method which can be used when the FTC system decides to switch to a non-faulty control method. This is important that the control scheme is able to perform the same functionality as the normal control scheme. Now, the last step toward our goal is to use both FDI system and control schemes to assemble a fault tolerant controller.

- **Chapter 5: Fault Tolerant Control of Ship-mounted Satellite Tracking Antenna**, (Soltani, Izadi-Zamanabadi, and Wisniewski, 2008c). Submitted to IEEE Transaction on Control Systems Technology.

A Fault Tolerant Control system is a control system that possesses the ability to accommodate for system failures automatically and to maintain overall system stability and acceptable performance in the event of component failures (Maki, Jiang, and Hagino, 2001). The Fault Tolerant Control design is normally done by means of modifying the control system's structure, laws, and parameters according to the result of the on-line FDI.

The contributions of this chapter are on two subjects: First, the FDI system for the satellite tracking antenna is designed and the result of the fault-disturbance discrimination is analyzed. Second, an FTC system, with ability to keep the performance of the antenna system in case of failures, is presented, where the approach is basically to alter the control system for the specific failures.

This chapter begins with the model of the working antenna in the normal operation as well as the fault description. Then a review on FDI and IMC design

procedure is brought. The FDI design is analyzed in more details where the separation between fault and disturbance is investigated by means of choosing the right weight filters. At the end, the results of the FDI design as well as the FTC system on a practical test set-up is demonstrated.

The results of this chapter are, indeed, directly points out to our goal, which was to construct a fault tolerant controller for the antenna capable of keeping the functionality of the system when the control system encounters a failure. As it is explained before, the FDI system, as an essential requirement of FTC, plays a vital role in our achievement. This leads us to pay extra attention to the FDI concept. A comparison of this FDI method with two other optimization based fault diagnosis methods are demonstrated in the next chapter. Another study case is used to illustrate more practical features of the technique.

- **Chapter 7: Robust FDI for Hopper Engine Subsystem**, (Soltani, Izadi-Zamanabadi, Wisniewski, Belau, and LeGonidec, 2008d) Accepted for the AIAA/ ASME/ SAE/ ASEE Joint Propulsion Conference, Hartford, Connecticut, USA, 2008.

The method which is used in this thesis considers the fact that the nature of the fault is parametric. This means that the FDI system tries to estimate the parameter which not only is a part of the model uncertainty, but also causes a failure. Every FDI method, depending on the demand, has its own preferences in the FDI problem e.g., observer-based and etc. This chapter includes the design of the FDI system for the Hopper satellite launch system. The optimization problem in FDI design is solved through two different tools ($\mathcal{H}_\infty$ and μ-synthesis). A comparison to two other optimization-based methods (Mixed $\mathcal{H}_2$ / $\mathcal{H}_\infty$ Fault Diagnosis and Mixed $\mathcal{H}_\infty$ / LMI Fault Diagnosis), which provide an observer for the fault, is demonstrated. The results of this comparison shows the effectiveness of the method, specifically, for parametric faults case.

- **Chapter 8: Conclusions and Recommendations**

Chapter 2

Satellite Tracking Antenna System

This chapter will describe the 2-axis F77 tracking antenna system provided by Space-Com A/S. A short review on the antenna system including the actuators and sensors will be described. Then the ship motion at sea as the disturbances to the system is introduced regarding the requirements by Inmarsat. A fault analysis is brought and the effect of different faults are qualitatively described.

2.1   System Overview

The Fleet F77 antenna is a fully developed antenna system, with well defined interfaces, since the product is already in production. The system originally contains a mechanical 3 axis antenna, with a stepper motor attached to each axis of rotation. The antenna has two joints: one joint in the socket base of the antenna (Azimuth), that rotates the entire antenna in the horizontal plane, the second joint allows the antenna to move in the vertical plane (Elevation), and the last joint rotates the plate of the antenna perpendicular to the elevation axis (Cross-elevation). However, in this thesis, the objective is to use the 2-axis antenna. Therefore, the cross-elevation axis is locked during analysis, design, and experiments.

For controlling the antenna, SpaceCom A/S has developed an embedded system, containing micro controller based on the PIC 16F series from Microchip, but in our verification tests all the interfaces communicate directly with the PC input/outputs using xPC Tools in MATLAB.

Figure 2.1 shows an overview of the 2-axis antenna and different blocks in this diagram are explained in the following.
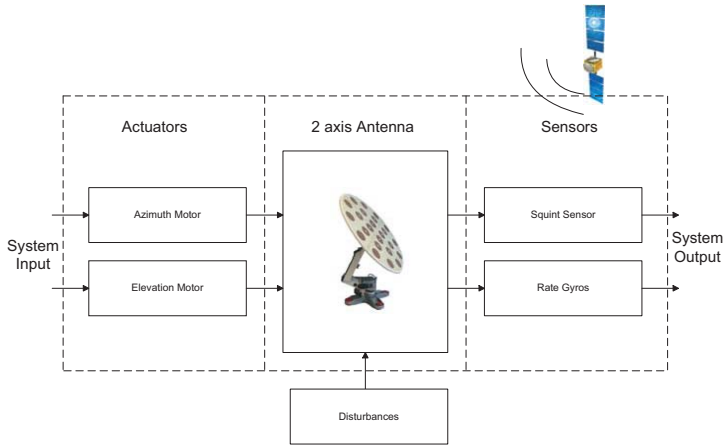
Figure 2.1: Overview of 2-axis F77 antenna system.

2.1.1 Sensors

The F77 antenna contains two types of sensors. As it can be seen in figure 2.1, the sensors are: rate gyro sensors and squint sensors. These sensors are used to measure the orientation of the antenna system. This section includes the sensors which has been used in the developed F77 Antenna. These sensors are briefly described in the following.

Beam Sensor (Squint Sensor)

The function of the SpaceCom squint sensor is to measure the error angles between satellite signal directional vector (SAT vector) and the electrical reference direction, i.e. the directional vector which provides a maximum signal reception, this is defined as the antenna Line Of Sight (LOS) and is typically the normal vector of the antenna array plane. The sensor output includes two values $S_{e,E}$ (elevation error) and $S_{e,CE}$ (cross-elevation error), which are an indication of the geometric angles φ_e and θ_e that can be seen in figure 2.2.

The indication $S_{e,E}$ and $S_{e,CE}$, of the error angles are not provided directly in radians or degrees as a unit, but as integer values. In order to use this sensor data in the control system, a mapping of the raw data is performed.
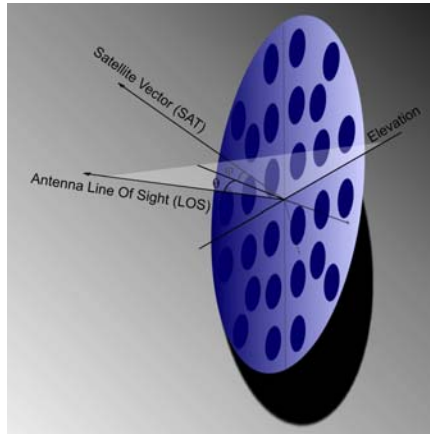
Figure 2.2: Geometric illustration of the squint sensor output angles φ_e and θ_e.

Principle of Operation

In this section, a brief explanation of the principle, that SpaceCom uses for angle estimation, is made. The SpaceCom antenna is divided into four elements as shown in figure 2.3. By phase shifting the signal between the elements 1 and 4, the antenna characteristic in this direction is altered. The phase shift is performed in two steps: first the signal of element 1 is delayed relative to element 4, second the signal of element 4 is delayed relative to element 1. By measuring the signal intensity while performing the two phase shifts in direction 1 - 4, it is possible to determine how much signal power comes from the two section of the antenna. From this measurement it is possible to determine the direction to the satellite. This is also done for the 2 - 3 elements as well, thereby
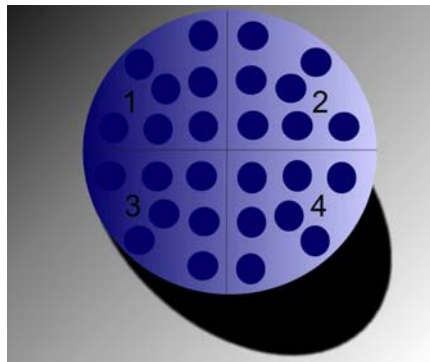
Figure 2.3: The F77 antenna array is divided into four elements.

a complete estimation of the direction of the target (satellite) is made. The phase shift delay between the elements are constant predetermined values.

In order to visualize the effect of the phase shifts figure 2.4 shows how the antenna characteristic is altered in 1-4 direction. This change is the same for the 2-3 direction.

In each of the altered direction the signal intensity is integrated over a certain time, and the difference of the measurements in the two directions are stored in data packages by the sensor, and transmitted via a standard RS-232 connection.

Gyros
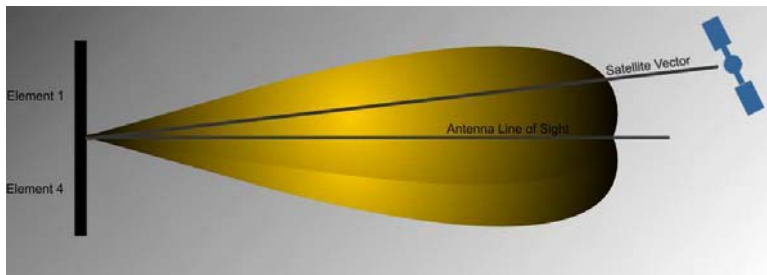
Figure 2.4: Varying the F77 antenna array characteristics by phase shifts of the antenna elements.

A rate gyro is capable of outputting a signal that is proportional with the angular velocity. Years ago the devices were large and mechanical, but today the significant smaller solid-state devices are widely used. In general, there are three types of solid-state rate gyro sensors: piezoelectric gyros, fiber-optic gyros (FOG's), and ring laser gyros (LRG's). The most common used solid-state gyro is the piezoelectric type, which uses either silicon, quartz or ceramic for measuring the Coriolis forces (see (Wertz, 1978) for more information about the principle). The piezoelectric sensors are refereed as MEMS (Micro Electro Mechanical Systems). This has to do with the vibrating turning force principle, which is electromechanical. The FOG's and LRG's are typically more precise devices, however the prices are 10-100 times higher.

Analog Devices has developed the ADXRS-series, which are reliable and cost-effective piezoelectric solid-state gyro sensors, with a good performance. ADXRS-series all has a built-in temperature sensor, that allows the developer to compensate for changes in temperature. The ADXRS series also offers custom bandwidth adjustment by the use of a 2nd order low-pass filter, which enables the developer to suppress noise from mechanical vibrations.

In order to use this sensor, a model of the gyro is derived. This models the ADXRS150 rate gyro sensor including the amplifiers, filters, analog-to-digital conversion and software driver. This is done to obtain the best estimate of the measured angular velocity. To estimate a model an ARX system identification is used while the sensors are placed on the ship simulator with a given sinusoidal frequency.

The estimated parameters for ARX model when converting the discrete ARX model to the complex domain gives the transfer function for the ADXRS150 rate gyro sensor as

$$G_{ADXRS150}(s) = \frac{1.0023}{4.673e^{-3}s + 1}.$$

(2.1)

This shows that the dynamics of the sensor is very fast and indeed for low frequencies the dynamic is negligible.
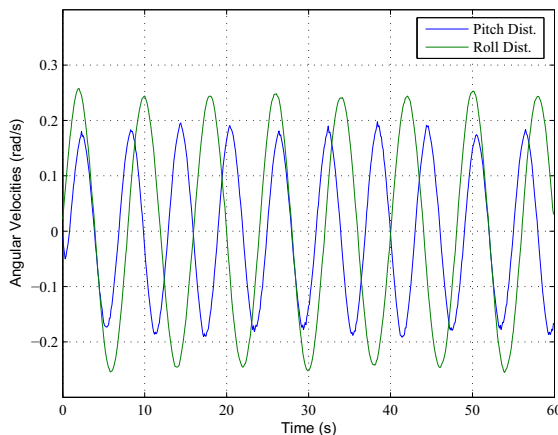
Figure 2.5: The low-pass filtered measurement output of the gyros under the maximum angular velocities and amplitudes (standard provided by Inmarsat) for pitch and roll motions.

2.1.2 Actuators

Stepper motors are used to rotate the antenna about the Azimuth and Elevation axis. When taking about stepper motors, the subject can be divided into three categories - variable reluctance(VR), permanent magnet (PM), and hybrid (HY) stepper motors. The variable reluctance stepper motor has no permanent magnet in the rotor, which means that it can move without constraint, but on the other hand it has a low degree of motor

torque. The permanent magnet stepper motor has a higher torque level, but operates typically at low speeds, and with big steps ($45°$ - $90°$). The hybrid stepper motor principle combines the best from the variable reluctance and the permanent magnet, which results in a stepper motor that can operate at high speed, has a high torque level, and a high step resolution, due to teeth on both rotor and stator.

In the antenna system provided by SpaceCom A/S the actuators consists of two different types of hybrid stepper motors, "Nanotec st4018m0706", and "Mae HY200-2220". The Nanotec motors are used on the elevation axes, and the Mae motor is used on the azimuth axes. Both motor types have two phases (A and B) and 50 rotor teeth (H_r), which results in a step resolution of $1.8°$/step in full stepping mode. To be able to give the input to the motor in the right order a power drive is used. The power drive is able to change the current in the phases, e.g. half in each, then the step resolution can be increased to e.g. half stepping mode, forth stepping mode, etc (If the step mode is 10 or more, it is normally referred to as micro stepping.). The power drives to the stepper motors are of type "Nanotec IMT901", and is able to run up to eight stepping mode, making the rotor step resolution $0,225°$/step.

To be able to fully control the dynamics of the stepper motors, it is necessary to have a model describing these dynamics. The input to the stepper motor is the value supplied to the PWM module, where the output of the PWM module are pulses made for the driver. The frequency of the pulses are indeed related to the angular velocity of the motor.

To estimate a model of the actuators (motors augmented in the antenna with gears), closed-loop identification is used while the motor angles (read from the driver) are used for a PID feedback to the motor driver input. The results were confirming that the dynamics of the actuators can be approximated by integrators as

$$\dot{\theta}_{bj}^j = u_{bj}^j \tag{2.2}$$

and

$$\dot{\theta}_{jp}^p = u_{jp}^p, \tag{2.3}$$

where u_{bj}^j and u_{jp}^p are the inputs, and θ_{bj}^j and θ_{jp}^p are the angles of the azimuth and elevation motors respectively.

The dynamics of the stepper motor, however is a big area of research itself, is considered in a simplified format, but there are still some consideration regrading the conditions under which this model is satisfied. Those conditions include the maximum speed and acceleration which cause physical constraints for the 2-axis antenna. This constraints are briefly expressed in Appendix B.
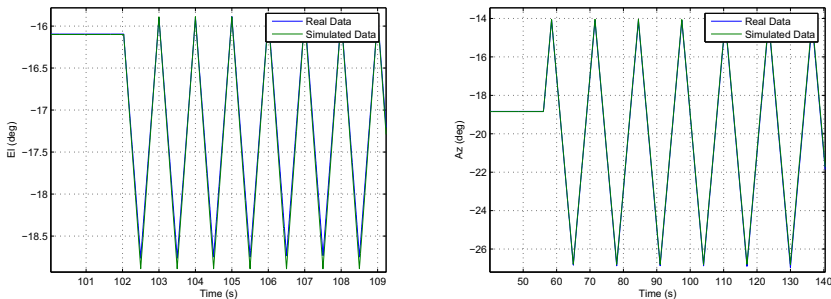
Figure 2.6: Verification of the model for Elevation and Azimuth motor angles (Soltani, 2006).

2.1.3 Ship Motion

When looking into the issue of ship motions at sea, at least three contributions to the movement should be considered: The wind acting on the ship, the waves generated by the wind, and the currents at sea (often referred to as ocean currents). Many works have been done on describing these stochastic processes. However, the resulting motion of the ship itself, caused by the wind, waves, and current is far less documented for generic purpose, the reason is that different ship structures, sizes and loads affect the dynamic behavior of the ship differently.

The main contributor to the ship motions, is the wind generated wave acting on the ship body. Thus, the disturbance on the ship, is assumed to be caused by waves for simplification. However, the disturbance specification provided by Inmarsat, will still be met.

Wave and Wind Disturbances

The wind generated waves at sea start with small wavelets growing bigger and bigger with the drag force of the wind until they finally break and disappear. It has been observed that a developing sea and storm have a high peak frequency in its spectrum. A storm that has lasted for long time, is said to make a fully developed sea. When the wind decreases, the waves peak frequency decreases and a low frequency decaying sea or swell is formed.

Ocean waves are usually described as a stochastic process, since the sea elevation is random in both time and space. At the moment the state of the art regarding sea elevation modeling, is based on free-running model test data, databases, and numerical simulation based on Computational Fluid Dynamics Methods (CFDM), (Perez and Blanke, 2002).

These models are very precise, but also very complex and not suitable for testing control strategies.
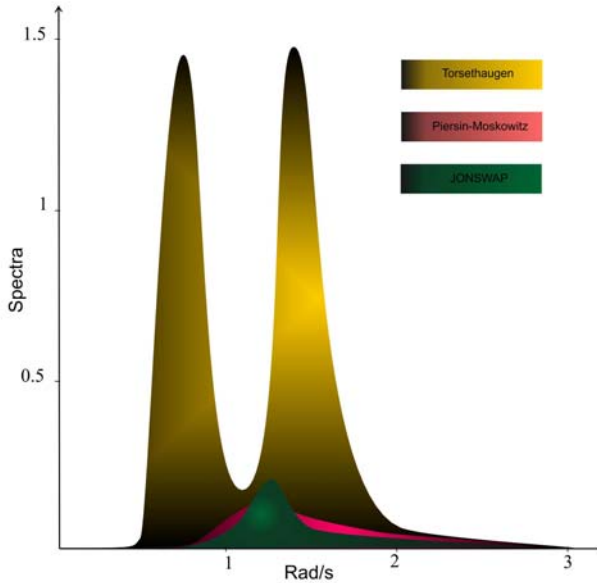
Figure 2.7: Comparison of the three different wave spectra.

To describe the spectrum of the elevation at the sea surface, many works have been carried out: The earliest spectrum formulation was a power spectral density function, founded by (Neumann, 1952), and was based upon one-parameter, an empirical constant, the wind speed, and gravity. Since (Bretschneider, 1959) added another parameter to the spectrum and in 1963 Pierson and Moskowitz developed the Pierson-Moskowitz spectrum (PM) (Neumann, 1963), based on observations from the North Atlantic Ocean, (Fossen, 2002). Today three other spectra are used: The Modified Pierson-Moskowitz spectrum, the JONSWAP spectrum or the Torsethaugen spectrum. For fully developed sea the two parameter Modified Pierson-Moskowitz spectrum (MPM) should be used. This spectrum is a one peak spectrum and has been highly recommended. In 1968 and 1969 an extensive measurement program was carried out in the North Sea. The program was named Joint North Sea Wave Project (JONSWAP). The spectral density function formulation is valid for not fully developed seas, which results in a more peaked spectrum compared to the developed sea spectrum. The JONSWAP spectral formulation describes wind-generated waves under the assumption of finite water depth and lim-

ited fetch. The Torsethaugen spectrum is based on empirical data and is proposed as a two peaked spectrum which includes the effect of swell and newly developed waves. The empirical spectrum is based on experimental data from the North Sea. Figure 2.7 compares the mentioned spectra.

The Effect of Waves on The Ship

As it is mentioned above, the main contribution to the disturbances is from the wind generated waves which affect the ship. This effect is influenced by several elements such as encounter frequency, ship speed, the angle between the wave and the ship heading, the mass, size, and the restoring forces of the ship (Fossen, 2002; Perez and Blanke, 2002).

The encountered frequency ω_e is related to the peak frequency spectrum ω_0 as

$$\omega_e = \omega - \frac{\omega^2 U_0 cos(\chi)}{g},$$
(2.4)

where χ is the encounter angle (the angle between ship heading and the wave direction (see figure 2.8)), g is the gravity acceleration, and U_0 is the total speed of the ship.
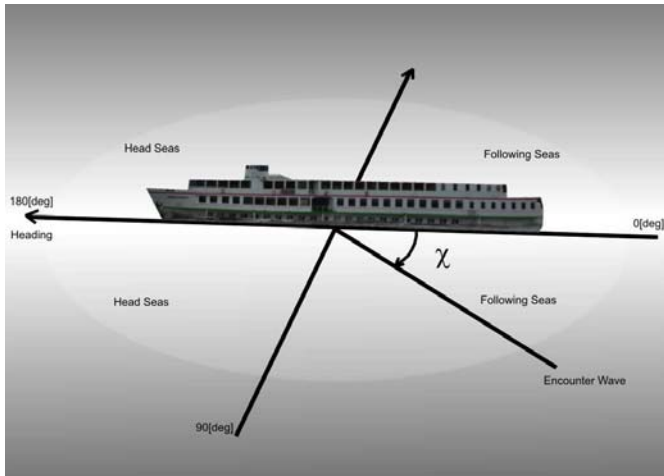
Figure 2.8: Encounter angle χ.

Besides, the dynamics of the vessel is acting as a low-pass filter (normally it is approximated by a 2nd order model) which weaken the effect of the high frequencies in the spectrum. Therefore, the effect of the waves can bee seen as sinusoidal motions on the

ship which is restricted in the frequency. The restrictions have been defined as the standard maximum values of the roll, pitch, and yaw disturbance frequency and amplitude by (Inmarsat, 2003).

Disturbance System

The sinusoidal disturbances are modeled by the following dynamics which is also called the *exosystem*:

$$\dot{w} = Sw, \tag{2.5}$$

where $w = \begin{bmatrix} p, \acute{p}, q, \acute{q}, r, \acute{r} \end{bmatrix}^T$,

$$S = diag(S_i), i = 1, 2, 3. \tag{2.6}$$

and

$$S_i = \begin{bmatrix} 0 & \Omega_i \\ -\Omega_i & 0 \end{bmatrix}, \tag{2.7}$$

where Ω_1, Ω_2, and Ω_3 are the frequencies of roll, pitch, and yaw disturbances. Also the initial value of w can determine the phase of sinusoidal disturbances.

2.1.4 Tracking Antenna Dynamics

To prevent duplications, the reader is referred to review the Section 5.3 where the different frames are defined for the satellite tracking antenna system. The rotation between frames are explained and linked together. Moreover, the tracking error is expressed in the dynamical system.

2.2 Fault Analysis

Failure Mode and Effect Analysis (FMEA) is initially introduced by system engineers and developed by (Jorgensen, 1995; Bøgh, 1997; Izadi-Zamanabadi, 1999) as a tool to analyze the components of a system for possible failures, their causes, and effects (Blanke et al., 2006). In FMEA, a qualitative model of the faults is made in each component of the system. This is done by dividing the system into suitable components. In each of these components the faults and their effects are explained via a FMEA table which is normally used to analyze and possibly make a table of the information for each failure about

- Failure Modes (FM),

- Failure Causes (FC),

- Failure Effects (FE),

- Failure Occurrence Risk (FOR),

- Failure Severity (FS),

- Priority Index (PI)

- Actions Required (AR),

where FOR and FS are expressed as numbers between 0 to 10 chosen by the user and the fault priority can be find out according to figure 2.9.
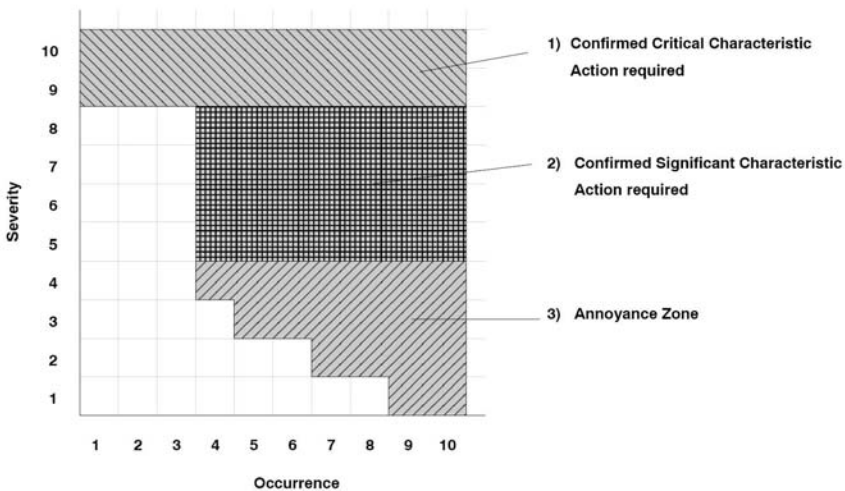
Figure 2.9: For priority 1 and 2 require action but for priority 3 the action is preferred.

In table 2.1, FMEA table for the antenna is developed. The beam sensor uses a high bandwidth communication link to the satellite. The strength of the signal as described in the last section determines the output of this sensor. Thus, the amount of the signal reaching the plate of the antenna is a crucial factor for this measurement. Consequently, any factor which prevents or changes the signal strength externally is actually a failure to the beam sensor. Those failures are mainly due to an object between the antenna and the satellite (signal blocking), temporary satellite shut down, and change in the atmosphere.

Failure Modes	Failure Causes
	Failure Effects
	Failure Occurrence Risk
	Failure Severity
	Priority Index
	Actions Required
signal blocking	incorrect feedback to the controller
	high noise in measurement
	5
	9
	1
	control reconfiguration
satellite shutdown	incorrect feedback
	large noise in measurement
	0.5
	9
	1
	control reconfiguration
atmosphere change	disturbed tracking performance
	low noise in measurement
	4
	1
	Acceptable Operation Mode
	no action
gyro temp and vibration	decrease performance in reconfiguration
	bias and noise in measurement
	5
	1
	Acceptable Operation Mode
	no action
position loose	decrease performance in reconfigurated controller
	bias in angle measurement
	2
	2
	Acceptable Operation Mode
	no action

Table 2.1: FMEA table for the tracking antenna.

The priority index also shows that the detection of those failures are necessary. The rate gyros might be affected by the change in temperature or vibrations. However, the used gyros have compensator for both factors. The actuator faults is mainly loosing the position. However, the FMEA table 2.1 shows that the priority index of the gyro and actuator faults are much lower than that of the beam sensor.

Chapter 3

Robust FDI for A Ship- mounted Satellite Tracking Antenna

Abstract- Overseas telecommunication is preserved by means of satellite communication. Tracking system directs the on-board antenna toward a chosen satellite while the external disturbances affect the antenna. Certain faults (beam sensor malfunction or signal blocking) cause interruption in the communication connection resulting in the loss of the tracking functionality. In this paper, an optimization based fault diagnosis system is proposed for the nonlinear model of the satellite tracking antenna (STA). The suggested method is able to estimate the fault for a class of nonlinear systems acting under external disturbances. The system is reformulated in the so-called standard problem setup. Finally, the applicability of the method has been verified through implementation on an antenna system.

3.1   Introduction

The ability to maintain communication over large distances has always been an important issue. Communication can be maintained through satellite communication as the constellation of the communication satellites ensures that it is always possible to make contact with a satellite, regardless of the actual position on Earth. The important factor in this case is to track the satellite and sustain contact with it. The challenge arises when the antenna is used in a non-stationary case, e.g. marine communication. Once the ship-mounted antenna has tracked a communication satellite, movements of the ship, partly due to waves, will force the antenna to point away from the satellite and thereby break the communication (Soltani et al., 2007). An advanced control algorithm is developed

for this antenna that compensates for these disturbances. Based on the received communication signals the antenna system determines the discrepancies from the antenna's line of sight and provides these to the control system.

The problem arises when the signal is blocked due to change in atmosphere, a hurdle between the antenna and satellite, or satellite shut down. This results in faulty data to the control loop and hence leading to the loss of tracking functionality and/or instability.

Fault diagnosis has since the 1980s been an active research topic. Depending on the models that have been used to describe the systems, linear or nonlinear, different approaches have been proposed by many researchers (Jørgensen, Patton, and Chen, 1995), (Blanke et al., 2006), and (Isermann, 2006). One of the important problems that has attracted attention of most in this research community is the robustness issue that arises due to the fact that there is some mismatch (however small) between the derived model and the real system dynamics. An early paper, which suggested combining methods for diagnosis and control was (Nett, Jacobson, and Miller, 1988). (Bokor and Keviczky, 1994) suggested to use $\mathcal{H}_\infty$ optimization to design fault diagnosis filters. A method that used dedicated and specialized filter structures was presented in (Mangoubi et al., 1995).

The focus of this paper is on designing a FDI system for the satellite tracking antenna (STA) which is robust to the uncertainties and disturbances in the system. In particular, the focus is on employing methods for fault diagnosis which have been inspired by and derived from the area of robust control theory, or in wider generality of optimization based control synthesis methods. A fault diagnosis approach for systems with parametric faults has been used for a linear model of a satellite launch vehicle in (Soltani, Izadi-Zamanabadi, and Stoustrup, 2008a). Such an approach was presented in (Stoustrup and Niemann, 1999), where the model is considered to be parameter varying and the fault is, in fact, a parameter. However, to the best of our knowledge, no application to the nonlinear case of this method has been reported. In this paper, the nonlinear system's case in (Stoustrup and Niemann, 2002) has been studied in more details and some practical notes has been added such as the problem of distinguishing between faults from disturbances.

A dynamical model of STA has been used to design the FDI system. Verification results show that the proposed dynamic model's behavior closely simulate the real system (Soltani, 2006). However, to illustrate the applicability of the presented method, the diagnosis system is verified against a real antenna system with successful results.

The paper is organized as follows: in Section 3.2, the dynamical model of the operating STA as well as the fault nature is presented. Section 3.3 renders the proposed method together with the FDI system design procedure. Section 3.4 presents the results in practical tests; eventually, conclusions and suggestions are brought in the last section of the paper.

3.2   Problem Formulation

3.2.1   Modeling of STA
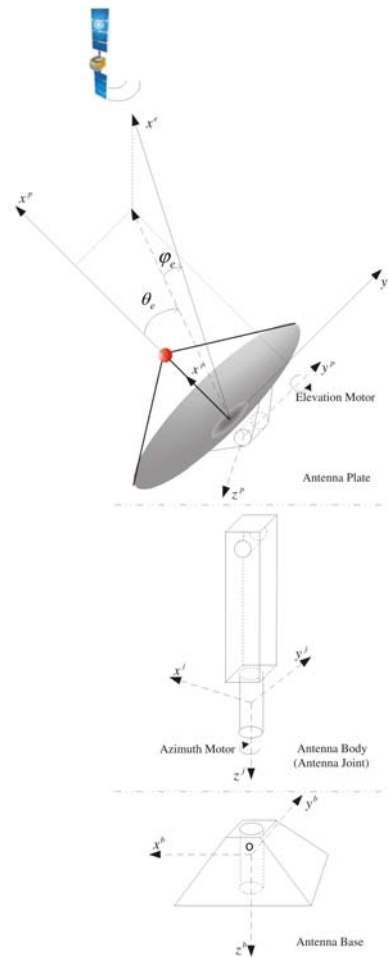
Figure 3.1: A satellite tracking antenna.

The dynamic model of the satellite tracking antenna consists of four main parts (See (Soltani et al., 2007) and (Soltani, 2006));

- *The model of the antenna joints dynamics*. It models the antenna as a combination of joints and analyzes the kinematic and dynamics of the mechanical system.

This part includes the assignment of proper frames to each joint and defining the relevant states together with the rotations between those frames. Figure 3.1 shows such procedure for the antenna.

- *The model of the satellite tracking system.* This model transforms the control problem to one framework. In fact, the measurement of the beam sensor, which the regulation of that is the main goal, is mapped to the control frame where the dynamics is described in. Figure 3.1 illustrates the measured angles φ_e and θ_e and that these angles are defined as the deviation of the vector x^e of the earth frame from the vectors x^p and y^p of the plate frame.

- *The model of the ship motion* which plays an important role to deviate the antenna from the true pointing vector is modeled (see (Johansen, Fossen, Sagatun, and Nielsen, 2003), (Fossen, 2002), (Tanaka and Nishifuji, 1995), (Tanaka and Nishifuji, 1994), (Tseng and Teo, 1997)) and the disturbance specifications provided by (Inmarsat, 2003) has been met.

- *The controller* (Soltani et al., 2007), which has been designed based on the internal model control (IMC), is able to handle simultaneously uncertainties in the plant parameters as well as in the trajectory which is to be tracked (Isidori et al., 2003b).
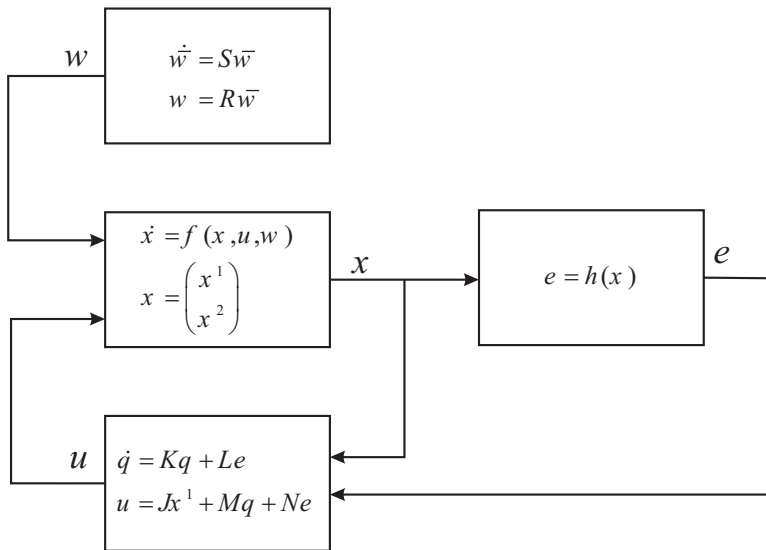
Figure 3.2: Block diagram of the antenna model.

The control system in (Soltani et al., 2007) used the gyro data for the purpose of control while in the current case the control system uses the data provided by the beam sensor to achieve the control objectives. Figure 3.2 shows the classical representation of the STA system which is using a linear controller. Defining special orthogonal group $SO(3) \subset \mathbb{R}^{3\times3}$ as the set

$$SO(3) = \{\mathcal{R} \in \mathbb{R}^{3\times3} : \mathcal{R}\mathcal{R}^T = I, det(\mathcal{R}) = 1\},$$

the state vector is $x = (x^1, x^2) \in \mathbb{R}^{2\times SO(3)}$, $u \in \mathbb{R}^2$ is the input vector to the motors, $\bar{w} \in \mathbb{R}^6$ is the vector of exogenous system states (produces the disturbance vector $w \in \mathbb{R}^3$ as roll, pitch, and yaw motions in the base of the antenna and consequently the ship body), $e \in \mathbb{R}^2$ is the vector of the measurement error from the beam sensor, and $q \in \mathbb{R}^2$ is the vector of the robust controller states.

Furthermore, the nonlinear smooth functions f, h are expressed in the following.

$$f : \mathbb{R}^2 \times SO(3) \times \mathbb{R}^{2\times3} \to \mathbb{R}^2 \times SO(3), \tag{3.1}$$

$$f(x, u, w) = \begin{pmatrix} f^1(u) \\ f^2(x^2, w) \end{pmatrix} = \begin{pmatrix} u \\ Skew(w)x^2 \end{pmatrix}, \tag{3.2}$$

where the function $Skew(w)$ is defined as

$$Skew(w) = \begin{pmatrix} 0 & -w_3 & w_2 \\ w_3 & 0 & -w_1 \\ -w_2 & w_1 & 0 \end{pmatrix}, \tag{3.3}$$

and

$$h : \mathbb{R}^2 \times SO(3) \to \mathbb{R}^2, h(x) =$$
$$\begin{pmatrix} tan^{-1}\left(\frac{-x_{11}^2 sin(x_1^1)+x_{21}^2 cos(x_1^1)}{x_{11}^2 cos(x_1^1)cos(x_2^1)+x_{21}^2 sin(x_1^1)cos(x_2^1)+x_{31}^2 sin(x_2^1)}\right) \\ sin^{-1}\left(\frac{-x_{11}^2 cos(x_1^1)sin(x_2^1)-x_{21}^2 sin(x_1^1)sin(x_2^1)+x_{31}^2 cos(x_2^1)}{1}\right) \end{pmatrix} \tag{3.4}$$

Moreover, the lower block in figure 3.2 is the state space representation of the controller with proper dimensions w.r.t. the dimensions of the defined vectors. The upper block in figure 3.2 also expresses the *exosystem*, which is the linear autonomous system (see (Isidori et al., 2003b)) and generates the disturbance w affecting the system. The matrix $S \in \mathbb{R}^{6\times6}$ is defined as

$$S = diag(S_i), i = 1, 2, 3 \tag{3.5}$$

where

$$S_i = \begin{bmatrix} 0 & \Omega_i \\ -\Omega_i & 0 \end{bmatrix}, \tag{3.6}$$

that Ω_1, Ω_2, and Ω_3 are the frequencies of roll, pitch, and yaw disturbances. The initial value of $\bar{w}$ determines the phase of sinusoids. Finally, the matrix $R \in \mathbb{R}^{3 \times 6}$ is the output map of the exosystem to the disturbances effecting the ship.

3.2.2   Fault Discussion

A failure in the beam sensor would mean that the pointing error feedback from the satellite is unknown and it will also result in loss of high bandwidth communication link depending on the severity of the fault. In order to maintain a good strength of satellite signal reaching the antenna, a controller keeps the pointing error between the antenna and the satellite to a minimum of less than a degree. However, a change in the strength of the signal measured by the beam sensor can occur by appearance of any hurdle between the antenna and the satellite or change in the atmosphere pressure and temperature. This is called a signal blocking. Blocking will result in an increase in the fluctuations on the pointing error measurement due to loss of signal strength. However, the amount of increase in the fluctuations depends on the amount of the signal reaching the antenna plate during blocking. In general deviations due to disturbances and initial conditions from the satellite sight vector cause the same fluctuations but they should not be considered as blocking since the controller will compensate for those deviations. That is a good reason in order not to use the measurement signal just-statistic properties to find the blocking faults.

Finally, the faulty system is effected by parameters $-1 \le \delta_i \le 1$, where δ_i ($i = 1, 2$) is the coefficients of the noise variance σ_i^2.

3.3   Method

3.3.1   Robust FDI in A Standard Set-up for A Nonlinear System

The generalized concept of fault detection architecture in a class of nonlinear systems is proposed in (Stoustrup and Niemann, 1999) as it is shown in figure 3.3.

In this set-up, the upper block Δ represents the nonlinearity that is assumed to be sector bounded in an $\mathcal{H}_\infty$ sense (Zhou et al., 1996). It is important that the linear plant $G(s)$ is
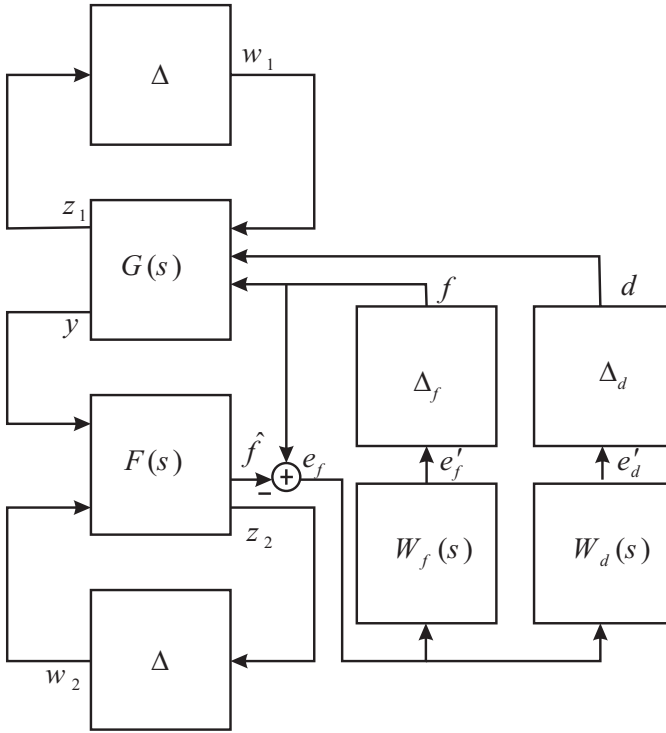
Figure 3.3: Fault detection architecture scheme.

such that it is possible to infer the stability of nonlinear loop with some specific Δ from robust stability with respect to the $\mathcal{H}_\infty$ unit ball.

The block $F(s)$ is the FDI system to be designed coupled by a copy of the nonlinear block Δ. The signal $\hat{f}$ is the estimation of f (fault affected signal) which is generated by FDI system. The signal d is the disturbance to the system. The blocks W_d and W_f are the weighting functions that, based on the design criteria, used to distinguish between fault and disturbance. Furthermore, w_2 would be the estimate of w_1 when z_2 is the estimate of z_1.

Defining e_f as $e_f = f - \hat{f}$, the problem will be transformed to make e_f small for any bounded f. This requires us to make the system augmented with the Δ_f and Δ_d blocks where $\|\Delta_f\|_\infty , \|\Delta_d\|_\infty \leq 1$ are robustly stable. This results in computing nonlinear FDI system by finding a linear filter which solves a μ problem for a linear system structure including four uncertainty blocks, i.e., two Δ blocks combined with Δ_f and Δ_d.

In fact, it is possible to write the system as

$$
\begin{pmatrix} z_1 \\ z_2 \\ \acute{e}_f \\ \acute{e}_d \\ \cdots \\ y \\ w_2 \end{pmatrix} = \tilde{G}(s) \begin{pmatrix} w_1 \\ w_2 \\ f \\ d \\ \cdots \\ \hat{f} \\ z_2 \end{pmatrix} \tag{3.7}
$$

or

$$
\begin{pmatrix} \tilde{z} \\ \tilde{y} \end{pmatrix} = \tilde{G}(s) \begin{pmatrix} \tilde{w} \\ \tilde{u} \end{pmatrix} \tag{3.8}
$$

and then design the FDI filter according to the following result (Stoustrup and Niemann, 2002):

Theorem 1 *Assume that the system*

$$
\tilde{G}(s) = \begin{pmatrix} \tilde{G}_{\tilde{z}\tilde{w}}(s) & \tilde{G}_{\tilde{z}\tilde{u}}(s) \\ \tilde{G}_{\tilde{y}\tilde{w}}(s) & \tilde{G}_{\tilde{y}\tilde{u}}(s) \end{pmatrix} \tag{3.9}
$$

and the linear filter $F(s)$ satisfies

$\left\| \tilde{G}_{\tilde{z}\tilde{w}}(.) + \tilde{G}_{\tilde{z}\tilde{u}}(.)F(s)\tilde{G}_{\tilde{y}\tilde{w}}(.) \right\|_{\mu} < \gamma$ *considering mentioned four uncertainty blocks, then the $\mathcal{L}_2 - \mathcal{L}_2$ operator gain from fault f to fault estimation error $e_f = f - \hat{f}$ when applying the FDI system in figure 3.3 is bounded by γ as well.*

3.3.2   Design of the Fault Detector for STA

The first step in design procedure is the introduction of two filters W_f and W_d to make sure that $\frac{\|e_f\|}{\|f\|}$ is minimized in the frequency area of interest. That is important to range the filters so that W_f passes the frequency range, $\Phi_f(\omega)$, where the fault is dominant and W_d does it for the frequency range, $\Phi_d(\omega)$ where the disturbance is dominant. Furthermore, it is desired that $\Phi_f(\omega) \cap \Phi_d(\omega) = \emptyset$. For instance $W_f(s)$ is specified by

$$
\begin{aligned}
\dot{x}_{ef} &= A_{ef}x_{ef} + B_{ef}e_f \\
\acute{e}_f &= C_{ef}x_{ef} + D_{ef}e_f,
\end{aligned} \tag{3.10}
$$

with $D_{ef} = 0$ thus $\acute{e}_f = W_f(s)e_f$. Correspondingly, the filter $W_d(s)$ is

$$\begin{aligned}
\dot{x}_{ed} &= A_{ed}x_{ed} + B_{ed}e_f \\
\acute{e}_d &= C_{ed}x_{ed} + D_{ed}e_f
\end{aligned}$$

(3.11)

i.e., $\acute{e}_d = W_d(s)e_f$.

The second step is to separate the linear and nonlinear parts of the system. This should be done with respect to the assumption that the nonlinear part is sector bounded. Considering the system dynamics, we have two nonlinear parts in $f^2(x^2, w)$ and $h(x)$. The outputs provided by these two blocks are always bounded ($x^2 \in SO(3)$ and $h(x)$ is composed of tan^{-1} and sin^{-1}). Consequently, the exosystem should be considered into the nonlinear Δ block. Thus, the linear part of the dynamics is

$$\begin{aligned}
\dot{x}^1 &= Jx^1 + Mq + Ne \\
\dot{q} &= Kq + Le.
\end{aligned}$$

(3.12)

The output error e is modeled as

$$e = h(x) + f + d.$$

(3.13)

Now, we need to present a combination of (3.12) and (3.13) in a linear format knowing that

$$w_1 = h(x)z_1.$$

(3.14)

This can be done by considering a unit input $v = 1$ as a known input where $z_1 = v$ as

$$\begin{aligned}
\dot{x}^1 &= Jx^1 + Mq + N\Delta z_1 + N\Delta_f \acute{e}_f + N\Delta_d \acute{e}_d \\
\dot{q} &= Kq + L\Delta z_1 + L\Delta_f \acute{e}_f + L\Delta_d \acute{e}_d.
\end{aligned}$$

(3.15)

The third step is to write the whole system in an standard way so that it could be used by the linear robust design tools such as μ synthesis. This set-up is presented as follows

$$
\begin{pmatrix}
\dot{x}^1 \\
\dot{q} \\
\dot{x}_{ef} \\
\dot{x}_{ed} \\
\cdots \\
z_1 \\
z_2 \\
\acute{e}_f \\
\acute{e}_d \\
\cdots \\
y \\
w_2
\end{pmatrix}
=
\left(
\begin{array}{ccccc}
A & \vdots & B_1 & \vdots & B_2 \\
\cdots & & \cdots & & \cdots \\
C_1 & \vdots & D_{11} & \vdots & D_{12} \\
\cdots & & \cdots & & \cdots \\
C_2 & \vdots & D_{21} & \vdots & D_{22}
\end{array}
\right)
\begin{pmatrix}
x^1 \\
q \\
x_{ef} \\
x_{ed} \\
\cdots \\
v \\
w_1 \\
w_2 \\
f \\
d \\
\cdots \\
\hat{f} \\
z_2
\end{pmatrix}
\qquad (3.16)
$$

where the matrix elements are

$$
A = \begin{pmatrix}
J & M & 0 & 0 \\
0 & K & 0 & 0 \\
0 & 0 & A_{ef} & 0 \\
0 & 0 & 0 & A_{ed}
\end{pmatrix}
$$

$$
B_1 = \begin{pmatrix}
N\Delta & 0 & 0 & N & N \\
L\Delta & 0 & 0 & L & L \\
0 & 0 & 0 & B_{ef} & 0 \\
0 & 0 & 0 & B_{ed} & 0
\end{pmatrix}
$$

$$
B_2 = \begin{pmatrix}
0 & 0 \\
0 & 0 \\
-B_{ef} & 0 \\
-B_{ed} & 0
\end{pmatrix}
$$

$$
C_1 = \begin{pmatrix}
0 & 0 & 0 & 0 \\
0 & 0 & 0 & 0 \\
0 & 0 & C_{ef} & 0 \\
0 & 0 & 0 & C_{ed}
\end{pmatrix}
$$

$$
D_{11} = \begin{pmatrix}
1 & 0 & 0 & 0 & 0 \\
0 & 0 & 0 & 0 & 0 \\
0 & 0 & 0 & 0 & 0 \\
0 & 0 & 0 & 0 & 0
\end{pmatrix}
$$

$$D_{12} = \begin{pmatrix} 0 & 0 \\ 0 & 1 \\ 0 & 0 \\ 0 & 0 \end{pmatrix}$$

$$C_2 = \begin{pmatrix} 0 & 0 & 0 & 0 \\ 0 & 0 & 0 & 0 \end{pmatrix}$$

$$D_{21} = \begin{pmatrix} \Delta & 0 & 0 & 1 & 1 \\ 0 & 0 & 0 & 0 & 0 \end{pmatrix}$$

$$D_{22} = \begin{pmatrix} 0 & 0 \\ 0 & \Delta \end{pmatrix}$$

and f and d are defined by:

$$\begin{aligned} f &= \Delta_f \acute{e}_f \\ d &= \Delta_d \acute{e}_d. \end{aligned} \tag{3.17}$$

The last step is to compute the fault detection filter by D-K algorithm. Hence, the solution is to apply standard D-K iterations by assuming

$$\begin{aligned} \Delta &= diag(\delta_i) \\ \Delta_f &= diag(\delta_{f_i}) \\ \Delta_d &= diag(\delta_{d_i}), \end{aligned} \tag{3.18}$$

where all δ_is, δ_{f_i}s, and δ_{d_i}s belong to unit circle in the complex plane for $i = 1, 2$.

3.4   Practical Results

The implementation of the designed FDI filter is according to figure 3.4. The measurements are e, x, and recall that $v = 1$ is assumed. Moreover, we need to build up the nonlinear Δ block which provides an estimation for the error e. This is done by implementing three gyros at the body of the antenna where it is fixed to the ship. The output of the gyros is the vector w which by integration gives the rotation matrix and finally it is possible to compute the error output $h(x)$ (see (Soltani et al., 2007) and (Soltani, 2006)).

The idea of having a real test led to evaluate the method while the antenna is placed on a tool called *ship simulator*. The ship simulator is able to simulate the movements of the ship in different conditions. This system provides a reliable simulation of the environment according to the requirements provided by (Inmarsat, 2003). When placing
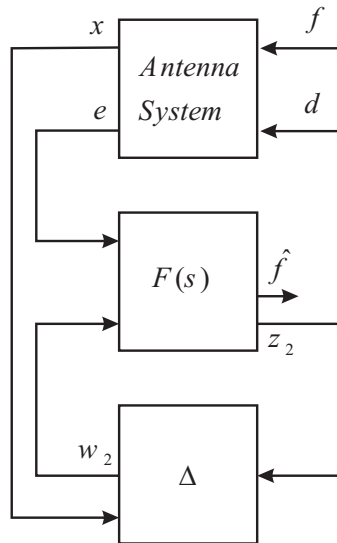
Figure 3.4: Implementation of the off-line designed filter to the on-line system.

the antenna on this device, the ship simulator moves the antenna in pitch, roll, and turn axes which are the most important movements affecting the antenna's plate direction. Eventually, to build up the real situation of the ship-mounted antenna, it is placed in an antenna laboratory which is equipped with a signal transmitter as a virtual satellite. Additionally, the lab walls are electromagnetically insulated in order to reduce the effect of the reflection of the signals to the antenna. In the verification tests, the maximum amplitude and frequency of the pitch, roll, and yaw disturbances, according to (Inmarsat, 2003), has been set to the ship simulator.

The ship simulator starts about time $t = 20s$. Figure 3.5-a(left column) shows the case that the fault happens as disconnection of the elevation receiver of the beam sensor during the time $40s < t < 70s$. Figure 3.5-b(left column) shows the output of the cross elevation receiver of the beam sensor and figure 3.5-c(left column) shows the estimated faults for elevation and cross elevation sensors which are $\hat{f}_1$ and $\hat{f}_2$ respectively. It illustrates that the fault has been detected and isolated at the right time.

Figure 3.5(right column) reveals the same scenario for the cross elevation beam sensor and declares that the fault diagnosis for this case is also well-performed.

Figure 3.6-a,b show the output of the beam sensor while a fault has happened to the test structure between time $95s$ and $144s$. This fault has been applied by turning the signal generator off in order to simulate the signal blocking during the tracking of satellite and/or satellite shutdown which are of importance during overseas satellite tracking.
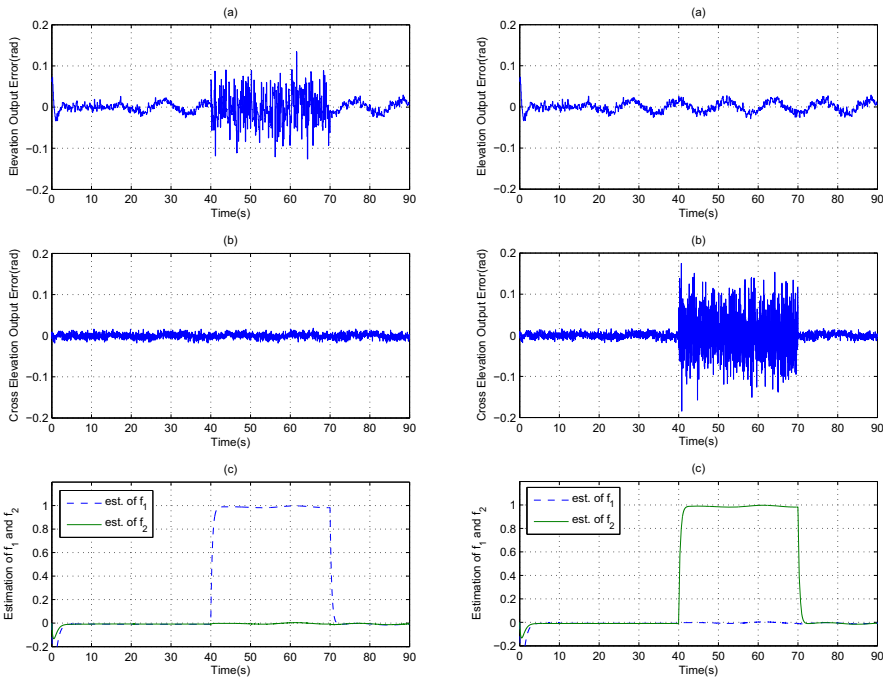
Figure 3.5: Fault on beam sensor elevation (left column) and cross-elevation (right column) signal.

Finally, figure 3.6-c shows the output of the implemented FDI system for this fault where obviously, in this case, both fault estimations indicate the fault.

3.5   Conclusions

The nonlinear model of the satellite tracking antenna was explained. The model was formulated in a standard problem set-up for robust control. A combination of a linear filter-obtained from an $\mathcal{H}_\infty$ approach- and a nonlinear block was employed as the fault detector system. The set-up was developed so that the designed FDI system reduces the effect of the disturbances to the estimated value of the fault. Finally, the implemented FDI algorithm has been checked on a ship simulator test device and it has been concluded that the proposed FDI system has fulfilled the desired fault diagnosis specifications.
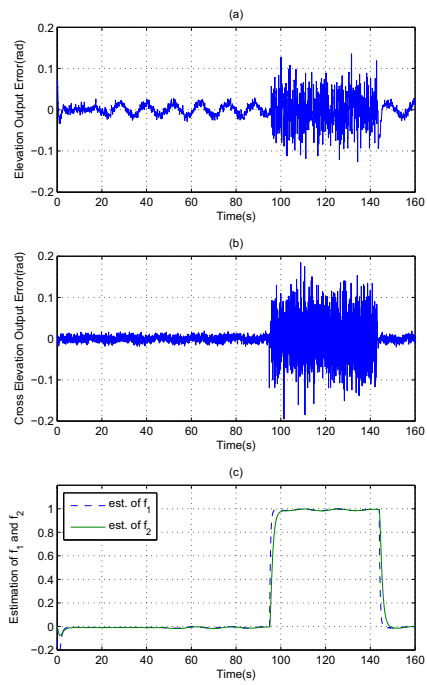
Figure 3.6: Total signal blocking or satellite shutdown.

Chapter 4

High Precision Control of Ship-mounted Satellite Tracking Antenna

Abstract- *The telecommunication on a modern merchandise ship is maintained by means of satellite communication. The task of the tracking system is to position the on-board antenna toward a chosen satellite. The control system is capable of rejecting the external disturbances which affect on the under-actuated antenna and ensures that it remains locked on the satellite. In this paper, a nonlinear internal model controller (NIMC), which achieves asymptotic tracking for the nonlinear antenna system with nonlinear exogenous dynamics, is proposed. Computer simulations as well as practical tests verify the effectiveness of this method to cope with the external disturbances that are imposed to the satellite tracking antenna (STA).*

4.1   Introduction

The ability to maintain communication over large distances has always been an important issue. Communication can be maintained through satellite communication as the constellation of the communication satellites ensures that it is always possible to make contact with a satellite, regardless of the actual position on Earth. The important factor in this case is to track the satellite and sustain contact with it. For stationary antennas this is simple: once the satellite has been tracked, the communication antenna on the ground will remain fixed on it. The challenge arises when the antenna is used in a non-stationary case, e.g. marine communication. Once the ship-mounted antenna has

tracked a communication satellite, movements of the ship, partly due to waves, will force the antenna to point away from the satellite and thereby break the communication. If the antenna system is not capable of compensating for the disturbances in an appropriate way, the antenna system will not be able to maintain contact with the satellite. In this case, it is of great importance that the antenna has a control system, which ensures the antenna to compensate for these disturbances and to remain locked on the satellite.

From this point of view, a similar problem has been previously considered and solved for a full-actuated (three axis actuated) antenna by means of linearization of the model. The antenna has been used for communication within L-Band. The present case has challenged our attention because of the quest for maintaining communication at higher frequencies and wider bandwidth (KU-Band), which requires higher control precision, combined with the requirement for using under-actuated antenna.

The focus of the paper is specifically on the tracking task; The problem of controlling the output of a system so as to achieve asymptotic tracking of prescribed trajectories and asymptotic rejection of disturbances is a central problem. Internal-model-based tracking is able to handle simultaneously uncertaintities in the plant parameters as well as in the trajectory which is to be tracked (Isidori et al., 2003b). Our approach is similar to that of (Isidori, Marconi, and Serrani, 2003a), where a model-based design is considered. We address the design of an internal-model-based controller for STA capable of rejecting the most effective disturbances which are ship's roll, pitch, and yaw motions detected in the base of the antenna (Tanaka and Nishifuji, 1994) (Tanaka and Nishifuji, 1995) (Johansen et al., 2003). In this work, we assume that the heave, surge, and sway forces to the ship are negligible during the operation of the antenna (Tseng and Teo, 1997) (Inmarsat, 2003) (Fossen, 2002). Verification results show that the proposed model's behaviour closely simulate the real system even under the mentioned assumption (Soltani, 2006).

The paper is organized as follows: in Section 4.2 the dynamical model of the operating STA, in both aspects of dynamics and disturbances acting on it, is developed. Section 4.3 renders the formulation of the problem and NIMC design procedure and proves the validity of the suggested controller. Section 4.4 presents the simulation results as well as practical tests; eventually, conclusions and suggestions are brought in the last section of the paper.

4.2   STA Modeling

The model consists of three parts; a model for satellite tracking, a model for antenna dynamics, and a model of ship motion, c.f., (Soltani, 2006).

4.2.1 Frame Assignment

To describe the relationship between satellite position, antenna element direction and ship disturbances, a common fixed inertial coordinate system is needed. The rotation of the ship with respect to the satellite will be defined by earth coordinates. To describe the orientation of the antenna element direction, two other frames are defined as Joint frame and Plate frame.

- Body-fixed frame F^b is used to show the effect of the wind and wave disturbances on the ship. The origin of this frame is placed in the point where the base of the antenna is located. The vector x^b is the heading vector of the ship, y^b is the right hand vector of the ship, and z^b is pointing downward the ship perpendicular to x^b and y^b. Figure 4.1 shows the frame F^b on the ship.

- Earth frame F^e describes the orientation of an Earth fixed frame to the Body-fixed frame F^b. The origin of this frame is placed on the origin of F^b. As long as the ship does not move, it is assumed that F^e does not move with respect to F^b. Furthermore, x^e is pointing toward the satellite and y^e and z^e are vectors perpendicular to x^e, where ye lays in the horizontal plane. They can also be aligned to y^b and z^b with two rotations of F^e around y^b and z^b axes. More details are shown in figure 4.1.

- Joint frame F^j describes the movement of the azimuth motor with respect to the frame F^b. The origin of F^j is placed on the antenna body. The vector z^j is always aligned with z^b. The vectors x^j and y^j are initially aligned with the vectors x^b and y^b respectively, but they change due to the rotation of the azimuth motor which rotate on z^b axis. Figure 4.2 illustrates this frame on the antenna body.

- Plate frame F^p describes the movement of the elevation motor with respect to F^j. The origin of F^p is placed on the antenna plate center. The vector y^p is always aligned with the vector y^j and F^p is rotating around y^p due to the rotation of elevation motor. The axis x^p is perpendicular to the plate of the antenna and y^p. Finally, z^p is perpendicular to both x^p and y^p as shown in figure 4.2.

4.2.2 Rotation Between Frames

Now, we should understand how these frames move with respect to each other. First of all, we cancel all translative motions and distances between the origins of frames and only analyze the rotations between the frames. It's due to the fact that we assume the movement of the ship is negligible with respect to the distance between the satellite and
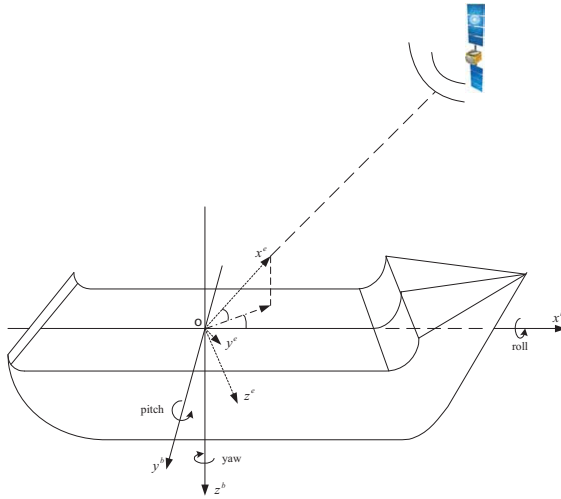
Figure 4.1: Body-fixed frame F^b and Earth frame F^e.
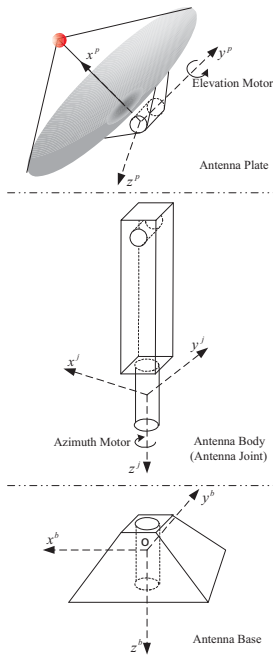
Figure 4.2: Joint frame F^j and Plate frame F^p.

the ship. Therefore, we begin from Earth frame F^e which is fixed on earth and then link other frames to each other one after another.

- Rotation between frame F^b and frame F^e is originated from the waves and winds effecting the dynamics of ship motion. The rotation matrix R_{eb} describes this rotation and the entries of the matrix are functions of time. This rotation matrix has the property of

$$\dot{R}_{eb} = R_{eb} Skew(\omega_{eb}^b), \tag{4.1}$$

where the entries of ω_{eb}^b are the coordinates of the angular velocity vector of F^b relative to F^e, resolved in F^b (Wertz, 1978).

$$\omega_{eb}^b = \begin{bmatrix} p & q & r \end{bmatrix}^T, \tag{4.2}$$

where p, q, and r are pitch, roll, and yaw angular velocities respectively. Also, the function $Skew$ is defined as

$$Skew(\omega_{eb}^b) = \begin{bmatrix} 0 & -r & q \\ r & 0 & -p \\ -q & p & 0 \end{bmatrix}. \tag{4.3}$$

These disturbances are illustrated in figure 4.1.

- The only change between F^b and F^j is caused by the azimuth motor which is installed on the base. This rotation can be computed directly from the rotation angle of the motor. Consider θ_{bj}^j as the rotation angle of the azimuth motor as shown in figure 4.2. We can represent this rotation matrix by

$$R_{bj} = \begin{bmatrix} cos(\theta_{bj}^j) & -sin(\theta_{bj}^j) & 0 \\ sin(\theta_{bj}^j) & cos(\theta_{bj}^j) & 0 \\ 0 & 0 & 1 \end{bmatrix}. \tag{4.4}$$

- The rotation between F^j and F^p is caused by the elevation motor which is installed on the plate around y^j axis. This rotation can be computed directly from the rotation angle of the elevation motor as illustrated in figure 4.2. Consider θ_{jp}^p as the rotation angle of the rotor of elevation motor. We can represent the rotation matrix as

$$R_{jp} = \begin{bmatrix} cos(\theta_{jp}^p) & 0 & -sin(\theta_{jp}^p) \\ 0 & 1 & 0 \\ sin(\theta_{jp}^p) & 0 & cos(\theta_{jp}^p) \end{bmatrix}. \tag{4.5}$$

4.2.3   Dynamics of Motors

The dynamics of the motors and kinematics of the antenna has been analyzed in (Soltani, 2006). Due to the inherent characteristics of the employed motors, which are step-motors, their dynamics are represented by the simplified equations

$$\dot{\theta}_{bj}^{j} = u_{bj}^{j} \tag{4.6}$$

and

$$\dot{\theta}_{jp}^{p} = u_{jp}^{p}, \tag{4.7}$$

where u_{bj}^{j} and u_{jp}^{p} are the inputs of the azimuth and elevation motors respectively.

4.2.4   Disturbances and Ship Dynamics

When looking into the issue of ship motions at sea, at least three contributions to the movement should be considered: The wind acting on the ship, the waves generated by the wind, and the currents at sea. Many works have been done on describing these stochastic processes, and many conclusions have been made in (Fossen, 2002). However, the resulting motion of the ship itself, caused by the wind, waves, and current, is far less documented for generic purposes. The reason for this is the fact that different ship structures, sizes and loads affect the dynamic behavior of the ship significantly.

The main contributor to the ship motions is the wave acting on the body. To simplify the model, it is assumed that the disturbances on the ship are affected only by waves. However, the disturbance specifications, provided by (Inmarsat, 2003), will still be met.

The roll and pitch disturbances affecting the dynamics of the ship are known to be locally well modeled by two sinusoidal waves (See also (Johansen et al., 2003), (Fossen, 2002), and (Tanaka and Nishifuji, 1994)). One of the sinusoidal waves has a short periodic length of about 6 sec and the other, long one, in the range of 6 to 10 sec. Moreover, the yaw disturbance can also be modeled as a small sinusoid wave. Thus, they can be modeled as

$$\dot{w} = Sw, \tag{4.8}$$

where $w = \begin{bmatrix} p, \acute{p}, q, \acute{q}, r, \acute{r} \end{bmatrix}^{T}$,

$$S = diag(S_i), i = 1, 2, 3. \tag{4.9}$$

and

$$S_i = \begin{bmatrix} 0 & \Omega_i \\ -\Omega_i & 0 \end{bmatrix}, \tag{4.10}$$
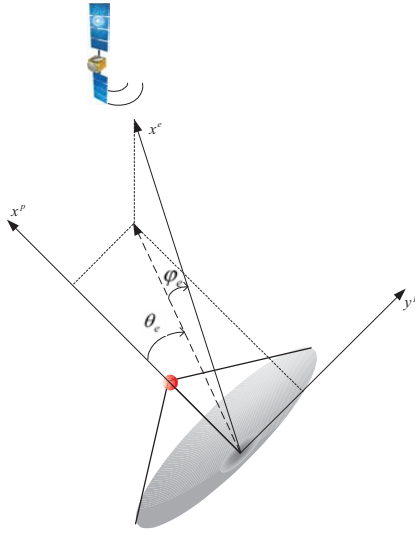
Figure 4.3: Error angles.

where Ω_1, Ω_2, and Ω_3 are the frequencies of roll, pitch, and yaw disturbances. The initial value of w determines the phase of sinusoids. This system is called the *exosystem*. Finally, disturbances make rotation between F^e and F^b as explained by (4.1).

4.3 NIMC Design

In order to define the control problem of under-actuated ship mounted STA, we should know about the operation of beam sensor and its measurement. Beam sensor measures the error angles between satellite signal directional vector x^e and the antenna plate vector x^p.

The sensor outputs are two angles φ_e and θ_e. θ_e is the angle between x^p and the projection of x^e on $x^p \times y^p$ surface of F^p. Also, φ_e is the angle between x^e and the projection of x^e on $x^p \times y^p$ surface of F^p as shown in figure 4.3.

It's clear that we can obtain the unit vector of x^e in F^p by

$$v^p = \left[\begin{array}{c} cos(\varphi_e)cos(\theta_e) \\ sin(\varphi_e)cos(\theta_e) \\ sin(\theta_e) \end{array} \right] . \tag{4.11}$$

4.3.1   Problem Formulation

The elements of the vector v^p are functions of time because of the motions of the ship and antenna motors. Obviously, we want the angles θ_e and φ_e to be zero, since we want the antenna to track the satellite. This is equivalent to

$$v^p = \begin{bmatrix} 1 & 0 & 0 \end{bmatrix}^T. \tag{4.12}$$

On the other hand, we can translate the vector x^e in F^p by

$$v^p = R_{pe}x^e, \tag{4.13}$$

where R_{pe} is the rotation matrix from F^e to F^p due to inputs and disturbances given by

$$R_{pe} = R_{pj}R_{jb}R_{be}, \tag{4.14}$$

where the orthogonal rotation matrices have the property of $R_{pj} = R_{jp}^T$, $R_{jb} = R_{bj}^T$, and $R_{be} = R_{eb}^T$. Finally, error angles can be calculated by

$$\varphi_e = tan^{-1}(\frac{\begin{pmatrix} 0 & 1 & 0 \end{pmatrix} v^p}{\begin{pmatrix} 1 & 0 & 0 \end{pmatrix} v^p}) \tag{4.15}$$

and

$$\theta_e = sin^{-1}(\begin{pmatrix} 0 & 0 & 1 \end{pmatrix} v^p). \tag{4.16}$$

Using (4.6), (4.7), (4.12), (4.13), (4.15), and (4.16) the system is formulated as follows

$$\begin{aligned} \dot{x} &= f(x, u, w) \\ e &= h(x, w) \\ y &= k(x, w) \\ \dot{w} &= s(w), \end{aligned} \tag{4.17}$$

where

$$\begin{aligned} x = (\theta_{bj}^j, \theta_{jp}^p, R_{be11}, R_{be21}, R_{be31}, R_{be12}, \\ R_{be22}, R_{be32}, R_{be13}, R_{be23}, R_{be33})^T \end{aligned} \tag{4.18}$$

is the state vector of the system,

$$u = (u_{bj}^j, u_{jp}^p)^T \tag{4.19}$$

is the control input vector,

$$w = (p, \acute{p}, q, \acute{q}, r, \acute{r})^T \tag{4.20}$$

is the disturbance vector,

$$e = (\varphi_e, \theta_e)^T \tag{4.21}$$

is the tracking error output, and

$$
\begin{aligned}
y = (\theta_{bj}^j, \theta_{jp}^p, R_{be11}, R_{be21}, R_{be31}, R_{be12}, \\
R_{be22}, R_{be32}, R_{be13}, R_{be23}, R_{be33})^T
\end{aligned}
\tag{4.22}
$$

is the measured output vector, where the elements of rotation matrix R_{be} are provided by a sensor fusion system (see also Appendix C) (Soltani, 2006). Furthermore, the nonlinear smooth functions f, h, k are expressed in the following.

$$f(x, u, w) = Ax + Bu, \tag{4.23}$$

where

$$
A = \begin{pmatrix}
\acute{A} & 0 & 0 & 0 \\
0 & Skew(\omega_{eb}^b) & 0 & 0 \\
0 & 0 & Skew(\omega_{eb}^b) & 0 \\
0 & 0 & 0 & Skew(\omega_{eb}^b)
\end{pmatrix}
$$

and

$$
B = \begin{pmatrix}
1 & 0 & 0 & \cdots & 0 \\
0 & 1 & 0 & \cdots & 0
\end{pmatrix}_{2 \times 11}^T,
$$

where $\acute{A} = \begin{pmatrix} 0 & 0 \\ 0 & 0 \end{pmatrix}$,
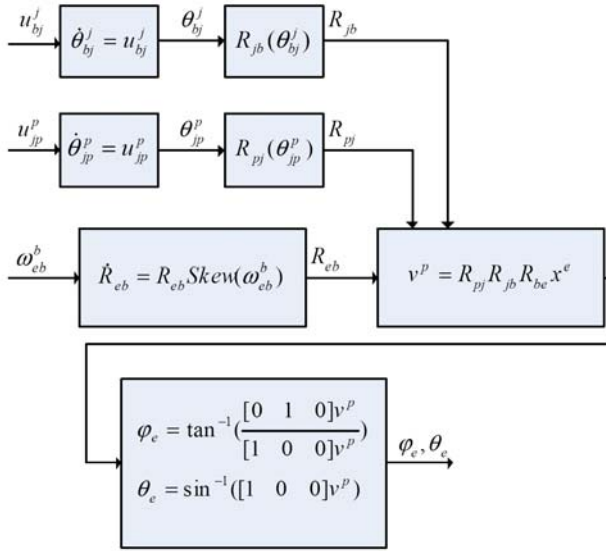
Figure 4.4: Block diagram of the open loop system with the effect of disturbances.

$$h(x) =$$

$$\begin{pmatrix} tan^{-1}(\dfrac{-R_{be11}sin(\theta^j_{bj})cos(\theta^p_{jp})+R_{be21}cos(\theta^j_{bj})cos(\theta^p_{jp})}{R_{be11}cos(\theta^j_{bj})cos(\theta^p_{jp})+R_{be21}sin(\theta^j_{bj})cos(\theta^p_{jp})+R_{be31}sin(\theta^p_{jp})}) \\ \\ sin^{-1}(\dfrac{-R_{be11}cos(\theta^j_{bj})sin(\theta^p_{jp})-R_{be21}sin(\theta^j_{bj})sin(\theta^p_{jp})+R_{be31}cos(\theta^p_{jp})}{1}) \end{pmatrix} \quad (4.24)$$

and

$$k(x) = x, \qquad (4.25)$$

where in this system h and k are not functions of w. Moreover, the last one of (4.17) expresses the exosystem, which is the linear autonomous system (4.8) and generates the disturbance w affecting the system.

For such system, suppose the controller has a form of

$$\begin{aligned} \dot{\xi} &= \phi(\xi, y) \\ u &= \theta(\xi, y), \end{aligned} \qquad (4.26)$$

in which $\phi(\xi, y)$ and $\theta(\xi, y)$ are smooth functions, satisfying $\phi(0, 0) = 0$ and $\theta(0, 0) = 0$. Then, the generalized tracking problem is as follows.

Given system (4.17) with exosystem (4.8), and two sets $\mathcal{X} \subset \mathbb{R}^n$ [1] and $\mathcal{W} \subset \mathbb{R}^r$ [2], find, a controller of the form (4.26) and a set $\mathcal{E} \subset \mathbb{R}^v$ [3], such that, in the closed-loop system:

1. the trajectory $(x(t), \xi(t), w(t))$ is bounded,

2. $lim_{t\to\infty} e(t) = 0$,

for every initial condition $(x(0), \xi(0), w(0)) \in \mathcal{X} \times \mathcal{E} \times \mathcal{W}$ (See (Isidori et al., 2003b).).

4.3.2   NIMC Design

The start point in NIMC design is to understand the basic idea of NIMC. Let $\pi : \mathbb{R}^r \to \mathbb{R}^n$ and $\sigma : \mathbb{R}^r \to \mathbb{R}^v$ be two smooth mappings, and suppose that the smooth manifold

$$\mathcal{M}_0 = \{(x, \xi, w) : x = \pi(w), \xi = \sigma(w)\}$$

is invariant for the forced closed-loop system (4.17) with (4.26). $\mathcal{M}_0$ being invariant for the closed-loop system means that $\pi(w)$ and $\sigma(w)$ are solutions of the pair of differential equations

$$\begin{aligned}
\frac{\partial \pi}{\partial w} s(w) &= f(\pi(w), \theta(\sigma(w), k(\pi(w), w)), w) \\
\frac{\partial \sigma}{\partial w} s(w) &= \phi(\sigma(w), k(\pi(w), w)).
\end{aligned} \tag{4.27}$$

Now assume that in the closed-loop system all trajectories with initial conditions in a set $\mathcal{X} \times \mathcal{E} \times \mathcal{W}$ are bounded and attracted by the manifold $\mathcal{M}_0$ and that the regulated output e is zero at each point of $\mathcal{M}_0$, i.e., that

$$0 = h(\pi(w), w). \tag{4.28}$$

Then, we can claim that if there are mappings $\pi(w)$ and $\sigma(w)$ such that closed-loop system (4.17) with (4.26) and (4.28) hold and, in forced closed-loop system (closed-loop system combined with exosystem), all trajectories with initial conditions in a set

---

[1] n is the dimension of states vector x

[2] r is the dimension of vector ζ

[3] v is the dimension of disturbance vector w

$\mathcal{X} \times \mathcal{E} \times \mathcal{W}$ are bounded and attracted by the manifold $\mathcal{M}_0$, the controller (4.26) solves the generalized tracking problem (Isidori et al., 2003b).

Moreover, the conditions (4.27) and (4.28) hold if and only if there exist a triplet of mappings $\pi(w), \sigma(w), c(w)$ such that

$$\frac{\partial \pi}{\partial w} s(w) = f(\pi(w), c(w), w)$$
$$0 = h(\phi(w), w)$$

(4.29)

and

$$\frac{\partial \sigma}{\partial w} s(w) = \phi(\sigma(w), k(\pi(w), w))$$
$$c(w) = \theta(\sigma(w), k(\pi(w), w)).$$

(4.30)

Finally, we accept following proposition as it has been proved in (Isidori et al., 2003b).

Proposition 1 *Suppose a controller of the form (4.26) is such that conditions (4.29) and (4.30) hold, for some triplet of mappings $\pi(w), \sigma(w), c(w)$. Suppose that all trajectories of the forces closed loop system, with initial conditions in a set $\mathcal{X} \times \mathcal{E} \times \mathcal{W}$, are bounded and attracted by the manifold $\mathcal{M}_0$. Then, the controller solves the generalized tracking problem.*

Going through design procedure, we depart from the fact that the dynamic of the controller is considered to be linear but the control output is considered to be nonlinear. Thus, the control system can be of the following form

$$\dot{\xi} = F\xi + Gy$$
$$u = H\xi + Ky + \theta(y).$$

(4.31)

The controller which satisfies the generalized tracking problem should satisfy (4.29) and (4.30). It is helpful to know that

$$f(x, u, w) = \begin{pmatrix} f_1(x, u) \\ f_2(x, w) \end{pmatrix},$$

(4.32)

where $f_1(x, u)$ is a linear function of x and u. Starting from (4.29), f_2 satisfies the first equation, since,

$$f_2(\pi(w), 0, w)$$

$$= \frac{\partial \pi}{\partial w} S w$$
$$= \frac{\partial \pi}{\partial t} \frac{\partial t}{\partial w} S w \quad (4.33)$$
$$= \frac{\partial \pi}{\partial t},$$

which is obvious due to (4.1). Furthermore, f_1 should satisfy

$$\dot{\hat{\pi}} = f_1(\acute{\pi}(w), c(w), w) = f_1(c(w)) = \acute{B}c(w), \quad (4.34)$$

where $\acute{\pi} = (\pi_1 \ \pi_2)^T$ (π_i, i= 1, 2,...11 are the elements of the vector π) and $\acute{B} = I_{2 \times 2}$. The second one of (4.29) gives a view of the nonlinear control low

$$tan(\pi_1) = \frac{\pi_6}{\pi_3}$$
$$tan(\pi_2)sin(\pi_1) = \frac{\pi_6 \pi_9}{(\pi_6)^2 - (\pi_3)^2}. \quad (4.35)$$

Equations (4.30) with the aid of (4.34) is reformulated to

$$\dot{\hat{\pi}} = H\sigma + \acute{\pi} + \theta(\pi)$$
$$\dot{\sigma} = F\sigma + G\pi, \quad (4.36)$$

where $\sigma = (\sigma_1 \ \sigma_2)^T$.

Defining $\theta(\pi)$ as $\theta(\pi) = (-tan^{-1}(\frac{\pi_6}{\pi_3}) \quad - tan^{-1}(\frac{\pi_6 \pi_9}{((\pi_6)^2 - (\pi_3)^2)sin(\pi_1)}))^T$, (4.36) will be reduced to

$$\dot{\hat{\pi}} = H\sigma$$
$$\dot{\sigma} = F\sigma + G\pi, \quad (4.37)$$

and the stability of σ and $\acute{\pi}$ is depending on having all real parts of the eigenvalues of $\begin{pmatrix} H & 0 \\ F & G \end{pmatrix}$ as negative.
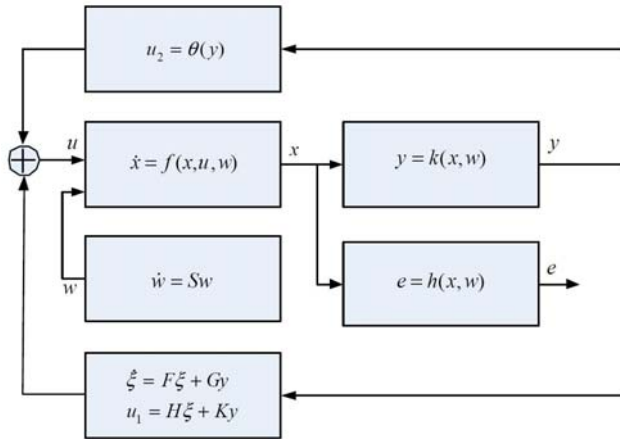
Figure 4.5: Block diagram of the closed-loop system with NIMC.

The block diagram of such NIMC is illustrated in figure 4.5.

4.4 Simulation and Practical Test

The effectiveness of the proposed methodology by means of both computer simulation and practical results has been demonstrated. Various simulations were done to confirm the algorithms.

4.4.1 Simulation Results

Figure 4.6 shows the phase portrait of the antenna tracking output error angles φ_e and θ_e with employed NIMC subject to sea motions. The objective of this simulation is to show that both errors go to zero from randomly chosen initial conditions. Sinusoidal waves are used to simulate the pitch and roll disturbances due to the wave effect standards according to (Inmarsat, 2003).

4.4.2 Practical Test Results

The idea of having a real test of STA resulted in taking a practical simulation of the antenna operation on a virtual ship. Ship simulator, figure 4.7, can simulate the move-
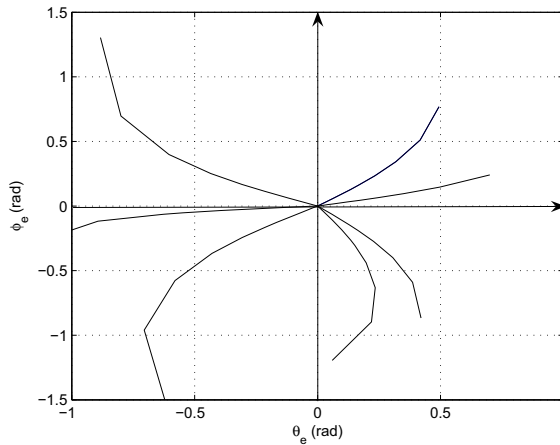
Figure 4.6: Phase portrait of output errors φ_e and θ_e.

ment of the ship in different conditions. This system provides a reliable simulation environment when heave forces are negligible.

In the verification tests, the maximum amplitude and frequency of the pitch, roll, and yaw disturbances, according to (Inmarsat, 2003), has been set to the ship simulator.
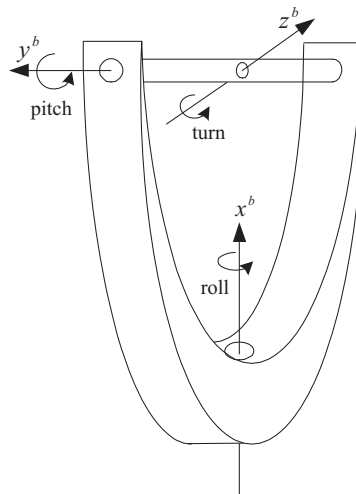
Figure 4.7: A conceptual illustration of the used ship simulator with its rotational axis.
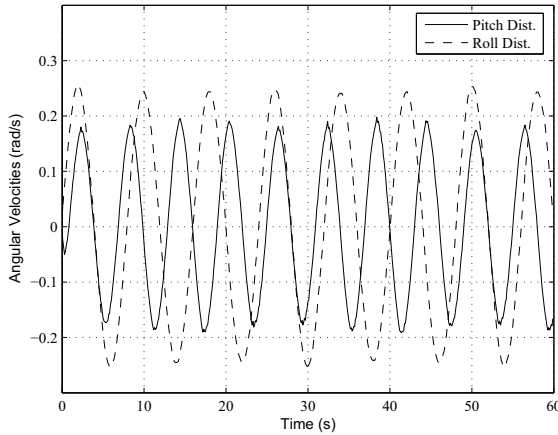
Figure 4.8: Measured disturbances from rate gyros.

Figure 4.8 shows the low-pas filtered output of the roll and pitch gyros. The azimuth and elevation angles are shown in figure 4.9. The motors move very fast (less than 1 second) at the beginning and bring the angles to the reference trajectory. Then they follow the trajectory which has been made by internal model. The low-pass filtered error angles of beam sensor are revealed in figure 4.10.
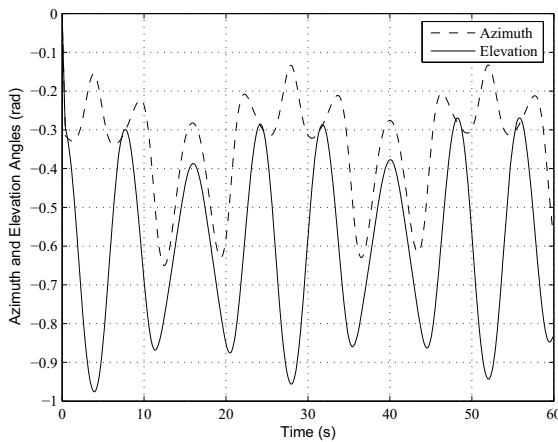
Figure 4.9: Azimuth motor angle θ_{bj}^{j} and elevation motor angle θ_{jp}^{p}.
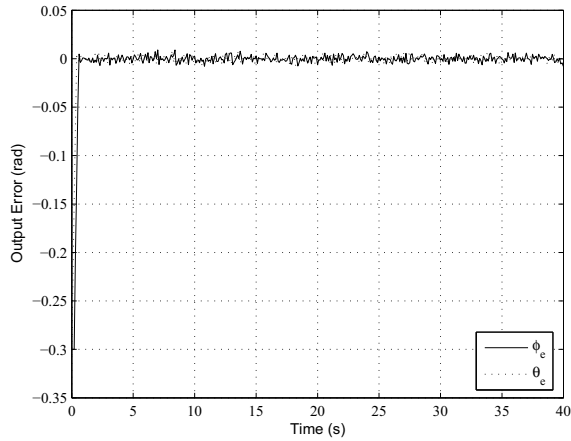
Figure 4.10: Output Errors φ_e and θ_e.

Finally, the absolute error value θ_{abs}, which is calculated by

$$\theta_{abs} = \sqrt{\theta_e^2 + \varphi_e^2} \qquad (4.38)$$

and determines the approximate error angle radius from zero error, is illustrated in figure 4.11.
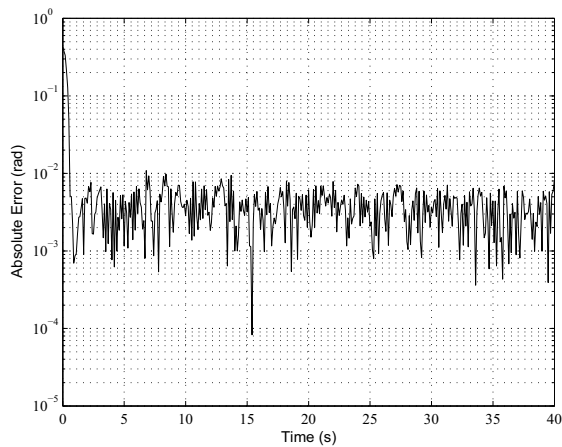
Figure 4.11: Absolute error value θ_{abs}.

4.5   Conclusions

Dynamic and kinematic modeling of a ship-mounted STA is described. The tracking problem of the antenna is formulated and an internal model controller, which guarantees asymptotical convergence of the tracking error to zero, is then proposed. Furthermore, the designed controller has been simulated regarding with the effect of disturbances coming to the ship due to the waves and wind according to specifications in (Inmarsat, 2003). Finally, the implemented control algorithm has been checked on a ship simulator test device and it has been concluded that NIMC has fulfilled the desired control specifications.

Chapter 5

Fault Tolerant Control of Ship-mounted Satellite Tracking Antenna

*   **Abstract-** Motorized antenna is a key element in overseas satellite telecommunication. The control system directs the on-board antenna toward a chosen satellite while the high sea waves disturb the antenna. Certain faults (communication system malfunction or signal blocking) cause interruption in the communication connection resulting in loss of the tracking functionality, and instability of the antenna. In this article, a fault tolerant control system is proposed for the satellite tracking antenna (STA). The suggested reconfigurable control system- which is supervised by a robust fault diagnosis system- uses two control strategies for the antenna system to keep the tracking functionality when a fault happens. The fault diagnosis system performs an optimized estimation of the fault for a class of nonlinear systems acting under external disturbances. Finally, the applicability of the method is verified through implementation on an antenna system.*

5.1   Introduction

The ability to maintain communication over large distances has always been an important issue. Communication can be maintained through satellite as the constellation of the communication satellites ensures that it is always possible to make contact with a satellite, regardless of the actual position on Earth. The important factor in this case is to track the satellite and sustain contact with it. The challenge arises when the antenna

is used in a non-stationary case, e.g. marine communication. Once the ship-mounted antenna has tracked a communication satellite, movements of the ship, partly generated by waves, will force the antenna to point away from the satellite and thereby break the communication (Soltani et al., 2007). An advanced control algorithm is developed for this antenna that compensates for these disturbances. Based on the received communication signals the antenna system determines the deviation from the antenna's line of sight and provides these to the control system.

The problem arises when the signal is blocked due to change in atmosphere, a hurdle between the antenna and satellite, or a satellite shut down. This results in faulty data to the control loop and hence leading to the loss of tracking functionality and/or instability. In addition, when the fault disappears, the antenna has to re-initialize and search the sky for the satellite and this is a time consuming task after the interruption. A fault tolerant control (FTC) system which is a combination of fault diagnosis and accommodation system is proposed in this article. This system detects the fault and reconfigure the control system so that it is still able to direct the antenna toward the satellite during the fault period.

Fault diagnosis has since the 1980s been an active research topic. Depending on the models that have been used to describe the system, stochastic or deterministic (linear/nonlinear), many different approaches have been proposed (Jørgensen et al., 1995), (Blanke et al., 2006), and (Isermann, 2006). One of the important problems that has attracted the most attention in this research community is the robustness issue that arises due to the fact that there is some mismatch (however small) between the derived model and the real system dynamics. An early paper, which suggested combining methods for diagnosis and control was (Nett et al., 1988). (Bokor and Keviczky, 1994) suggested to use $\mathcal{H}_\infty$ optimization to design fault diagnosis filters. A method that used dedicated and specialized $\mathcal{H}_\infty$ - based filter structures was presented in (Mangoubi et al., 1995).

A particular focus of this paper is on designing a FDI system for the satellite tracking antenna (STA) that is robust to the uncertainties and disturbances in the system. Especially, the emphasis is on employing methods for fault diagnosis which have been inspired by and derived from the area of robust control theory, or in wider generality of optimization based control synthesis methods. A fault diagnosis approach for systems with parametric faults has been used. Such an approach was presented in (Stoustrup and Niemann, 1999). However, to the best of our knowledge, no application to the nonlinear case has been reported. In this article, the proposed method for the nonlinear system's fault detection in (Stoustrup and Niemann, 2002) has been studied in details and extra notes has been added such as the problem of distinguishing faults from disturbances. Moreover, when the FDI system acknowledges the presence of fault, the control system has to reconfigure to the the second control strategy that is not affected by the fault.

A nonlinear internal model control (NIMC) is suggested to be used for the faulty case

scenario. NIMC is able to simultaneously handle uncertainties in the plant parameters as well as in the trajectory which is to be tracked (Isidori et al., 2003b). Our approach is similar to that of (Isidori et al., 2003a), where a model-based design is considered. We address the design of an internal-model-based controller, capable of rejecting the dominant disturbances which are ship's roll, pitch, and yaw motions detected in the base of the antenna (Tanaka and Nishifuji, 1994) (Tanaka and Nishifuji, 1995) (Johansen et al., 2003).

A dynamical model of STA has been used to design the FDI system. Verification results showed that the proposed dynamic model closely simulates the real system (Soltani, 2006). However, to illustrate the applicability of the presented method, the FTC system is verified against a real antenna system with successful results.

The paper is organized as follows: in Section 5.2, the problem statement is addressed. The dynamical model of the operating STA, the beam control strategy, and the fault nature is presented in Section 5.3. Section 5.4 renders the proposed FDI method and the FDI design procedure. In Section 5.5 the FTC scenario together with NIMC design for the system are described. Section 5.6 presents the results in practical tests and especially analyzes the FDI design; eventually, conclusions are brought in the last section of the paper.

5.2   Problem Statement

Given a communication antenna platform, develop a fault-tolerant control system that reliably detects a class of commonly occurred faults and accommodates for these by means of control reconfiguration.
The solution to the stated problem is achieved by addressing the following three specific objectives:

- Develop a comprehensive (nonlinear) model that adequately describes the dynamic/kinematic behavior of the antenna system .

- Develop/employ fault diagnosis algorithms that detect the faults while being robust toward system uncertainties and external disturbances.

- Develop an alternative control strategy for the nonlinear system suitable for reconfiguration purposes.

The mentioned objectives are subsequently addressed in the corresponding sections.
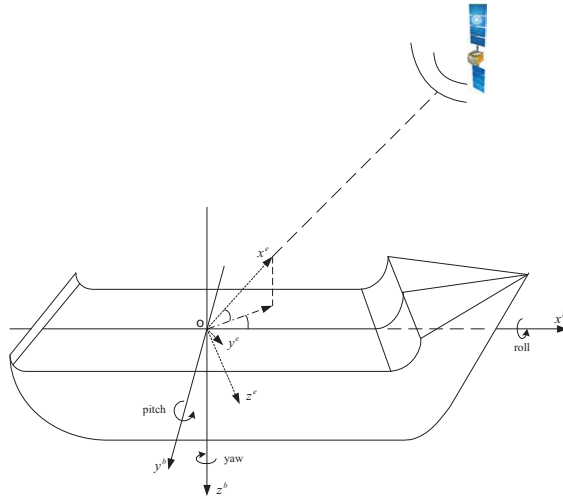
Figure 5.1: Body-fixed frame F^b and Earth frame F^e.

5.3   Satellite Tracking Antenna (STA) System

The prerequisite for designing the model-based fault diagnosis and control algorithm is a comprehensive model for the system's behavior. In the first part of this section the model for the STA is derived. In the second part we briefly describe the original control strategy for the STA system. In addition the effect of interesting faults was discussed.

5.3.1   Modeling of STA

To describe the relationship between satellite position, antenna element direction and ship disturbances, a common fixed inertial coordinate system is needed. Earth frame F^e describes the position of the satellite in an earth-fixed frame with the origin on the ship body. Since, the chosen satellite is geo-stationary, its position is fixed in F^e. We use the fact that the translative movements of the origin of F^e (ship) is negligible when comparing with the distance from the ship to the satellite. Furthermore, x^e is pointing toward the satellite and y^e and z^e are vectors perpendicular to x^e where ye lays on the horizontal plane. More details are shown in figure 5.1. Body-fixed frame F^b describes the orientation of the ship body to the earth fixed frame. The origin of this frame is placed in the point where the base of the antenna is located. The vector x^b is the heading vector of the ship, y^b is the right side vector of the ship, and z^b is pointing downward the ship. Figure 5.1 shows the frame F^b on the ship. y^e and z^e can also be aligned to y^b and

z^b with two rotations of F^e around y^b and z^b axes. The rotation between frame F^b and frame F^e is originated from the waves and winds affecting the dynamics of ship motion. The rotation matrix R_{eb} describes this rotation. This rotation matrix has the property of

$$R_{eb} = R_{be}^{-1} = R_{be}^T, \tag{5.1}$$

and

$$\dot{R}_{eb} = R_{eb}Skew(\omega_{eb}^b), \tag{5.2}$$

where the entries of ω_{eb}^b are the coordinates of the angular velocity vector of F^b relative to F^e, resolved in F^b (Wertz, 1978) and

$$\omega_{eb}^b = \begin{bmatrix} p & q & r \end{bmatrix}^T, \tag{5.3}$$

where p, q, and r are roll, pitch, and yaw angular velocities respectively- illustrated in figure 5.1. The function $Skew$ is defined as

$$Skew(\omega_{eb}^b) = \begin{bmatrix} 0 & -r & q \\ r & 0 & -p \\ -q & p & 0 \end{bmatrix}. \tag{5.4}$$

When analyzing the ship motions at sea, at least three contributions to the movement should be considered: The wind acting on the ship, the waves generated by the wind, and the currents at sea. In several works these contributions have been modeled by stochastic processes (Fossen, 2002). However, the resulting motion of the ship itself, caused by the wind, waves, and current, is far less documented for generic purposes. The reason is that differences in ship structures, sizes and loads affect the dynamic behavior of the ships significantly. The main contributor to the ship motions is the wave acting on the body. To simplify the model, it is assumed that the disturbances on the ship are affected only by waves. However, the disturbance specifications, provided by (Inmarsat, 2003), will still be met. The roll and pitch disturbances affecting the dynamics of the ship are known to be locally well modeled by two sinusoidal waves (See also (Johansen et al., 2003), (Fossen, 2002), and (Tanaka and Nishifuji, 1994)). One of the sinusoidal waves has a short periodic length of about 6 sec and the other is in the range of 8 to 10 sec. Moreover, the yaw disturbance can also be modeled as a small sinusoid wave. Thus, they can be modeled as

$$\dot{w} = Sw, \tag{5.5}$$

where $w = \begin{bmatrix} p & \dot{p} & q & \dot{q} & r & \dot{r} \end{bmatrix}^T$,

$$S = diag(S_i), i = 1, 2, 3. \tag{5.6}$$

and

$$S_i = \begin{bmatrix} 0 & \Omega_i \\ -\Omega_i & 0 \end{bmatrix}, \tag{5.7}$$

where Ω_1, Ω_2, and Ω_3 are the frequencies of roll, pitch, and yaw disturbances. The initial value of w determines the phase of sinusoids. This system is called the *exosystem*. Finally, disturbances make rotation between F^e and F^b as explained by (5.2), generated by (5.5), and mapped by

$$\omega_{eb}^b = \begin{bmatrix} 1 & 0 & 0 & 0 & 0 & 0 \\ 0 & 0 & 1 & 0 & 0 & 0 \\ 0 & 0 & 0 & 0 & 1 & 0 \end{bmatrix} w. \tag{5.8}$$

To describe the orientation of the antenna element direction, two frames are defined as Joint frame and Plate frame. Joint frame F^j describes the movement of the azimuth motor with respect to the frame F^b. The origin of F^j is placed on the antenna joint geometrical center. The vector z^j is always aligned with z^b. The vectors x^j and y^j are initially aligned with the vectors x^b and y^b respectively, but they change due to the rotation of the azimuth motor which rotates around z^b axis. Figure 5.2 illustrates this frame on the antenna body. Plate frame F^p describes the movement of the elevation motor with respect to F^j. The origin of F^p is placed on the center of the antenna plate. The vector y^p is always aligned with the vector y^j and F^p is rotating around y^p due to the rotation of elevation motor. The axis x^p is perpendicular to the plate of the antenna (which is also called as the antenna line of sight (LOS)) and y^p. Finally, z^p is perpendicular to both x^p and y^p as shown in figure 5.2. The only change between F^b and F^j is caused by the azimuth motor which is installed on the base. This rotation can be measured directly from the rotation angle of the motor. Consider θ_{bj}^j as the rotation angle of the azimuth motor as shown in figure 5.2. We can represent this rotation matrix by

$$R_{bj} = \begin{bmatrix} cos(\theta_{bj}^j) & -sin(\theta_{bj}^j) & 0 \\ sin(\theta_{bj}^j) & cos(\theta_{bj}^j) & 0 \\ 0 & 0 & 1 \end{bmatrix}. \tag{5.9}$$

In the same way, the rotation between F^j and F^p is caused by the elevation motor which is installed on the plate around y^p axis. Consider θ_{jp}^p as the rotation angle of the rotor of elevation motor. We can represent the rotation matrix as

$$R_{jp} = \begin{bmatrix} cos(\theta_{jp}^p) & 0 & -sin(\theta_{jp}^p) \\ 0 & 1 & 0 \\ sin(\theta_{jp}^p) & 0 & cos(\theta_{jp}^p) \end{bmatrix}. \tag{5.10}$$

The dynamics of the motors and kinematics of the antenna has been analyzed in (Soltani, 2006). Due to the inherent characteristics of the employed motors, here step-motors, their dynamics are simplified as

$$\dot{\theta}_{bj}^j = u_{bj}^j \tag{5.11}$$

and

$$\dot{\theta}_{jp}^p = u_{jp}^p, \tag{5.12}$$

where u_{bj}^j and u_{jp}^p are the inputs of the azimuth and elevation motors respectively.

In order to define the control problem of the ship-mounted STA, the tracking error should be formulated. Beam sensor measures the error angles between the satellite signal directional vector x^e and the antenna line of sight x^p. The sensor outputs are two angles ϕ_e and θ_e. θ_e is the angle between x^p and the projection of x^e on $x^p \times y^p$ surface of F^p. Also, ϕ_e is the angle between x^e and the projection of x^e on $x^p \times y^p$ surface of
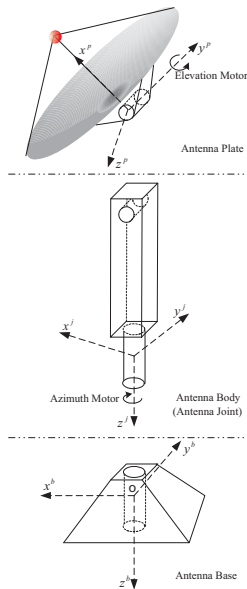
Figure 5.2: Joint frame F^j and Plate frame F^p.

F^p as shown in figure 5.3. Clearly, we can obtain the unit vector x^e in F^p by

$$(x^e)^p = v^p = \begin{bmatrix} cos(\phi_e)cos(\theta_e) \\ sin(\phi_e)cos(\theta_e) \\ sin(\theta_e) \end{bmatrix}. \tag{5.13}$$

Thus, error angles can be calculated by

$$\phi_e = tan^{-1}(\frac{\begin{pmatrix} 0 & 1 & 0 \end{pmatrix} v^p}{\begin{pmatrix} 1 & 0 & 0 \end{pmatrix} v^p}) \tag{5.14}$$

and

$$\theta_e = sin^{-1}(\begin{pmatrix} 0 & 0 & 1 \end{pmatrix} v^p). \tag{5.15}$$

On the other hand, we can obtain v^p from the vector x^e in F^e by

$$v^p = R_{pe}(x^e)^e = R_{pe} \begin{bmatrix} 1 & 0 & 0 \end{bmatrix}^T, \tag{5.16}$$

where R_{pe} is the rotation matrix from F^e to F^p due to joints and ship orientation given by
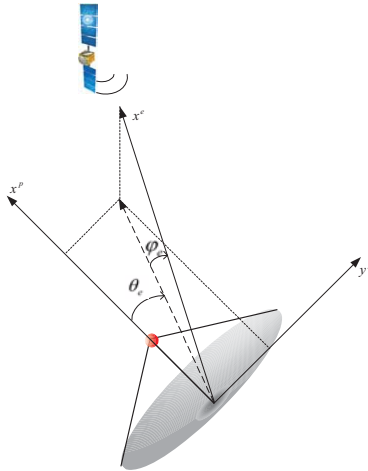
Figure 5.3: Error angles.

$$R_{pe} = R_{pj}R_{jb}R_{be}, \tag{5.17}$$
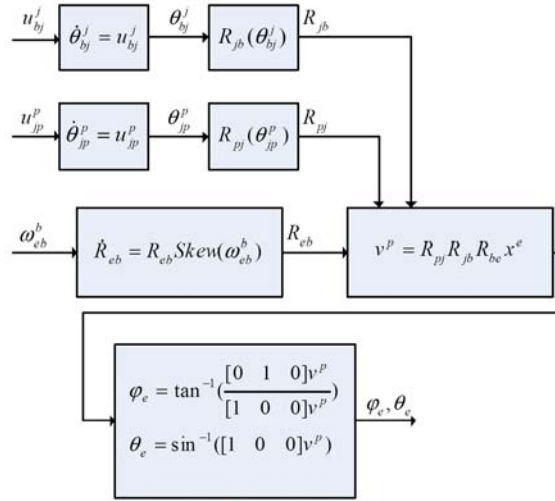
Figure 5.4: Block diagram of the open loop system with the effect of disturbances.

where the orthogonal rotation matrices ($R_{pj} = R_{jp}^T$, $R_{jb} = R_{bj}^T$, and $R_{be} = R_{eb}^T$). Defining special orthogonal group $SO(3) \subset \mathbb{R}^{3\times3}$ as the set

$$SO(3) = \{\mathcal{R} \in \mathbb{R}^{3\times3} : \mathcal{R}\mathcal{R}^T = I, det(\mathcal{R}) = 1\},$$

the nonlinear dynamics of the STA system is defined as follows

$$
\begin{aligned}
\dot{x} &= f(x, u, w) \\
e &= h(x) \\
y &= k(x) \\
\dot{w} &= Sw,
\end{aligned}
$$

(5.18)

where $x = (x^1, x^2) \in \mathbb{R}^2 \times SO(3)$ is the state vector ($x^1 = (\theta_{bj}^j, \theta_{jp}^p)^T$ and $x^2 = R_{be}$), $u \in \mathbb{R}^2$ is the input vector to the motors ($u = (u_{bj}^j, u_{jp}^p)^T$), $w \in \mathbb{R}^6$ is the vector of exogenous system states (produces the disturbance vector $\omega_{eb}^b \in \mathbb{R}^3$ as roll, pitch, and yaw motions in the base of the antenna and consequently the ship body), $e \in \mathbb{R}^2$ is the vector of the output error from the beam sensor ($e = (\phi_e, \theta_e)^T$), and $y \in \mathbb{R}^4$ is the measurement vector ($y = (\theta_{bj}^j, \theta_{jp}^p, \phi_e, \theta_e)^T$). Furthermore, the nonlinear smooth functions f, h, and k are expressed as following.

$$f : \mathbb{R}^2 \times SO(3) \times \mathbb{R}^{2\times 3} \to \mathbb{R}^2 \times SO(3), f(x, u, \omega_{eb}^b)$$
$$= \left(\begin{array}{c} f^1(u) \\ f^2(x^2, \omega_{eb}^b) \end{array} \right) = \left(\begin{array}{c} u \\ -Skew(\omega_{eb}^b)x^2 \end{array} \right), \tag{5.19}$$

$$h : \mathbb{R}^2 \times SO(3) \to \mathbb{R}^2, h(x) =$$
$$\left(\begin{array}{c} tan^{-1}\left(\frac{-x_{11}^2 sin(x_1^1)cos(x_2^1)+x_{21}^2 cos(x_1^1)cos(x_2^1)}{x_{11}^2 cos(x_1^1)cos(x_2^1)+x_{21}^2 sin(x_1^1)cos(x_2^1)+x_{31}^2 sin(x_2^1)}\right) \\ \\ sin^{-1}\left(\frac{-x_{11}^2 cos(x_1^1)sin(x_2^1)-x_{21}^2 sin(x_1^1)sin(x_2^1)+x_{31}^2 cos(x_2^1)}{1}\right) \end{array} \right) \tag{5.20}$$

and

$$k : \mathbb{R}^2 \times SO(3) \to \mathbb{R}^4, k(x) = \left(\begin{array}{c} x^1 \\ h(x) \end{array} \right). \tag{5.21}$$

5.3.2 Beam Control

In the normal operation scenario, the antenna works based on the measurement of the output error from the beam sensor. The control system is designed for the linearized model of the antenna about an equilibrium point. To simplify the model, the rotation matrix R_{be} is considered as the disturbance input. With this respect, the linearized model of the STA system around the equilibrium point $x^{1*} = 0$, $x^{2*} = I_{3\times 3}$, and $u^* = 0$ is
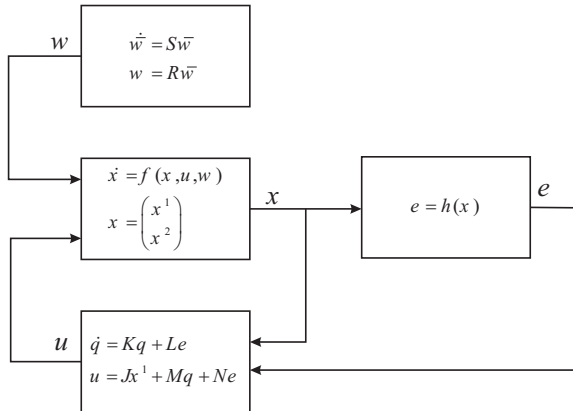
Figure 5.5: Block diagram of the antenna model.

$$\dot{x}^1 = u$$
$$e = \bar{C}x^1 + \bar{D}x^2$$
$$y = \begin{pmatrix} x^1 \\ e \end{pmatrix},$$

(5.22)

where $\bar{C} = \frac{dh}{dx^1}|_{x^*}$, and $\bar{D} = \frac{dh}{dx^2}|_{x^*}$. The original control problem was solved by designing a robust feed-back controller of the form

$$\dot{q} = Kq + Le$$
$$u = Jx^1 + Mq + Ne,$$

(5.23)

so that the error e vanishes to zero as $t \to \infty$ (The matrices J, K, L, M, and N are obtained by solving the standard $\mathcal{H}_\infty$ control problem for linear the system (eq:imc171)).

5.3.3 Fault Discussion

A failure in the beam sensor would mean that the pointing error feedback from the satellite is unknown and it will also result in loss of high bandwidth communication link depending on the severity of the fault. In order to maintain a good strength of satellite signal reaching the antenna, the controller keeps the pointing error between the antenna and the satellite to a minimum of less than a degree. A change in the strength of the signal measured by the beam sensor can occur by appearance of any hurdle between the antenna and the satellite or change in the atmosphere pressure and temperature which is so-called a signal blocking. Blocking will result in an increase of the fluctuations in the pointing error measurement due to loss of signal strength. However, the amount of increase in the fluctuations depends on the amount of the signal reaching the antenna plate during blocking. In general deviations due to disturbances and initial conditions from the satellite sight vector cause the same fluctuations but they should not be considered as blocking since the controller will compensate for those deviations. This is the main reason for not utilizing detection methods that only use the statistical properties of the measurement signals for detecting the mentioned blocking faults.

Finally, the faulty system is affected by parameters $-1 \leq \delta_i \leq 1$, where δ_i $(i = 1, 2)$ is the coefficient of the colored noise variance σ_i^2. The effect of these faults on the beam sensor output are shown in figure 5.6-(a) and (b), where the fault is injected to the STA system as interruption in signal transmission in the time interval $96s$ to $144s$.
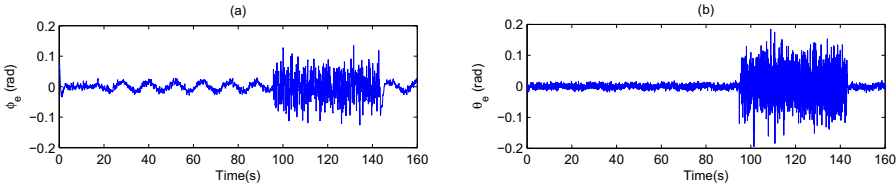
Figure 5.6: Faulty beam sensor measurement (a) elevation error ϕ_e and (b) cross-elevation error θ_e.

5.4   Robust Fault Diagnosis

5.4.1   Standard Set-up Formulation

The generalized concept of fault detection architecture in a class of nonlinear systems (proposed in (Stoustrup and Niemann, 1999)) is employed in this section.

In this set-up (see figure 5.7.), the upper block Δ represents the nonlinearity that is assumed to be sector bounded in an $\mathcal{H}_\infty$ sense (Zhou et al., 1996). It is important that the linear plant $G(s)$ is such that it is possible to infer the stability of nonlinear loop with some specific Δ from robust stability with respect to the $\mathcal{H}_\infty$ unit ball.

The block $F(s)$ is the FDI system to be designed which will be combined by a copy of the nonlinear block Δ. The signal $\hat{f}$ is the estimation of f (fault affected signal) which is generated by FDI system. The signal d is the disturbance to the system. The blocks W_d and W_f are the weighting functions that, based on the design criteria, used to distinguish between fault and disturbance. Furthermore, w_2 would be the estimate of w_1 when z_2 is the estimate of z_1.

Defining e_f as $e_f = f - \hat{f}$, the problem will be transformed to make e_f sufficiently small for any bounded f. This requires to make the system augmented with the Δ_f and Δ_d blocks where $\|\Delta_f\|_\infty \leq 1$ and $\|\Delta_d\|_\infty \leq 1$ are norm bounded. This results in computing nonlinear FDI system by finding a linear filter which solves a μ problem for a linear system structure including four uncertainty blocks, i.e., two Δ blocks combined with Δ_f and Δ_d. In fact, it is possible to write the system as

$$
\begin{pmatrix}
z_1 \\
z_2 \\
\acute{e}_f \\
\acute{e}_d \\
\hline
y \\
w_2
\end{pmatrix}
= \tilde{G}(s)
\begin{pmatrix}
w_1 \\
w_2 \\
f \\
d \\
\hline
\hat{f} \\
z_2
\end{pmatrix}
\tag{5.24}
$$
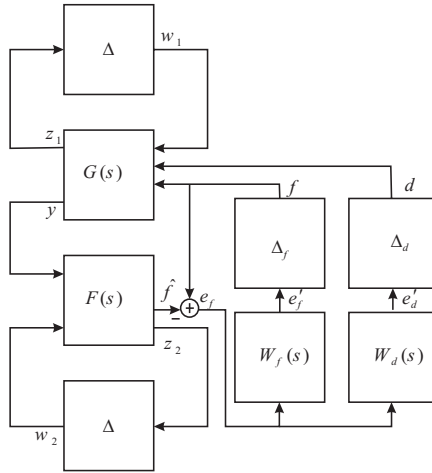
Figure 5.7: Block diagram of the FDI system in robust standard set-up.

or

$$\begin{pmatrix} \tilde{z} \\ \tilde{y} \end{pmatrix} = \tilde{G}(s) \begin{pmatrix} \tilde{w} \\ \tilde{u} \end{pmatrix} \tag{5.25}$$

and then design the FDI filter according to the following result (Stoustrup and Niemann, 2002):

Theorem 1 *Assume that the system*

$$\tilde{G}(s) = \begin{pmatrix} \tilde{G}_{\tilde{z}\tilde{w}}(s) & \tilde{G}_{\tilde{z}\tilde{u}}(s) \\ \tilde{G}_{\tilde{y}\tilde{w}}(s) & \tilde{G}_{\tilde{y}\tilde{u}}(s) \end{pmatrix} \tag{5.26}$$

and the linear filter $F(s)$ satisfies

$$\left\| \tilde{G}_{\tilde{z}\tilde{w}}(s) + \tilde{G}_{\tilde{z}\tilde{u}}(s)F(s)\tilde{G}_{\tilde{y}\tilde{w}}(s) \right\|_{\mu} < \gamma$$

considering mentioned four uncertainty blocks, then the $\mathcal{L}_2 - \mathcal{L}_2$ operator gain from fault f to fault estimation error $e_f = f - \hat{f}$ when applying the FDI system in figure 5.7 is bounded by γ as well.

5.4.2   Design of FDI Filter for The STA System

The first step to design procedure is to introduce two filters W_f and W_d to make sure that $\frac{\|e_f\|}{\|f\|}$ is minimized in the frequency area of interest. That is important to range the filters so that W_f passes the frequency range, $\Phi_f(\omega)$, where the fault is dominant and W_d does it for the frequency range, $\Phi_d(\omega)$ where the disturbance is dominant. Furthermore, it is desired that $\Phi_f(\omega) \cap \Phi_d(\omega) = \emptyset$.

The second step is to separate the linear and nonlinear parts of the system. This should be done with respect to the assumption that the nonlinear part is sector bounded. Considering the system dynamics, we have two nonlinear parts in f^2 and $h(x)$. The outputs provided by these two blocks are always norm-bounded ($x^2 \in SO(3)$ and $h(x)$ is composed of tan^{-1} and sin^{-1}). Thus, the linear part of the dynamics is

$$
\begin{aligned}
\dot{x}^1 &= Jx^1 + Mq + Ne \\
\dot{q} &= Kq + Le.
\end{aligned}
\tag{5.27}
$$

The output error e is modeled as

$$
e = h(x) + f + d.
\tag{5.28}
$$

Now, we need to present a combination of (5.27) and (5.28) in a LFT format knowing that

$$
w_1 = h(x)z_1.
\tag{5.29}
$$

This can be done by considering a unit input $v = 1$ as a known input (with $z_1 = v$) in

$$
\begin{aligned}
\dot{x}^1 &= Jx^1 + Mq + N\Delta z_1 + N\Delta_f \acute{e}_f + N\Delta_d \acute{e}_d \\
\dot{q} &= Kq + L\Delta z_1 + L\Delta_f \acute{e}_f + L\Delta_d \acute{e}_d.
\end{aligned}
\tag{5.30}
$$

The third step is to write the whole system in an standard set-up so that it could be used by the linear robust design tools such as μ synthesis (Soltani et al., 2008b,a). This set-up is presented as follows

$$\begin{pmatrix} \dot{x}^1 \\ \dot{q} \\ \dot{x}_{ef} \\ \dot{x}_{ed} \\ \hline z_1 \\ z_2 \\ \acute{e}_f \\ \acute{e}_d \\ \hline y \\ w_2 \end{pmatrix} = \left(\begin{array}{c|c|c} A & B_1 & B_2 \\ \hline C_1 & D_{11} & D_{12} \\ \hline C_2 & D_{21} & D_{22} \end{array} \right) \begin{pmatrix} x^1 \\ q \\ x_{ef} \\ x_{ed} \\ \hline v \\ w_1 \\ w_2 \\ f \\ d \\ \hline \hat{f} \\ z_2 \end{pmatrix} \qquad (5.31)$$

where the matrix elements are

$$A = \begin{pmatrix} J & M & 0 & 0 \\ 0 & K & 0 & 0 \\ 0 & 0 & A_{ef} & 0 \\ 0 & 0 & 0 & A_{ed} \end{pmatrix}$$

$$B_1 = \begin{pmatrix} N\Delta & 0 & 0 & N & N \\ L\Delta & 0 & 0 & L & L \\ 0 & 0 & 0 & B_{ef} & 0 \\ 0 & 0 & 0 & B_{ed} & 0 \end{pmatrix}$$

$$B_2 = \begin{pmatrix} 0 & 0 \\ 0 & 0 \\ -B_{ef} & 0 \\ -B_{ed} & 0 \end{pmatrix}$$

$$C_1 = \begin{pmatrix} 0 & 0 & 0 & 0 \\ 0 & 0 & 0 & 0 \\ 0 & 0 & C_{ef} & 0 \\ 0 & 0 & 0 & C_{ed} \end{pmatrix}$$

$$D_{11} = \begin{pmatrix} 1 & 0 & 0 & 0 & 0 \\ 0 & 0 & 0 & 0 & 0 \\ 0 & 0 & 0 & 0 & 0 \\ 0 & 0 & 0 & 0 & 0 \end{pmatrix}$$

$$D_{12} = \begin{pmatrix} 0 & 0 \\ 0 & 1 \\ 0 & 0 \\ 0 & 0 \end{pmatrix}$$

$$C_2 = 0$$

$$D_{21} = \begin{pmatrix} \Delta & 0 & 0 & 1 & 1 \\ 0 & 0 & 0 & 0 & 0 \end{pmatrix}$$

$$D_{22} = \begin{pmatrix} 0 & 0 \\ 0 & \Delta \end{pmatrix},$$

where f and d are defined by:

$$\begin{aligned} f &= \Delta_f \acute{e}_f \\ d &= \Delta_d \acute{e}_d. \end{aligned} \tag{5.32}$$

The last step is to compute the fault detection filter by D-K algorithm. Hence, the solution is to apply standard D-K iterations by assuming

$$\begin{aligned} \Delta &= diag(\delta_i) \\ \Delta_f &= diag(\delta_{f_i}) \\ \Delta_d &= diag(\delta_{d_i}), \end{aligned} \tag{5.33}$$

where all δ_is, δ_{f_i}s, and δ_{d_i}s belong to unit circle in the complex plane for $i = 1, 2$.

5.5   Control Reconfiguration

The accommodation strategy is chosen so that the control system should be able to keep the direction of the antenna plate toward the satellite in the faulty situation. In other words, when a fault, such as the disconnection of the communication, occurs then

the beam sensor data will be invalid and therefor the control system become unstable (figure 5.8 shows such instability) and this causes a system shutdown. In this case, after the interruption period, the antenna has to search the sky and find the satellite again which is a time consuming task. The accommodation system has to switch the control system to the NIMC controller which is not working with the beam sensor. Thus, the antenna still tracks the satellite direction and this results in fast re-establishment of the communication just after the interruption is finished and prevents the waste of time for satellite searching and etc. The overview of the reconfigurable system is shown in figure 5.9, where the reconfiguration system is actually using a threshold on estimated fault $\hat{f}$ to decide whether the system is faulty.
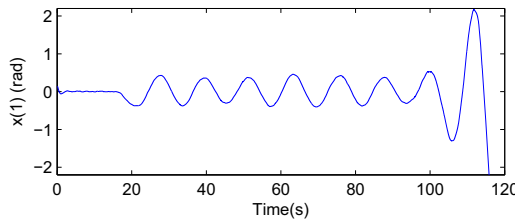
Figure 5.8: The antenna azimuth angle become unstable during interruption at 96s.

5.5.1 Nonlinear Internal Model Control

For the system (5.18), suppose that there exists a controller of the form

$$\begin{aligned}
\dot{\xi} &= \varphi(\xi, y) \\
u &= \vartheta(\xi, y),
\end{aligned} \tag{5.34}$$

in which $\varphi(\xi, y)$ and $\vartheta(\xi, y)$ are smooth functions, satisfying $\varphi(0, 0) = 0$ and $\vartheta(0, 0) = 0$. Then, the generalized tracking problem is as follows.

Given system (5.18) with exosystem (5.5), and two sets $\mathcal{X} \subset \mathbb{R}^{n}$ [1] and $\mathcal{W} \subset \mathbb{R}^{r}$ [2], find, a controller of the form (5.34) and a set $\mathcal{E} \subset \mathbb{R}^{v}$ [3], such that, in the closed-loop system:

1. the trajectory $(x(t), \xi(t), w(t))$ is bounded,

---

[1] n is the dimension of states vector x

[2] r is the dimension of vector ξ

[3] v is the dimension of disturbance vector w
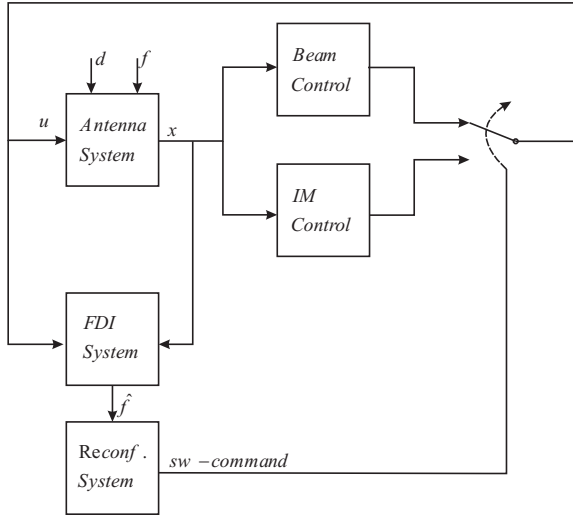
Figure 5.9: STA system reconfiguration overview.

2. $lim_{t \to \infty} e(t) = 0$,

for every initial condition $(x(0), \xi(0), w(0)) \in \mathcal{X} \times \mathcal{E} \times \mathcal{W}$ (see (Isidori et al., 2003b)).

The solution to the generalized tracking problem is given by NIMC. Let $\pi : \mathbb{R}^r \to \mathbb{R}^n$ and $\sigma : \mathbb{R}^r \to \mathbb{R}^v$ be two smooth mappings, and suppose that the smooth manifold
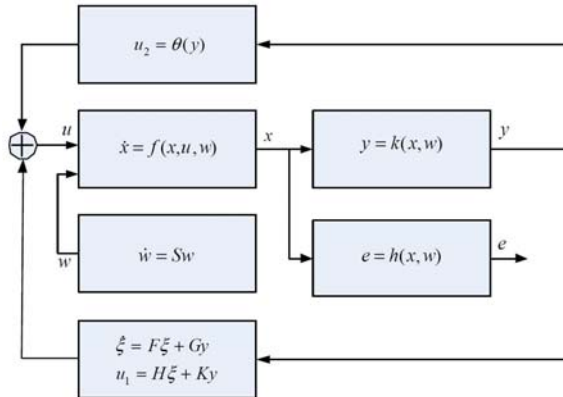
Figure 5.10: Block diagram of the closed-loop system with NIMC.

$$\mathcal{M}_0 = \{(x, \xi, w) : x = \pi(w), \xi = \sigma(w)\}$$

is invariant for the forced closed-loop system (5.18) with (5.34). $\mathcal{M}_0$ being invariant for the closed-loop system means that $\pi(w)$ and $\sigma(w)$ are solutions of the pair of differential equations

$$\frac{\partial \pi}{\partial w} Sw = f(\pi(w), \vartheta(\sigma(w), k(\pi(w))), w)$$
$$\frac{\partial \sigma}{\partial w} Sw = \varphi(\sigma(w), k(\pi(w))). \tag{5.35}$$

Now assume that in the closed-loop system all trajectories with initial conditions in a set $\mathcal{X} \times \mathcal{E} \times \mathcal{W}$ are bounded and attracted by the manifold $\mathcal{M}_0$ and that the regulated output e is zero at each point of $\mathcal{M}_0$, i.e., that

$$0 = h(\pi(w)). \tag{5.36}$$

Then, we can claim that if there are mappings $\pi(w)$ and $\sigma(w)$ such that closed-loop system (5.18) with (5.34) and (5.36) hold and, in forced closed-loop system (closed-loop system combined with exosystem), all trajectories with initial conditions in a set $\mathcal{X} \times \mathcal{E} \times \mathcal{W}$ are bounded and attracted by the manifold $\mathcal{M}_0$, the controller (5.34) solves the generalized tracking problem (Isidori et al., 2003b).

Moreover, the conditions (5.35) and (5.36) hold if and only if there exist a triplet of mappings $\pi(w), \sigma(w), c(w)$ such that

$$\frac{\partial \pi}{\partial w} Sw = f(\pi(w), c(w), w)$$
$$0 = h(\pi(w)) \tag{5.37}$$

and

$$\frac{\partial \sigma}{\partial w} Sw = \varphi(\sigma(w), k(\pi(w)))$$
$$c(w) = \vartheta(\sigma(w), k(\pi(w))). \tag{5.38}$$

Finally, we make use of the following proposition as it has been proved in (Isidori et al., 2003b).

Proposition 1 *Suppose a controller of the form (5.34) is such that conditions (5.37) and (5.38) hold, for some triplet of mappings $\pi(w), \sigma(w), c(w)$. Suppose that all trajectories*
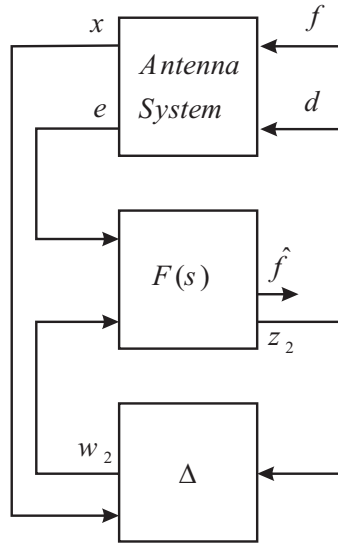
Figure 5.11: Implementation of the off-line designed filter to the on-line system.

of the forced closed loop system, with initial conditions in a set $\mathcal{X} \times \mathcal{E} \times \mathcal{W}$, are bounded and attracted by the manifold $\mathcal{M}_0$. Then, the controller solves the generalized tracking problem.

Going through design procedure, we depart from the fact that the dynamic of the controller is considered to be linear but the control output is considered to be nonlinear. Thus, the control system can be of the following form

$$
\begin{aligned}
\dot{\xi} &= F\xi + Gy \\
u &= H\xi + Ky + \Theta(y).
\end{aligned}
\tag{5.39}
$$

The controller which satisfies the generalized tracking problem should satisfy (5.37) and (5.38). Starting from (5.37), f^2 satisfies the first equation, since,

$$f^2(\pi^2(w), w) = \frac{\partial \pi^2}{\partial w} Sw$$
$$= \frac{\partial \pi^2}{\partial t} \frac{\partial t}{\partial w} Sw \qquad (5.40)$$
$$= \frac{\partial \pi^2}{\partial t},$$

which is obvious due to (5.2) (π^1 and π^2 are the maps corresponding to x^1 and x^2 respectively). Furthermore, f^1 should satisfy

$$\dot{\pi}^1 = f^1(\pi^1(w), c(w), w) = c(w). \qquad (5.41)$$

The second one of (5.37) gives the nonlinear control low

$$tan(\pi_1^1) = \frac{\pi_{21}^2}{\pi_{11}^2}$$
$$tan(\pi_2^1)sin(\pi_1^1) = \frac{\pi_{21}^2 \pi_{31}^2}{(\pi_{21}^2)^2 - (\pi_{11}^2)^2}. \qquad (5.42)$$

Equations (5.38) with the aid of (5.41) is reformulated to

$$\dot{\pi}^1 = H\sigma + K\pi^1 + \Theta(\pi)$$
$$\dot{\sigma} = F\sigma + G\pi, \qquad (5.43)$$

where $K = I_{2\times2}$. Defining $\Theta(\pi)$ as

$$\Theta_1(\pi) = -tan^{-1}(\frac{\pi_{21}^2}{\pi_{11}^2})$$
$$\Theta_2(\pi) = -tan^{-1}(\frac{\pi_{21}^2 \pi_{31}^2}{((\pi_{21}^2)^2 - (\pi_{11}^2)^2)sin(\pi_1^1)}), \qquad (5.44)$$

(5.43) will be reduced to
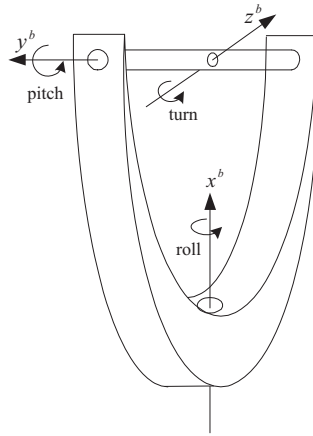
Figure 5.12: A conceptual illustration of the used ship simulator with its rotational axis.

$$\dot{\pi} = H\sigma$$
$$\dot{\sigma} = F\sigma + G\pi, \qquad (5.45)$$

and the stability of σ and π^1 is depending on having all real parts of the eigenvalues of $\begin{pmatrix} H & 0 \\ F & G \end{pmatrix}$ negative. The block diagram of such NIMC is illustrated in figure 5.10.

5.6   Results

5.6.1   Real-time Implementation

The implementation of the designed FDI filter is according to figure 5.11. The measurements are e, x, and recall that $v = 1$ is assumed. Moreover, we need to construct the nonlinear Δ block which provides an estimation for the error e. This is done by implementing three gyros at the body of the antenna where it is fixed to the ship. The output of the gyros is the vector w which by integration gives the rotation matrix and finally it is possible to compute the error output $h(x)$ (see (Soltani et al., 2007) and (Soltani, 2006)).

In order to evaluate the method in a real test scenario, the antenna was mounted on a *ship simulator*. The ship simulator, as shown in figure 5.12, can simulate the movements of the ship in different operational conditions. This system provides a reliable simulation

Filter	Type	$\omega_{b_1}(\frac{rad}{s})$	$\omega_{b_2}(\frac{rad}{s})$
W_{f_1}	BW band-pass	1100	1300
W_{f_2}	BW band-pass	600	1300
W_{f_3}	BW band-pass	300	1300
W_{f_4}	BW band-pass	60	1300
W_{d_1}	BW low-pass	-	10
W_{d_2}	BW low-pass	-	1
W_{d_3}	BW low-pass	-	0.1

Table 5.1: Table of the fault and disturbance filters type and cut-off frequencies.
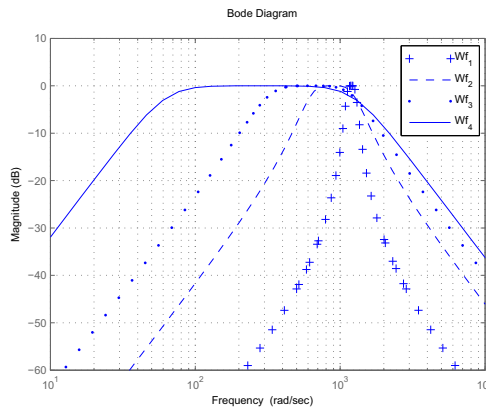
Figure 5.13: Bode diagram of the fault gain filters.

of the environment according to the requirements provided by (Inmarsat, 2003). When placing the antenna on z^b axis, the ship simulator moves the antenna in pitch, roll, and turn axes which are the most important movements affecting the antenna's plate direction. Eventually, to build up the real situation of the ship-mounted antenna, it is placed in an antenna laboratory which is equipped with a signal transmitter as a virtual satellite. Additionally, the lab walls are electromagnetically insulated in order to reduce the effect of the reflection of the signals to the antenna- which makes non-realistic noise for the beam sensor. In the verification tests, the maximum amplitude and frequency of the pitch, roll, and yaw disturbances, according to (Inmarsat, 2003), has been generated by the ship simulator.
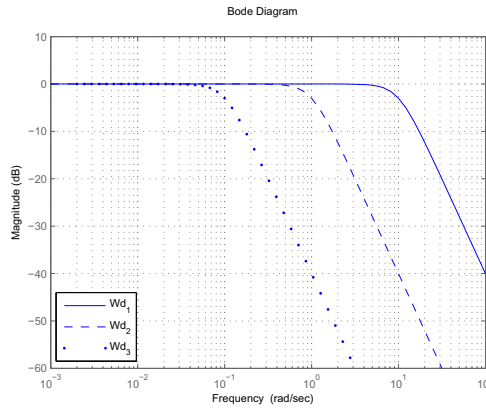
Figure 5.14: Bode diagram of the disturbance gain filters.

5.6.2   Design Considerations

The issue of designing a FDI system which is able to distinguish faults from disturbance has been discussed in the last section. In practice, we designed those filters for different frequency bands. This has been done due to our knowledge about the nature of the disturbance and faults. For the STA system, the effect of the faults appear in the higher frequency range than the frequency range for the disturbances. In the following, we analyzed the effect of this factor on the FDI system.

The filters are chosen as band-pass and low-pass Butter Worth filters with cut-off frequencies described in table 5.1. Figure 5.13 and figure 5.14 show the bode diagram of
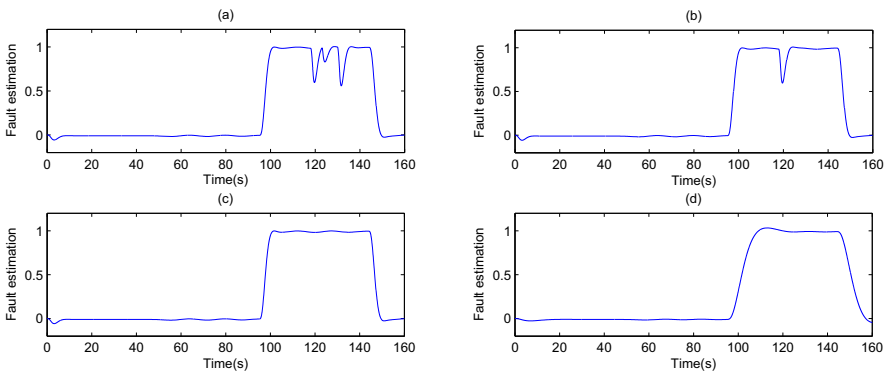
Figure 5.15: Estimated fault using (a) W_{f_1} (b) W_{f_2} (c) W_{f_3} (d) W_{f_4}.
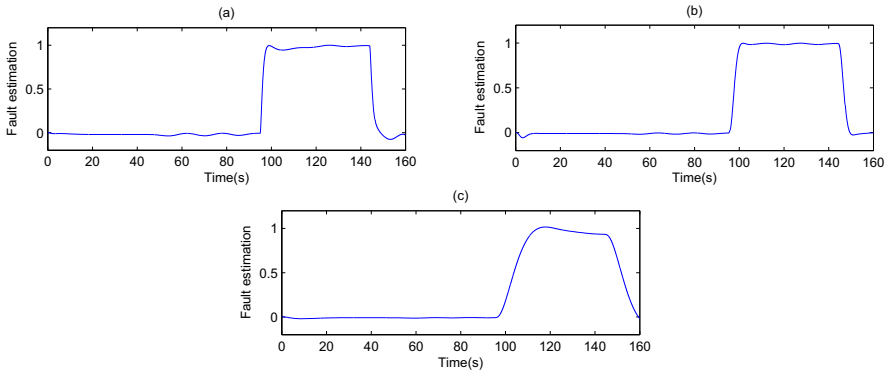
Figure 5.16: Estimated fault using (a) W_{d_3} (b) W_{d_2} (c) W_{d_1}.

the fault and disturbance filters used in our analysis.

The results are according to the fault shown in figure 5.6. Only the fault $\hat{f}_1$ is illustrated here to suppress the space in this article. In figure 5.15, four different filters are used for the fault gain filter in each design according to table 5.1. The estimated fault shows that by choosing more narrow band-width filter we can detect the fault faster; however, we have less robustness, e.g., by using W_{f_1} the faulty area is not safe enough (see figure 5.15-(a)) while by a wider filter (see figure 5.15-(d)) the estimated value is more robust and at the same time the detection is slower. In fact, there is a trade-off between the speed of detection and robustness when choosing the right filter for the design of the fault estimator. Figure 5.15-(c) shows the result of the fault estimation by using W_{f_3}.

The same procedure on the disturbance gain filters shows that by choosing a wider band filter for the disturbance, the estimation become robust and slow but using more narrow band-width we obtain faster detection but less robustness to the disturbances in the estimation. Figure 5.16 reveals that there is another trade-off for choosing the right disturbance gain filter. As it is mentioned in table 5.1 the chosen filter W_{d_3} in figure 5.16-(a) is too narrow and the estimation is affected by the disturbance while the filter W_{d_1} in figure 5.16-(c) is too wide therefore the resulted estimation is slow. Figure 5.16-(b) shows the result when W_{d_2} is used as the disturbance fault filter.

Moreover, figure 5.17-(a) and (b) show the azimuth and elevation angles before and after the reconfiguration system changes the control method. Figure 5.18-(a) and (b) show the error calculated by NIMC controller during the fault.

Finally, it should be noted that the fault diagnosis algorithm that we employed has been originally proposed for fault estimation purposes. Estimation of the fault in our case has shown to be an extremely challenging task due to the stochastic nature of the considered faults (see figure 5.6). Therefore, the fault diagnosis filter's output has only been used

for the detection purposes. The estimation of faults with such characteristics is the subject for further research.
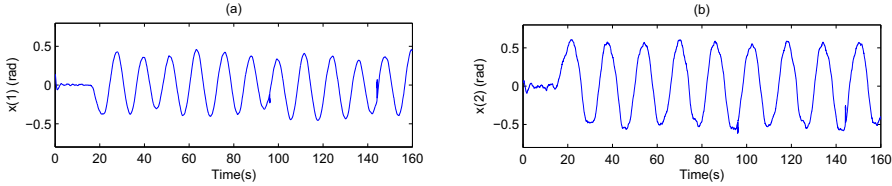
Figure 5.17: Motor angles (a) azimuth and (b) elevation.
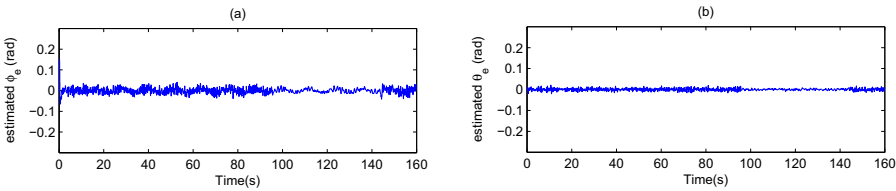
Figure 5.18: Calculated errors via IMC (a) elevation and (b) cross-elevation.

5.7 Conclusion

The nonlinear dynamical model of the satellite tracking antenna was explained. The model was formulated in a standard problem set-up for robust control. A combination of a linear filter- obtained by solving a $\mathcal{H}_\infty$ control problem- and a nonlinear system was employed for the fault detector system. The set-up was developed so that the designed FDI system reduces the effect of the disturbances on the estimated value of the fault. An internal model controller, which guarantees asymptotic convergence of the tracking error to zero, is designed as a second control strategy to handle the control task during the faults. Finally, the implemented FTC algorithm has been analyzed on a ship simulator test device and it has been concluded that the proposed FTC system has fulfilled the desired specifications for STA.

Chapter 6

Robust FDI for Hopper Engine Subsystem

Abstract- The ability of diagnosis of the possible faults is a necessity for satellite launch vehicles during their mission. In this paper, an structural analysis method is employed to divide the complex propulsion system into simpler subsystems for fault diagnosis filter design. A robust fault diagnosis method, which is an optimization based approach, is applied to the subsystems of the propulsion system. The optimization problem has been solved within two different tools and the results are compared with two other optimization based approaches. The turbopump system is used to illustrate the employed methods and obtained results.

6.1   Introduction

Reliability is a highly demanded topic in many industrial applications, particularly in aerospace. The mission objectives of a spacecraft may not be disrupted by any possible fault. A fault diagnosis system is able to monitor the system performance and alert the control system when a fault has occurred. In this regards, the problem of model-based fault diagnosis has been receiving increasing attention from the research communities (Willsky, 1996).

By the early 90's the logic of the conventional methods for fault diagnosis problem, which included annihilating the matrices, was substituted by the methods based on norm minimization. This phenomenon opened the doors of the $\mathcal{H}_2$, $\mathcal{H}_\infty$, and other optimization approaches to the field of fault diagnosis (Frank and Ding, 1994; Mangoubi et al., 1995; Edelmayer et al., 1996; Edelmayer and Bokor, 2000). Most of those

FD approaches (except parameter identification methods) have considered the models with additive fault input to the system. In other words, they are modeled as exogenous perturbations to the system (Basseville, 1988; Chen and Patton, 1999; Frank, 1990).

In this paper, the fault is modeled as a parameter, since the nature of many faults are indeed parametric. One of the most important reasons is that an exogenous input cannot, for example, de-stabilize a system while a parameter change might do that, which is also the case for our application. A fault diagnosis approach for systems with parametric fault which has been proposed by (Stoustrup et al., 1997; Niemann and Stoustrup, 1997) is used here. The optimization problem has been defined in the so-called standard set-up for robust control based on LFT. In this approach the residual is in fact an estimation of the fault.

A "Hopper", which is a horizontally launched and horizontally landing rocket-propelled launch vehicle comprising a nondisposable primary stage and one expendable upper stage, is under consideration as a reusable launch vehicle to replace the existing expandable launch vehicles in ESA (European Space Agency) in the future. The advantages include: reduction of transportation cost to orbit, return capability from orbit, and less environmental pollution.

A key element for the re-usability and maintainability is given by the health management system (HMS) being an integral part of the system design (Belau and Sommer, 2006). The HMS shall be able to diagnose faults of which the effect is hardly recognizable due to system uncertainties (unpredictable environmental conditions or system parameters) or sensor noise.

The main engine is a complex system with various subsystems. Designing a filter for this system, which is capable of indicating faults in a reliable manner, is shown to be a nearly impossible task. To address and solve this problem a structural analysis approach was employed. The structural analysis of the system leads to identifying subsystems with inherent redundant information required for designing appropriate filters. In order to illustrate the applicability of our approach we focus only on one subsystem that is chosen to be the turbopump system.

The contributions of this paper are two-fold: 1- illustrating the advantage of combined utilization of qualitative as well as quantitative methods to design a fault diagnosis system; Structural analysis method, which is a qualitative method, is used to analyze the system and divide the system into manageable (and monitorable) parts while quantitative (here, optimization based robust methods) are used for the detailed design. 2 - the application of the parametric fault diagnosis filter design based on the $\mathcal{H}_\infty$ as well as the μ synthesis, in the set-up presented in (Stoustrup and Niemann, 2002; Niemann and Stoustrup, 2000). In addition, the main results of the designed filter has been compared with two other optimization based methods to show the capability of this approach.

This paper is organized as follows: Section 6.2 presents an structural analysis on the propulsion system while the turbopump has been chosen as a subsystem. The fault diagnosis method has been presented and the fault estimator design procedure has been described in Section 6.3. In Section 6.4, the results of fault estimation are illustrated and compared with two other methods, and eventually, the conclusions are brought in Section 6.5.

6.2   Structural Analysis of The Propulsion System

6.2.1   Motivation

The overall nonlinear system of the considered engine model is translated to a model block diagram. The blocks in the diagram, which is shown in figure 6.1 on the following page, represent the functionalities of the engines main parts; valves, pumps, combustion chamber, and the gas generator. The considered plant has 14 independent inputs, 18 outputs, 14 intermittent (nonmeasurable) variables, and 6 dynamic/continuous states. 12 failure cases were considered in this system. There are 6 differential equations which describe the dynamic behavior of the valves and pumps (Soltani and Izadi-Zamanabadi, 2007). The number of the states in the system suggests that designing a model-based fault diagnosis algorithm should be a fairly manageable task. However, the obtained experience shows the contrary; due to the level of system nonlinearity the different applied methods illustrated a very limited success in detecting most of the chosen faults.

The complexity of this system appeals for a method that enables the design engineer(s) to break the system into small and manageable parts for which the detailed design can be carried out. In addition, it would be an advantage to be able to obtain additional knowledge about which parts of the system are monitorable and whether the selected faults can be detected and isolated.

6.2.2   Structural Analysis

Structural analysis is concerned with the properties of the system structural model, which is an abstraction of its behavior model in the sense that only the structure of the constraints, i.e. the existence of links between variables and parameters is considered and not the constraints themselves (Blanke et al., 2006). The links are represented by a bi-partite graph, which is independent of the nature of the variables and parameters and also of the value of the parameters. Hence, the structural model is a qualitative, very low level and easy to obtain, model of the system behavior. The structural analysis provides the following information: 1- monitorable parts of the system, i.e., the
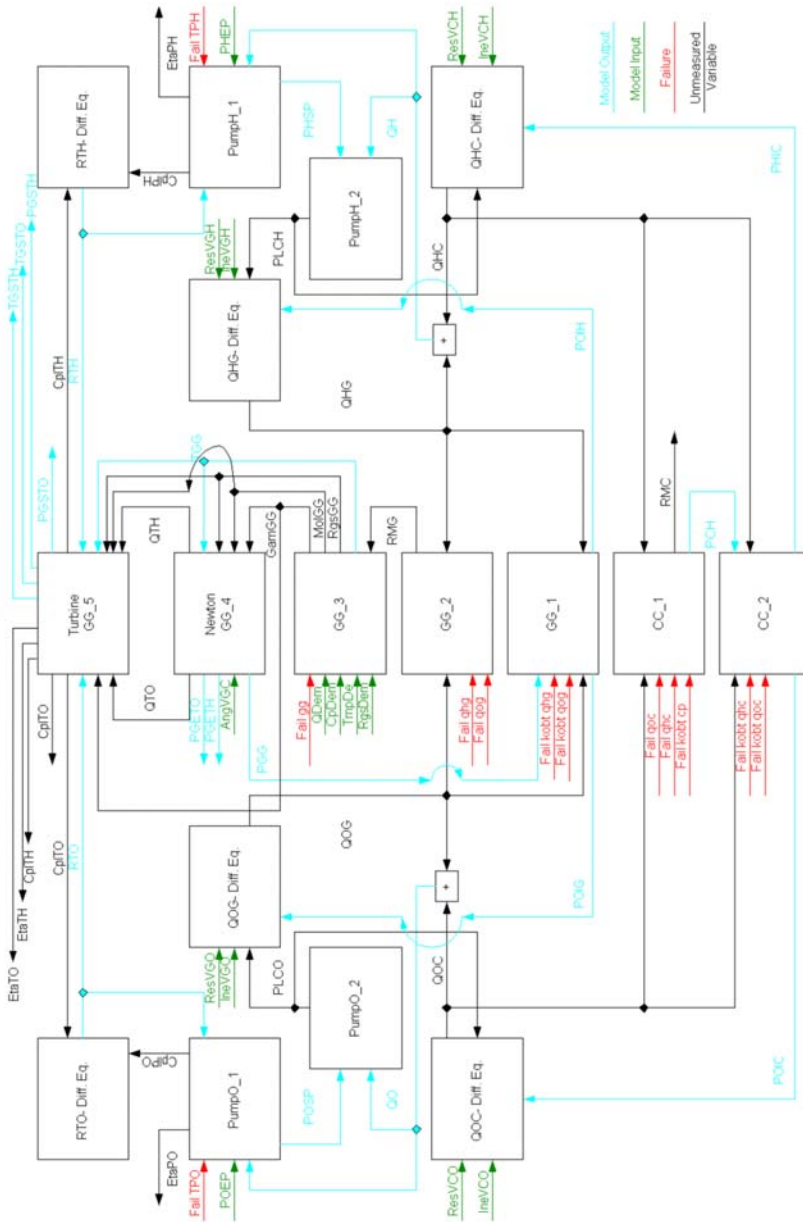
Figure 6.1: Modular decomposition of engine system. (Known) Inputs to each block are shown by green color, faults have red color, Blue color represents the measured outputs, and black color represents internal variables which are not known (not measured).

subset of the components, where the faults can be detected and isolated, 2- the possibility of designing residuals that meet some specific requirements, and 3- the existence of reconfiguration possibilities.

	R_o	p_1	p_3	p_8	p_{13}	m_1	m_4	m_6	m_{14}	m_{15}	m_{16}
c_1	×				①			1	1	1	1
c_2	①					1					
c_3			①				1		1	1	
c_4			1	①					1		
c_5		①	1	1		1	1		1	1	
c_6		1	1	1	1		1		1	1	1

Table 6.1: Structural model of the LOX pump system.

In order to demonstrate the use of the structural analysis we have taken the results for the liquid oxygen (LOX) turbopump. The structural model of the LOX pump is shown in table 6.1. The constraints are $\mathcal{C} = \{c_1, c_2, c_3, c_4, c_5, c_6\}$, the unknown variables and (intermittent) parameters are $\mathcal{X} = \{R_o, p_1, p_3, p_8, p_{13}\}$, and the known (measured) variables are $\mathcal{M} = \{m_1, m_4, m_6, m_{14}, m_{15}, m_{16}\}$. A *matching* between an unknown variable/parameter and a constraint, denoted by a ① in the cross section between the variable column and the constraint row, indicates that the matched variable can be calculated/computed through the corresponding constraint. For instance, p_{13} can be calculated through c_1 when the values of R_o and m_6 are known. The constraint $c_1(R_o, p_{13}, m_6) = 0$ represents the following dynamical behavior:

$$\dot{R}_o = ap_{13} - a(\alpha(\max(0, m_6))^2 + \beta max(0, m_6)R_o - \gamma R_o^2) \tag{6.1}$$

where a, α, β, γ are known parameters. The × in the table indicates that the value of corresponding variable can not be uniquely calculated through the corresponding constraint, hence can not be matched. The table shows that all unknown variables/parameters are matched. On the other hand, the constraint c_6 is not matched. However, c_6 contains unknown variables that are already matched (and hence can be calculated uniquely). Therefore, c_6 can be used to derive a relation that contains only known variables. The obtained relation is hence a redundancy relation. From the fault diagnosis viewpoint, the subsystem that is represented by constraints $c_1, c_2, c_3, c_4, c_5, c_6$ is observable (i.e. monitorable) and since it includes dynamical behavior. Therefore, it is suited for detailed model-based fault diagnosis design.

The nonlinear version of the LOX pump's system dynamic is written in a compact form

as:

$$\dot{R}_o = \frac{a_o Q_o^2}{R_{oh}} + b_o T_o + c_o Q_o R_o + d_o R_{oh} R_0^2 \qquad (6.2)$$
$$y_1 = R_o$$

where a_o, b_o, c_o, and d_o are constant coefficients depending on the design of the turbopump and T_o is the LOX turbine torque. The pump speed is represented by R_o, the pump flow by Q_o, and the mixture ratio by R_{oh}.

6.2.3   The fault augmented model

The efficiency loss (δ) has been considered as a parametric fault for LOX turbopump, that affects the pump shaft speed. The dynamic equation is satisfied only for no fault case ($\delta = 0$). The fault augmented model is

$$\dot{R}_o = \left(\frac{a Q_o^2}{R_{oh}} + c_o Q_o R_o + d_o R_{oh} R_0^2 \right)(1 - \delta) + b_o T_o \qquad (6.3)$$
$$y_1 = R_o.$$

6.3   Fault Estimation Method

6.3.1   Robust Parametric FDI in A Standard Set-up

A general concept of parametric fault detection architecture in a robust standard set-up is proposed in (Stoustrup and Niemann, 2002). The approach is to model a potentially faulty component as a nominal component in parallel with a (fictitious) error component. The optimization procedure suggested here then tries to estimate the ingoing and outgoing signals from the error component. This works well only in cases where the component is reasonably well excited, but on the other hand, if the component is not active at all, there is absolutely no way to detect whether it is faulty. The considered plant is described by the model

$$\begin{cases} \dot{x} = A_\Delta x + B_u u \\ y = C_y x + D_{yu} u \end{cases} \qquad (6.4)$$

where A_Δ is the deviated matrix from the nominal value (A) by a dependency to the fault where the dependency can be nonlinear. The possibly nonlinear parameter dependency of A_Δ is approximated with a polynomial. Therefore, $A_\Delta = A + p(\delta)A$, where p is a polynomial or rational function of the parameter δ satisfying $p(0) = 0$ (the non-faulty operation mode). Finally, the model (6.4) is written in linear fractional transformation form. As a result we get a system of the form

$$\begin{bmatrix} \dot{x} \\ z \\ y \end{bmatrix} = \left[\begin{array}{c|cc} A & B_f & B_u \\ \hline C_f & D_{zf} & 0 \\ C_y & 0 & D_{yu} \end{array} \right] \begin{bmatrix} x \\ f \\ u \end{bmatrix} \tag{6.5}$$

where z is the external output, f is the fault input signal, the matrix D_{zf} is well-posed (LFT's are normally used), and the connection between z and f is given by

$$\begin{aligned} f &= \Delta_{par} z \\ \Delta_{par} &= \delta I. \end{aligned} \tag{6.6}$$

The next step in setting up the fault estimation problem as a standard problem is to introduce two fault estimation errors e_f ad e_z as

$$\left\{ \begin{array}{l} e_f = f - \hat{f} \\ e_z = z - \hat{z} \end{array} \right\},$$

where $\hat{f}$ and $\hat{z}$ are the estimation of f and z to be generated by the filter respectively. Figure 6.2 shows the setup for this approach. In order to design a filter F such that applying F to u and y provides the two desired estimates $\hat{f}$ and $\hat{z}$ one additional step is required, which is the introduction of a fictitious performance block Δ_{perf} ; suggesting that the input u was generated as a feedback Δ_{perf} from the outputs $\begin{bmatrix} e_f \\ e_z \end{bmatrix}$:

$$u = \Delta_{perf} \begin{bmatrix} e_f \\ e_z \end{bmatrix}. \tag{6.7}$$

Therefore, two filters ($W_f(s)$ and $W_z(s)$) are introduced to make sure that the norm of $\frac{\|e_f\|}{\|f\|}$ is minimized in the frequency area of interest (For incipient faults a low frequency
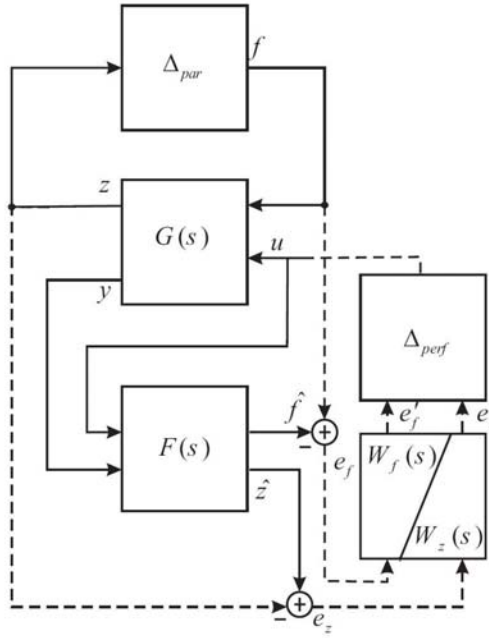
Figure 6.2: Standard problem set-up for parametric fault detection combined with fictitious performance block (The dashed lines are the connections which are artificially assumed only for the design and they do not exist in implementation).

filter is used). In fact, we introduce these filters to handle the high excitation level of the inputs. Finally we introduce

$$\Delta = \begin{bmatrix} \Delta_{par} & 0 \\ 0 & \Delta_{perf} \end{bmatrix}. \tag{6.8}$$

The significance of the Δ_{perf} block is the following. According to the small gain theorem, the $\mathcal{H}_\infty$ norm of the transfer function from u to $\begin{bmatrix} \dot{e}_f \\ \dot{e}_z \end{bmatrix}$ is bounded by γ if and only if the system in figure 6.2 is stable for all Δ_{perf}, $\| \Delta_{perf} \|_\infty < \gamma$. Hence, the problem of making the norm of the fault estimation error bounded by some quantity has been transformed to a stability problem. Eventually, the main result for FDI problem with parametric fault is provided by the following (Stoustrup and Niemann, 2002):

Theorem 1 *Let $F(s)$ be a linear filter applied to the system as in figure 6.2 as $\begin{bmatrix} \hat{f} \\ \hat{z} \end{bmatrix} = F \begin{bmatrix} u \\ y \end{bmatrix}$, and assume that $F(s)$ satisfies:*

$$\| \mathcal{F}_l(G_{\tilde{z}\tilde{w}}, F) \|_\infty < \gamma, \tag{6.9}$$

where $\tilde{z} = \begin{bmatrix} z \\ \acute{e}_f \\ \acute{e}_z \end{bmatrix}$, $\tilde{w} = \begin{bmatrix} f \\ u \end{bmatrix}$, and $\mathcal{F}_l(.)$ is the lower Linear Matrix Transformation (LFT) representation of the two connected blocks (Zhou et al., 1996). Then the resulting fault estimation error is bounded by

$$\| \begin{bmatrix} \acute{e}_f \\ \acute{e}_z \end{bmatrix} \|_\infty < \gamma N \tag{6.10}$$

where N is the excitation level of the system i.e., $\| u \|_\infty = N$.

6.3.2   Design of The Fault Detector for Turbopump

As an example of the fault estimation method, we brought one of the subsystems to present and analyze the results. The Oxygen turbopump subsystem is actually the combination of the RTO and PUMP O-1 blocks in figure 6.1. The dynamic model of this block is written as following

$$\dot{x} = (-ax - cQ_o)(1 - p(\delta)) + bT_o, \tag{6.11}$$

where a, b, and c are constants from the linearization, x is the shaft speed , Q_o is the pump flow , and T_o is the turbine torque and

$$p(\delta) = \lambda \delta^3 + \delta^2 - \lambda \delta \tag{6.12}$$

is the fault model with constant λ. The system is formulated in a standard form as

$$\dot{x} = -ax - x_u + bT_o + \lambda f_1 + f_2 - \lambda f_3$$
$$\dot{x}_u = -Wx_u + WcQ_o$$
$$\dot{x}_{ef} = A_{ef}x_{ef} + B_{ef}(\lambda f_1 + f_2 - \lambda f_3 - \hat{f})$$
$$\dot{x}_{ez} = A_{ez}x_{ez} + B_{ez}(\lambda z_1 + z_2 - \lambda z_3 - \hat{z})$$
$$z_1 = ax + x_u$$
$$z_2 = f_1$$
$$z_3 = f_2 \tag{6.13}$$
$$\acute{e}_f = C_{ef}x_{ef} + D_{ef}e_f$$
$$\acute{e}_z = C_{ez}x_{ez} + D_{ez}e_z$$
$$y_1 = x$$
$$y_2 = T_o$$
$$y_3 = Q_o$$

where W is a relatively big constant used to include the actuator fault in the state variables. The standard model (with $D_{ef} = D_{ez} = 0$) becomes

$$
\begin{bmatrix} \dot{x} \\ \dot{x}_u \\ \dot{x}_{ef} \\ \dot{x}_{ez} \\ \cdots \\ z_3 \\ z_2 \\ z_1 \\ \acute{e}_f \\ \acute{e}_z \\ \cdots \\ y_1 \\ y_2 \\ y_3 \end{bmatrix}
=
\left[\begin{array}{ccccc}
A_1 & \vdots & B_1 \quad B_f & \vdots & B_2 \\
\cdots & & \cdots \quad \cdots & \cdots & \cdots \\
C_1 & \vdots & D_{11} \quad D_{1f} & \vdots & D_{12} \\
\cdots & & \cdots \quad \cdots & \cdots & \cdots \\
C_2 & \vdots & D_{21} \quad D_{2f} & \vdots & D_{22}
\end{array} \right]
\begin{bmatrix} x \\ x_u \\ x_{ef} \\ x_{ez} \\ \cdots \\ T_o \\ Q_o \\ f_1 \\ f_2 \\ f_3 \\ \cdots \\ \hat{z}_1 \\ \hat{f}_1 \end{bmatrix}, \tag{6.14}
$$

where the matrix values can be found in Section A.3. Finally, a $\mathcal{H}_\infty$ filter F, which estimates $\hat{f}$ and $\hat{z}$ and takes u and y as inputs, is designed using *hinfsyn* in **MATLAB**. This filter results in e_f and e_z vanishing to zero as time goes to infinity.

6.4 Results

6.4.1 Comparable fault estimation/diagnosis algorithms

In order to evaluate the described algorithm in the previous section, three other suggested optimization based robust methods are employed. These methods are described in the following subsections.
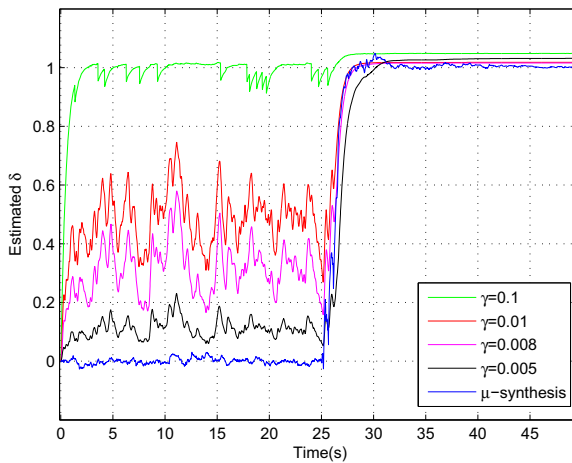
μ-Synthesis

Figure 6.3: The result of the $\mathcal{H}_\infty$ (with different γ values) and μ-synthesis method to the injected step fault.

The optimization problem in theorem 1 can be solved using D-K iteration as a numerical method for μ-synthesis. The set-up, should be formulated in a way so that δ is augmented in the set-up and considered to be in the unit circle of the complex plane.

$$
\begin{aligned}
\dot{x} &= -ax - x_u + bT_o + (ax + x_u)\lambda\delta^3 + (ax + x_u)\delta^2 - (ax + x_u)\lambda\delta \\
\dot{x}_u &= -Wx_u + WcQ_o \\
\dot{x}_{ef} &= A_{ef}x_{ef} + B_{ef}((ax + x_u)\lambda\delta^3 + (ax + x_u)\delta^2 - (ax + x_u)\lambda\delta - \hat{f}) \\
\dot{x}_{ez} &= A_{ez}x_{ez} + B_{ez}((ax + x_u)\lambda\delta^2 + (ax + x_u)\delta - (ax + x_u)\lambda - \hat{z}) \\
\acute{e}_f &= C_{ef}x_{ef} + D_{ef}e_f \\
\acute{e}_z &= C_{ez}x_{ez} + D_{ez}e_z \\
y_1 &= x \\
y_2 &= T_o \\
y_3 &= Q_o,
\end{aligned}
\qquad (6.15)
$$

Mixed $\mathcal{H}_2$ / $\mathcal{H}_\infty$ Fault Diagnosis

In (Khosrowjerdi, Nikoukhah, and SafariShad, 2005), the residual for the system

$$
\begin{aligned}
\dot{x} &= Ax + Bu + B_f f_a + B_d d_a \\
y &= Cx + Du + D_f f_s + D_d d_s
\end{aligned}
\qquad (6.16)
$$

is given by

$$
\begin{aligned}
\dot{\hat{x}} &= (A - KC)\hat{x} + [B - KD \ \ K][u \ \ y_m]^T \\
\hat{\delta} &= -Cx + [-D \ \ 1][u \ \ y_m]^T,
\end{aligned}
\qquad (6.17)
$$

where the gain K is obtained trough solving the convex optimization problem in (Khosrowjerdi et al., 2005) and $\hat{\delta}$ is the estimated residual here.

Mixed $\mathcal{H}_\infty$ / LMI Fault Diagnosis

In (Zhong, Ding, Lam, and Wang, 2003), a model-matching problem is solved by minimizing the $\mathcal{H}_\infty$ norm of the difference between the residual reference model and the real residual. In this method, the residual for the system (6.16) is given by

Figure 6.4: The result of the mixed $\mathcal{H}_2$ / $\mathcal{H}_\infty$ method to the injected step fault (The upper graph is zoomed and illustrated in the lower graph).

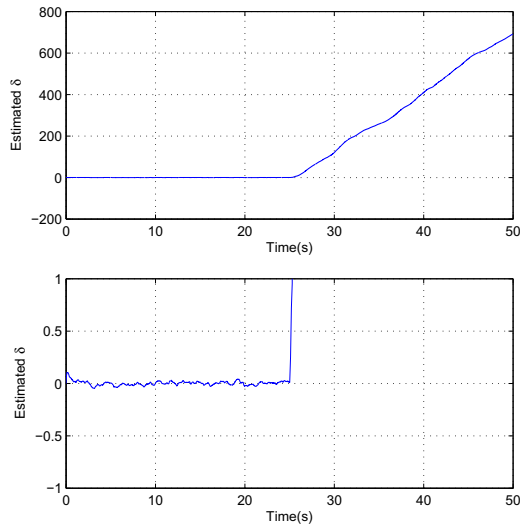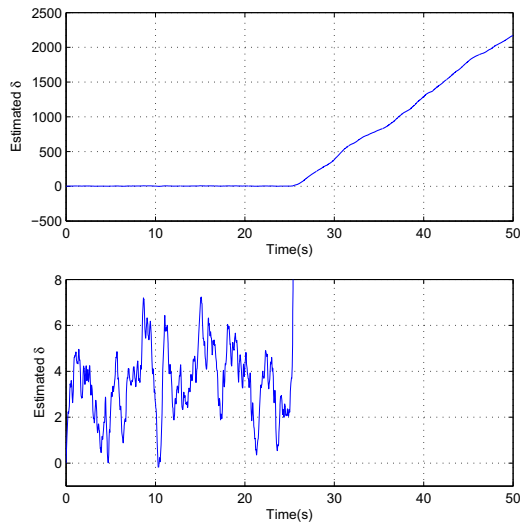**Figure 6.5:** The result of the mixed $\mathcal{H}_\infty$ / LMI method to the injected step fault (The upper graph is zoomed and illustrated in the lower graph).

$$\dot{\hat{x}} = (A - HC)\hat{x} + [B - HD \ \ H][u \ \ y_m]^T$$
$$\hat{y}_m = C\hat{x} + Du \tag{6.18}$$
$$\hat{\delta} = V[y_m - \hat{y}_m],$$

where $\hat{x}$ and $\hat{y}_m$ are the estimates of the state and measurement output vectors and the filter gains H and V are designed according to theorem 2 in (Zhong et al., 2003).

6.4.2   Comparison of Estimation Results

Figure 6.3 shows the comparison of the different designs for $\mathcal{H}_\infty$ and μ synthesis. It also shows that by reducing the γ of $\mathcal{H}_\infty$ optimization the estimation become more robust to the disturbances. The comparison of the $\mathcal{H}_\infty$ with μ-synthesis shows that in the no-fault interval (0-25s), the estimation has lower amount of fluctuations and is more robust. However, in the fault interval (25s-50s), the residual generated by $\mathcal{H}_\infty$ design is more robust to the disturbances.

Figure 6.4 shows the output of the estimated residual generated by the mixed $\mathcal{H}_2$ / $\mathcal{H}_\infty$ design method. As the change in the parameter results in instability, the estimated residual is also unbounded. Consequently, the estimated residual is not corresponding to the injected fault; however, it represents the existence of a fault.

In figure 6.5, a similar type of output (unbounded) is observed. The residual is the result of the mixed $\mathcal{H}_\infty$ / LMI design method which does not represent the estimation of the fault, though it is less robust to the disturbances compared to $\mathcal{H}_2$ / $\mathcal{H}_\infty$ design method.

In figures 6.6, 6.7, 6.8, 6.9, 6.10, 6.11, 6.12, and 6.13, the output of all four different FD filters are illustrated for different injected faults δ. These results show that the filter designed through μ-synthesis approach gives the best estimation of the injected fault in different scenarios.

6.4.3   Structural Analysis Results

The structural analysis, carried out on the propulsion engine model, identified 11 independent subsystems with inherent redundant information (hence it is possible to derive 11 different and linearly independent residual expressions). 6 of these subsystems exhibit dynamic behavior while the other 5 are of algebraic nature. 12 different faults were considered in this system. A preliminary analysis of the fault impacts on each subsystem (represented by a corresponding residual) suggested that all faults were detectable. In addition, 7 faults were isolable while the other faults were group-wise isolable, i.e.

a group of 2 faults and a group of 3 faults were isolable, but with no possibility of isolating the faults from each other in each group (Soltani and Izadi-Zamanabadi, 2007). Detailed design of fault diagnosis algorithms for each subsystem (in particular those with dynamic behavior) were then carried out and the results were compared with the evaluation results of the fault detectability/isolability from structural analysis. They showed an exact match. Despite being a simple qualitative method the structural analysis showed to be an extremely powerful tool for developing health monitoring systems in complex dynamical systems.

6.5   Conclusion

The structural analysis approach was used in the research project to identify the monitorable parts/subsystems of a complex propulsion system and provide information about the possibility of detecting and isolating the considered faults in the system. In this paper, the process of using the structural analysis was briefly illustrated by applying it on a turbopump subsystem. A model-based fault estimation filter was employed to this subsystem. The filter was designed based on the parametric fault diagnosis filter design approach and used the $\mathcal{H}_\infty$ as well as the μ synthesis to solve the optimization problem. The chosen turbopump subsystem was used as the benchmark. To illustrate the capability of the employed methods the main results of the designed filters have been compared with the results from two other optimization based methods.
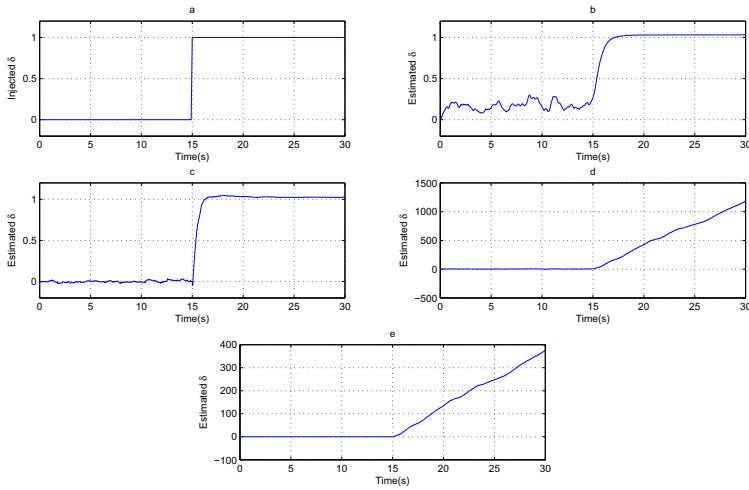
Figure 6.6: Fault injected as a step (a) the injected δ, (b) the residual provided by $\mathcal{H}_\infty$ design, (c) the residual provided by μ design, (d) the residual provided by $\mathcal{H}_2$ / $\mathcal{H}_\infty$ design, and (e) the residual provided by $\mathcal{H}_\infty$LMI design.
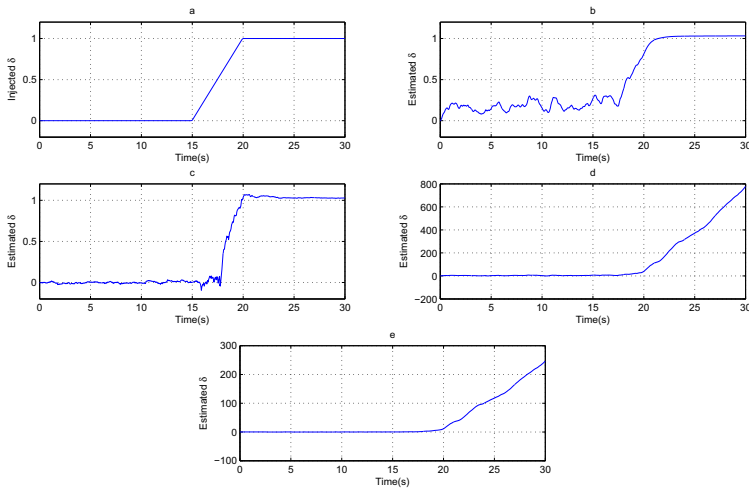
Figure 6.7: Fault injected as a fast ramped-raising step (a) the injected δ, (b) the residual provided by $\mathcal{H}_\infty$ design, (c) the residual provided by μ design, (d) the residual provided by $\mathcal{H}_2$ / $\mathcal{H}_\infty$ design, and (e) the residual provided by $\mathcal{H}_\infty$ / LMI design.
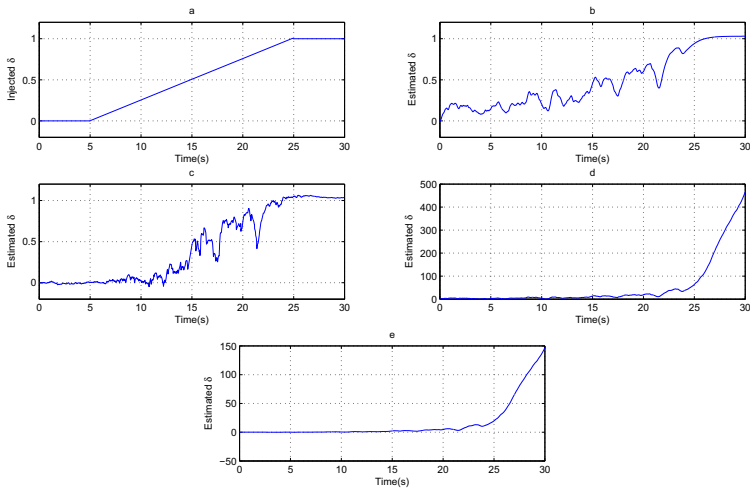
Figure 6.8: Fault injected as a slow ramped-raising step (a) the injected δ, (b) the residual provided by $\mathcal{H}_\infty$ design, (c) the residual provided by μ design, (d) the residual provided by $\mathcal{H}_2 / \mathcal{H}_\infty$ design, and (e) the residual provided by $\mathcal{H}_\infty$ / LMI design.
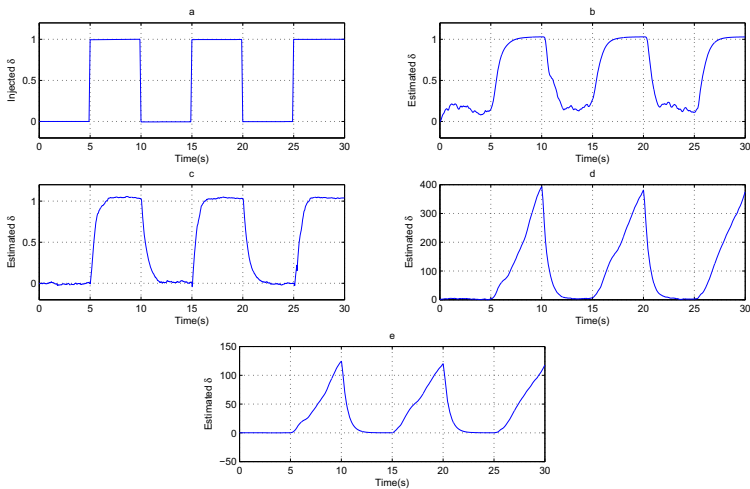
Figure 6.9: Fault injected as rectangular pulses (a) the injected δ, (b) the residual provided by $\mathcal{H}_\infty$ design, (c) the residual provided by μ design, (d) the residual provided by $\mathcal{H}_2 / \mathcal{H}_\infty$ design, and (e) the residual provided by $\mathcal{H}_\infty$ / LMI design.
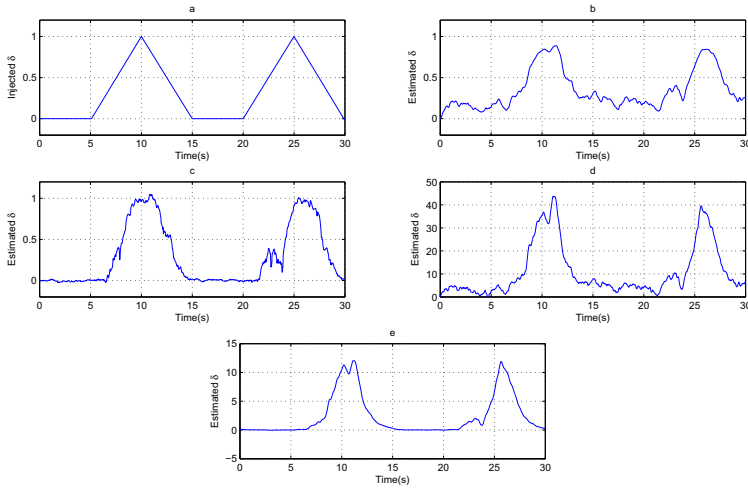
Figure 6.10: Fault injected as triangular pulses (a) the injected δ, (b) the residual provided by $\mathcal{H}_\infty$ design, (c) the residual provided by μ design, (d) the residual provided by $\mathcal{H}_2$ / $\mathcal{H}_\infty$ design, and (e) the residual provided by $\mathcal{H}_\infty$ / LMI design.
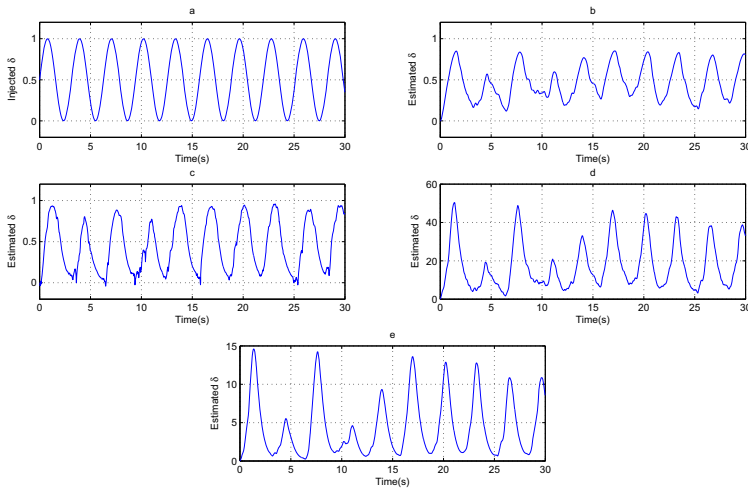
Figure 6.11: Fault injected as sine with the frequency of $2\frac{rad}{s}$ (a) the injected δ, (b) the residual provided by $\mathcal{H}_\infty$ design, (c) the residual provided by μ design, (d) the residual provided by $\mathcal{H}_2$ / $\mathcal{H}_\infty$ design, and (e) the residual provided by $\mathcal{H}_\infty$ / LMI design.
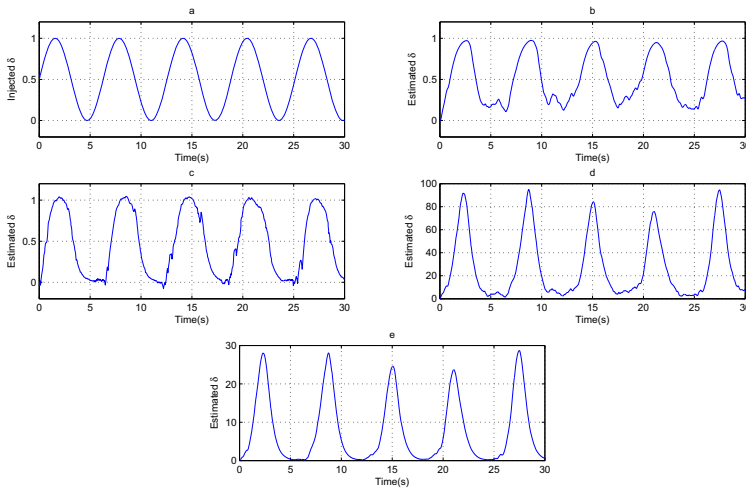
Figure 6.12: Fault injected as sine with the frequency of $1\frac{rad}{s}$ (a) the injected δ, (b) the residual provided by $\mathcal{H}_\infty$ design, (c) the residual provided by μ design, (d) the residual provided by $\mathcal{H}_2$ / $\mathcal{H}_\infty$ design, and (e) the residual provided by $\mathcal{H}_\infty$ / LMI design.
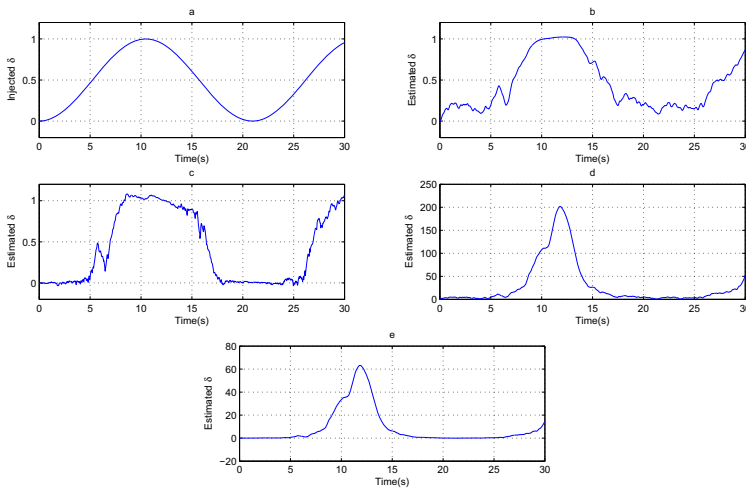
Figure 6.13: Fault injected as sine with the frequency of $0.3\frac{rad}{s}$ (a) the injected δ, (b) the residual provided by $\mathcal{H}_\infty$ design, (c) the residual provided by μ design, (d) the residual provided by $\mathcal{H}_2$ / $\mathcal{H}_\infty$ design, and (e) the residual provided by $\mathcal{H}_\infty$ / LMI design.

Chapter 7

Conclusions and Recommendations

This thesis considered analysis, design, and implementation of the fault diagnosis and fault tolerant control system on mechanical systems, namely, ship-mounted satellite tracking antenna. This chapter briefly reviews the main contributions and achievements of the work and proposes directions for further research.

7.1 Conclusions

In this thesis, both theoretical and practical aspects of fault diagnosis and fault tolerant control in an antenna system were combined together. In each chapter, the theoretical part of the method as well as the practical model were presented. The verification of the employed method was examined by means of experiments. The results of the implementations on the application verified the capabilities of the method. The conclusions are made according to the accomplishments in the following:

- The model of the satellite tracking antenna was derived in Chapter 2. This model included the sensors, actuators, tracking dynamics, and ship motions. The dynamic and kinematic parts of the model was combined together and formulated in order to be used by the control and/or fault diagnosis system design. The verification of the model in (Soltani, 2006) showed that the mentioned model could closely simulate the real tracking antenna. Furthermore, the possible faults on the system have been analyzed and the most severe faults, which were on the beam sensor, were chosen to be detected.

- A fault diagnosis method, based on optimization approaches that are commonly used in robust control theory, was employed. In this method, the system dynamics

has been formulated in a standard set-up for robust control based on LFT's. In this set-up the parametric faults were estimated and introduced as the residuals of the FDI system.

- As the generated dynamical model of the satellite tracking antenna was highly nonlinear, a nonlinear version of the aforementioned fault estimation method was introduced and implemented on the antenna system. The implementation results verified that the method is suitable for detecting the considered faults.

- Beside the nonlinearity, it was emphasized that the waves were the major disturbances acting on the ship-mounted antenna system. The proposed fault diagnosis system was developed in a format so that it was able to distinguish between the faults and the disturbances. The goal was achieved by introducing different weighting filters to the fault and disturbance system in the design procedure.

- The design of the weighting filters was investigated and it was concluded that choosing narrow-band filters for fault/disturbance results in less robust estimation while choosing wide-band filters causes slower estimation.

- A nonlinear internal model control was introduced as an additional control algorithm to be employed by the fault tolerant control system. The internal model control was able to simultaneously solve the tracking problem and reject the external disturbances. The dynamic behavior of these disturbances were generated by a system, called exosystem, which emulated the effect of the waves on the ship motion. The employed exosystem belongs to the class of the dynamical systems for which the internal model control can suitably handle the disturbance rejection problem. Implementation and test of the proposed controller on the ship simulator test facility illustrated the success of the designed controller.

- To cope with the considered faults in the system a fault tolerant control strategy was employed. The fault tolerant control system, which works based on switching between the controllers, was able to keep the direction of the antenna toward the satellite in the situations where the fault occurred and/or the disturbances forced the pointing vector to diverge. This was beneficial since the antenna does not need to perform the time consuming sky search (to find the satellite) after the fault (signal blocking or satellite temporal shut down) is disappeared. Furthermore, it prevents the antenna system to become unstable. Eventually, the results of the FTC system implementation on the ship simulator test set-up verified the capability of the developed fault tolerant control strategy.

- The robust fault diagnosis method was compared with two other methods while the FD approach itself was solved through two different optimization tools- $\mathcal{H}_\infty$

and μ-synthesis. The comparison of four mentioned FD filter designs on the Hopper's propulsion subsystem showed that the μ-synthesis method gave the best results for fault detection/estimation.

7.2 Recommendations

This thesis did not cover a number of issues. It is suggested to continue the further investigations in the following directions:

- The residuals generated by the fault diagnosis system is in fact the estimation of the fault. By the aid of the designed fault diagnosis system, it becomes possible to estimate the faulty parameter. In this thesis, a threshold on the residual was used to determine when the controller should change the strategy. It is suggested for the future research to design a FTC system which is able to make an adaptive change to the control system regarding the estimation of the fault.

- The motor saturations can be considered as the constraints of the states of the system in further investigations. The control problem of the satellite tracking can be formulated into a hybrid control design problem when the model together with its constraints (see Appendix B) is considered. In particular, this becomes relevant when the antenna is used on ships sailing near the equator while the satellite is flying directly above the ship.

Bibliography

K. Adjallah, D. Maquin, and J. Ragot. Non-linear observer-based fault detection. *Control Applications, 1994., Proceedings of the Third IEEE Conference on*, pages 1115–1120 vol.2, 1994. doi: 10.1109/CCA.1994.381359.

M. Basseville. Detecting changes in signals and systems- a survey. *Automatica*, 24(3): 309–326, 1988.

R. V. Beard. *Failure accommodation in linear systems through self-Reorganization*. PhD thesis, Dep. Aeronautics and Astronautics, MIT, Cambridge, 1971.

W. Belau and J. Sommer. Definition of rsts reference scenarios, missions, vehicle configurations and s/s layout. *EADS report*, may 2006.

S. A. Bøgh. *Fault Tolerant Control Systems- A Development Method and Real-life Case Study*. PhD thesis, Dep. of Contr. Eng., Aalborg University, Denmark, 1997.

S. A. Bøgh, R. Izadi-Zamanabadi, and M. Blanke. Onboard supervisor for the ørsted satellite attitude control system. *The 5th Workshop on Artificial Intelligence and Knowledge Based Systems for Space*, pages 137–152, 1995.

M. Blanke. Consistent design of dependable control system. *Control Engineering Practice*, 4(9):1305–1312, 1996.

M. Blanke, M. Staroswiecki, and N. Wu. Concepts and methods in fault-tolerant control. *American Control Conference, 2001. Proceedings of the 2001*, 4:2606–2620 vol.4, 2001. doi: 10.1109/ACC.2001.946264.

M. Blanke, M. Kinnaert, J. Lunze, and M. Staroswieski. *Diagnosis and Fault-Tolerant Control*. Springer, 2006.

E. Bokor and L. Keviczky. An $\mathcal{H}_\infty$ filtering approach to robust detection of failures in dynamical systems. In *Proceedings of the 33rd Conference on Decision and Control*, pages 3037–3039, Lake Buena Vista, FL, USA, 1994.

C. L. Bretschneider. Wave variability and wave spectra for wind generated gravity waves. Technical report, Beach Erosion Board, Corps. of Engineers. 118, 1959.

C. Cheah, C. Liu, and J. Slotine. Adaptive jacobian tracking control of robots with uncertainties in kinematic, dynamic and actuator models. *Automatic Control, IEEE Transactions on*, 51(6):1024–1029, 2006a. ISSN 0018-9286. doi: 10.1109/TAC.2006. 876943.

C. C. Cheah, C. Liu, and J. J. E. Slotine. Adaptive Tracking Control for Robots with Unknown Kinematic and Dynamic Properties. *The International Journal of Robotics Research*, 25(3):283–296, 2006b. doi: 10.1177/0278364906063830.

J. Chen and R. J. Patton. Robust model-based fault diagnosis for dynamic system. *Kluwer Academic Publishers*, 1999.

W. Chung and J. Speyer. A game theoretic fault detection filter. *Automatic Control, IEEE Transactions on*, 43(2):143–161, 1998. ISSN 0018-9286. doi: 10.1109/9. 661064.

J. De Cuyper and M. Verhaegen. State Space Modeling and Stable Dynamic Inversion for Trajectory Tracking on an Industrial Seat Test Rig. *Journal of Vibration and Control*, 8(7):1033–1050, 2002.

C. De Persis and A. Isidori. A geometric approach to nonlinear fault detection and isolation. *Automatic Control, IEEE Transactions on*, 46(6):853–865, 2001. ISSN 0018-9286. doi: 10.1109/9.928586.

S. Devasia, D. Chen, and B. Paden. Nonlinear inversion-based output tracking. *Automatic Control, IEEE Transactions on*, 41(7):930–942, 1996. ISSN 0018-9286. doi: 10.1109/9.508898.

R. Douglas and J. Speyer. An h-infinity bounded fault detection filter. *American Control Conference, 1995. Proceedings of the*, 1:86–90 vol.1, 1995.

A. M. Edelmayer and J. Bokor. Scaled h-infinity filter for sensitivity optimization of detection filters. *in Proceeding of the 17th Triennial World Congress of IFAC*, pages 324–330, 2000.

A. M. Edelmayer, J. Bokor, and L. Keviczky. H-infinity filter design for linear systems: comparison of two approaches. *in Proceeding of the 13th Triennial World Congress of IFAC*, pages 37–42, 1996.

C. Edwards, S. Spurgeon, and R. Patton. Sliding mode observers for fault detection and isolation. *Automatica*, 36:541–553(13), 2000. doi: doi:10.1016/S0005-1098(99) 00177-6.

T. Fossen. *Marine Control Systems: Guidance, Navigation and Control of Ships, Rigs, and Underwater Vehicles*. Marine Cybernetics, Trondheim, Norway, 2002.

P. Frank. Fault diagnosis in dynamic systems using analytic and knowledge-based redundancy - A survey and some new results. *Automatica*, 26:459–474, 1990.

P. M. Frank. Fault diagnosis in dynamic system via state estimation- a survey. *in Tzafestas, Singh, and Schmidt (eds), System fault diagnostics, reliability, and related knowledge based approaches*, 1:35–98, 1987.

P. M. Frank and X. Ding. Frequency domain approach to optimally robust residual generation and evaluation for model-based fault diagnosis. *Automatica*, 30(5):789–804, 1994. ISSN 0005-1098.

P. M. Frank and L. Keller. Sensitivity discriminating observer design for instrument failure detection. *IEEE Trans. Aero. and Electron. Syst.*, AES-16:460–467, 1981.

P. M. Frank and J. Wunnenberg. robust fault diagnosis using unknown input schemes. *Book chapter, Fault diagnosis in dynamic systems: theory and application, Printice Hall, chpter 3*, pages 47–98, 1989.

E. Frisk and L. Nielsen. Robust residual generation for diagnosis including a reference model for residual behavior. *in Proceeding of the 16th Triennial World Congress of IFAC*, 1999.

Z. Gao and P. Antsaklis. On the stability of the pseudo-inverse method for reconfigurable control systems. *Aerospace and Electronics Conference, 1989. NAECON 1989., Proceedings of the IEEE 1989 National*, pages 333–337 vol.1, 1989. doi: 10.1109/NAECON.1989.40232.

D. Hengy and P. M. Frank. Component failure detection via nonlinear state observer. *in Proceeding of IFAC Workshop on Fault Detection and Safety in Chemical Plants*, pages 153–157, 1986.

R. F. Huang and C. Y. Stangel. Restructurable control using proportional integral implicit model following. *Journal of Guidance, Control, and Dynamics*, 13:303–309, 1990.

L. Hunt, G. Meyer, and R. Su. Computing particular solutions. *Decision and Control, 1994., Proceedings of the 33rd IEEE Conference on*, 3:2520–2521 vol.3, 1994. doi: 10.1109/CDC.1994.411522.

Inmarsat. *Ship Motion Specifications*. Inmarsat Global Ltd, London, 2003.

R. Isermann. *Fault-Diagnosis Systems: An Introduction from Fault Detection to Fault Tolerance*. Springer, 2006.

A. Isidori, L. Marconi, and A. Serrani. Robust nonlinear motion control of a helicopter. *IEEE Trans. Automat. Contr.*, 48:413 – 426, 2003a.

A. Isidori, L. Marconi, and A. Serrani. *Robust Autonomous Guidance: An Internal Model Approach*. Springer, London, England, 2003b.

R. Izadi-Zamanabadi. *Fault-tolerant Supervisory Control System Analysis and Logic Design*. PhD thesis, Dep. of Contr. Eng., Aalborg University, Denmark, 1999.

T. Johansen, T. Fossen, S. Sagatun, and F. Nielsen. Wave synchronizing crane control during water entry in offshore moonpool operation-experimental results. *IEEE J. Oceanic Eng.*, 28:720 – 728, 2003.

H. L. Jones. *Failure detection in linear system*. PhD thesis, Dep. Aeronautics and Astronautics, MIT, Cambridge, 1973.

R. Jørgensen, R. Patton, and J. Chen. An eigenstructure assignment approach to FDI for the industrial actuator benchmark test. *Control Eng. Practice*, 3:1751–1756, 1995.

R. B. Jorgensen. *Development and Test of Methods for Fault Detection and Isolation*. PhD thesis, Aalborg University, Department of Electronic Systems, 1995.

M. J. Khosrowjerdi, R. Nikoukhah, and N. SafariShad. Fault detection in a mixed $h2/h_\infty$ setting. *IEEE Trans. on Automatic Control*, 50(7):1063–1068, 2005.

V. Krishnaswami and G. Rozzoni. Nonlinear parity equation residual generation for fault detection and isolation. *Preprints of the IFAC Sympo. on Fault Detection, Supervision and Safety for Technical Processes, SAFEPROCESS'94*, 1:317–322, 1994.

V. Krishnaswami, G.-C. Luh, and G. Rizzoni. Nonlinear parity equation based residual generation for diagnosis of automotive engine faults. *Control Engineering Practice*, 3: 1385–1392(8), 1995. doi: doi:10.1016/0967-0661(95)00141-G.

J. Lunze. Qualitative modelling of linear dynamical systems with quantized state measurements. *Automatica*, 30(3):417–431, 1994. ISSN 0005-1098.

J. Lunze and F. Schiller. Logic-based process diagnosis utilizing the causal structure of dynamical systems. *IFAC/IFIP/IMACS Int. Sympo. on Artificial Intelligence in Real-time Control*, pages 649–654, 1992.

J. M. Maciejowski, editor. *Predictive Control with Constraints*. Prentice Hall, 2002.

M. Maki, J. Jiang, and K. Hagino. A stability guaranteed active fault-tolerant control system against actuator failures. *Decision and Control, 2001. Proceedings of the 40th IEEE Conference on*, 2:1893–1898 vol.2, 2001. doi: 10.1109/.2001.981182.

R. Mangoubi, B. Appleby, and J. Farrell. Robust estimation in fault detection. *Decision and Control, 1992., Proceedings of the 31st IEEE Conference on*, 2:2317–2322, 1992.

R. Mangoubi, B. Appleby, G. Verghese, and W. Vander Velde. A robust failure detection and isolation algorithm. *Decision and Control, 1995., Proceedings of the 34th IEEE Conference on*, 3:2377–2382 vol.3, 1995. doi: 10.1109/CDC.1995.480694.

R. S. Mangoubi, editor. *A Robust Estimation and Failure Detection: A Consise Treatment*. Springer Verlag, 1998.

R. S. Mangoubi and A. M. Edelmayer. Model based fault detection: the optimal past, the robust present, and a few thoughts on the future. *in Proceeding of the 17th Triennial World Congress of IFAC*, pages 64–75, 2000.

M.-A. Massoumnia. A geometric approach to the synthesis of failure detection filters. *Automatic Control, IEEE Transactions on*, 31(9):839–846, 1986. ISSN 0018-9286.

M.-A. Massoumnia, G. Verghese, and A. Willsky. Failure detection and identification. *Automatic Control, IEEE Transactions on*, 34(3):316–321, 1989. ISSN 0018-9286. doi: 10.1109/9.16422.

R. K. Mehra and J. Peschon. An innovations approach to fault detection andiagnosis in dynamic systems. *Automatica*, 7:637–640, 1971.

M. R. Napolitano, C. Neppach, V. Casdorf, S. Naylor, M. Innocenti, and G. Silvestri. Neural-netwotk-based scheme for sensor failure detection, identification, and accommodation. *J. of Guidance, Contr. and Dynamics*, 16(6):1280–1286, 1995.

C. Nett, C. Jacobson, and A. Miller. An integrated approach to controls and diagnostics: The 4-parameter controller. In *Proceedings of the American Control Conference*, pages 824–835, 1988.

G. Neumann. *On Wind-Generated Ocean Waves with Special Reference to the Problem of Wind Forecasting*. New York University, College of Eng. Res. Div., 1952.

G. Neumann. *A Proposed Spectral Form for Fully Developed Wind Seas Based on The Similarity Theory of S. A. Kitaigorodskii*. U.S. Naval Oceanographic, 1963.

H. Niemann and J. Stoustrup. Design of fault detectors using h-infinity optimization. *Proceedings of the 39th IEEE Conference on Decision and Control*, pages 4327–4328, Dec. 2000.

H. Niemann and J. Stoustrup. Integration of control and fault detection: nominal and robust design. *IFAC Fault Detection, Supervision and Safety for Technical Processes. Hull, UK. pp. 341– 346.*, 1997.

R. Nikoukhah. Innovations generation in the presence of unknown inputs: application to robust failure detection. *Automatica*, 30(12):1851–1867, 1994. ISSN 0005-1098.

J. Park and G. Rizzoni. A new interpretation of the detection filter: Part i- a closed form algorithm. *International Journal of Control*, 60:767–787, 1994.

R. Patton and J. Chen. Neural networks in nonlinear dynamic systems fault diagnosis. *Engineering Simulation (on Engineering Diagnostics)*, 13(6):905–924, 1996.

R. Patton, J. Chen, and T. Siew. Fault diagnosis in nonlinear dynamic systems via neural networks. *Control, 1994. Control '94. Volume 2., International Conference on*, pages 1346–1351 vol.2, 1994.

R. J. Patton. Fault-tolerant control: The 1997 situation. *Preprints of the IFAC Sympo. on Fault Detection, Supervision and Safety for Technical Processes*, pages 1033–1055, 1997.

R. J. Patton and J. Chen. Robust fault detection of jet engine sensor system using aigenstructur assignment. *Journal of Guidance, Control, and Dynamics*, 15:1491–1497, 1992.

R. J. Patton and S. M. Kangethe. Robust fault diagnosis using eigenstructure assignment of observers. *Fault diagnosis in dynamic systems: theory and application, Print-ice Hall, chpter 3*, pages 99–154, 1989.

T. Perez and M. Blanke. A simple method to tune shaping filters for simulation of ship motion in irregular seas. Technical report, University of Newcastle and Technical University of Denmark, 2002.

H. Rauch. Autonomous control reconfiguration. *Control Systems Magazine, IEEE*, 15 (6):37–48, 1995. ISSN 0272-1708. doi: 10.1109/37.476385.

D. Sauter and F. Hamelin. Frequency-domain optimization for robust fault detection and isolation in dynamic systems. *Automatic Control, IEEE Transactions on*, 44(4): 878–882, 1999. ISSN 0018-9286. doi: 10.1109/9.754839.

S. M. N. Soltani. Model verification of a satellite tracking antenna. Technical report, Aalborg University, Denmark, June 2006.

S. M. N. Soltani and R. Izadi-Zamanabadi. Fault detection and diagnosis of hopper engine. Technical report, Aalborg University, June 2007.

S. M. N. Soltani, R. Izadi-Zamanabadi, and R. Wisniewski. High precision control of ship-mounted satellite tracking antenna. In *Proceedings European Control Conference*, pages 368–374, Kos, Greece, 2007.

S. M. N. Soltani, R. Izadi-Zamanabadi, and J. Stoustrup. Parametric fault estimation based on $\mathcal{H}_\infty$ optimization in a satellite launch vehicle. In *Proceedings of IEEE Multi-conference on Systems and Control (CCA)*, San Antonio, Texas (USA), 2008a.

S. M. N. Soltani, R. Izadi-Zamanabadi, and R. Wisniewski. Robust fdi for a ship-mounted satellite tracking antenna: A nonlinear approach. In *Proceedings of IEEE Multi-conference on Systems and Control (CCA)*, San Antonio, Texas (USA), 2008b.

S. M. N. Soltani, R. Izadi-Zamanabadi, and R. Wisniewski. Fault tolerant control of ship-mounted satellite tracking antenna. *Submitted to IEEE Trans. Contr. Syst. Technol.*, 2008c.

S. M. N. Soltani, R. Izadi-Zamanabadi, R. Wisniewski, W. Belau, and S. LeGonidec. Robust fdi for hopper engine subsystem. *Accepted for the AIAA/ ASME/ SAE/ ASEE Joint Propulsion Conference, Hartford, Connecticut, USA*, 2008d.

J. Sommer and W. Belau. System engineering requirements and features impacting the hms. *EADS report*, may 2006.

J. Stoustrup and H. Niemann. Fault detection and isolation in systems with parametric faults. In *Proc. IFAC World Congress*, pages 139–144, Volume P, Beijing, China, July 1999.

J. Stoustrup and H. Niemann. Fault estimation-a standard problem approach. *Int. J. Robust Nonlinear Control*, 12:649–673, 2002.

J. Stoustrup, M. Grimble, and H. Niemann. Design of integrated systems for the control and detection of actuator/sensor faults. *Sensor Review*, 17(2):138 – 149, 1997. doi: 10.1108/02602289710170311.

G. P. Sutton and O. Biblarz. *Rocket Propulsion Elements*. Wiley Interscience, New York, 2001.

S. Tanaka and S. Nishifuji. Automatic on-line measurement of dynamic ship's attitude. In *20th International Conference on Industrial Electronics, Control and Instrumentation, 1994. IECON '94.*, volume 3, pages 2005 – 2010, Sept. 1994.

S. Tanaka and S. Nishifuji. On-line sensing system of dynamic ship's attitude by use of servo-type accelerometers. *IEEE J. Oceanic Eng.*, 20:339 – 346, 1995.

M. T. Tham. *Lecture Notes on Introduction to Robust Control*. University of Newcastle Upon tyne, 2002.

H. Tseng and D. Teo. Ship-mounted satellite tracking antenna with fuzzy logic control. *IEEE Trans. Aerosp. Electron. Syst.*, 34:639–645, 1997.

M. Tyler and M. Morari. Optimal and robust design of integrated control and diagnostic modules. *In Proceedings of the 1994 American Control Conference, pages 2060–2064, Baltimore, MD*, 1994.

N. Viswanadham and R. Srichander. Fault detection using unknown input observers. *Control Theory and Advanced Technology*, 3(2):91–101, 1987.

K. Watanabe, I. Matsuura, M. Abe, M. Kubota, and D. M. Himmelblau. Incipient fault diagnosis of chemical processes via artificial neural networks. *AIChE Journal*, 35(11): 1803–1812, 1989. ISSN 1547-5905.

J. Wertz. *Spacecraft Attitude Determination and Control*. Kluwer Academic Publishers, Boston, USA, 1978.

J. White and J. Speyer. Detection filter design: Spectral theory and algorithms. *Automatic Control, IEEE Transactions on*, 32(7):593–603, 1987. ISSN 0018-9286.

M. Willis, C. Di Massimo, G. Montague, M. Tham, and A. Morris. Artificial neural networks in process engineering. *Control Theory and Applications, IEE Proceedings D [see also IEE Proceedings-Control Theory and Applications]*, 138(3):256–266, 1991. ISSN 0143-7054.

A. S. Willsky. A survey of design methods for failure detection in dynamic systems. *Automatica*, 12:601–611, 1996.

A. S. Willsky and H. L. Jones. A generalized likelihood ratio approach to the detection and estimation of jumps in linear systems. *IEEE Trans. Automat. Contr.*, AC-21(1): 108–112, 1976.

W. M. Wonham, editor. *Linear Multivariable Control: A Geometric Approach*. Springer-Verlag. 2nd Edition, 1985.

J. Wunnenberg. *Linear and Nonlinear Robust Fault Detection in Dynamic Systems*. PhD thesis, University of Duesburg, FRG, 1990.

H. Yang and M. Saif. State observation, failure detection and isolation (fdi) in bilinear systems. *Decision and Control, 1995., Proceedings of the 34th IEEE Conference on*, 3:2391–2396 vol.3, 1995. doi: 10.1109/CDC.1995.480697.

Z. Yang and M. Blanke. The robust control mixer module method for control reconfiguration. *American Control Conference, 2000. Proceedings of the 2000*, 5:3407–3411 vol.5, 2000. doi: 10.1109/ACC.2000.879200.

D. Yu and D. N. Shields. A bilinear fault detection filter. *International Journal of Control*, 68:417–430(14), 1997.

D. Yu, D. Shields, and J. Mahtani. Fault detection for bilinear systems with application to a hydraulic system. *Control Applications, 1994., Proceedings of the Third IEEE Conference on*, pages 1379–1384 vol.2, 1994a. doi: 10.1109/CCA.1994.381323.

D. Yu, D. Shields, and J. Mahtani. A nonlinear fault detection method for a hydraulic system. *Control, 1994. Control '94. Volume 2., International Conference on*, pages 1318–1322 vol.2, 1994b.

M. Zhong, S. X. Ding, J. Lam, and H. Wang. An lmi approach to design robust fault detection filter for uncertain lti systems. *Automatica*, 39:543–550, 2003.

K. Zhou, K. Glover, B. Bodenheimer, and J. Doyle. Mixed h-2 and h-infinity performance objectives. i. robust performance analysis. *Automatic Control, IEEE Transactions on*, 39(8):1564–1574, 1994. ISSN 0018-9286. doi: 10.1109/9.310030.

K. Zhou, J. C. Doyle, and K. Glover, editors. *Robust and Optimal Control*. Prentice Hall, 1996.

Appendix A

Parametric Fault Estimation Based on $\mathcal{H}_\infty$ Optimization in A Satellite Launch Vehicle

Abstract- *Correct diagnosis under harsh environmental conditions is crucial for space vehicles' health management systems to avoid possible hazardous situations. Consequently, the diagnosis methods are required to be robust toward these conditions. Design of a parametric fault detector, where the fault estimation is formulated in the so-called standard set-up for $\mathcal{H}_\infty$ control design problem, is addressed in this paper. In particular, we investigate the tunability of the design through the dedicated choice of the fault model. The method is applied to the model of turbopump as a subsystem of the jet engine for the satellite launch vehicle and the results are discussed.*

A.1   Introduction

Reliability is an essential topic within many industrial sectors, in particular the aerospace industry as no possible and foreseeable fault should interrupt the mission objectives of a spacecraft (or a launch vehicle). In this regards, having the capability of continuous monitoring of the system states e.g., the ability to diagnose the system's dynamics behavior, is a necessity in order to implement fault tolerant strategies.

Fault diagnosis has since the 1980s been an active research topic. Depending on the models that have been used to describe the systems, model based (linear/nonlinear) or others, different approaches have been proposed (Jørgensen et al., 1995), (Blanke et al., 2006), and (Isermann, 2006). One of the important problems that has attracted attention

of most in this research community is the robustness issue that arises due to the fact that there is some mismatch (however small) between the derived model and the real system dynamics.

The particular focus in this paper is on employing methods for fault diagnosis which have been inspired by and derived from the area of robust control theory, or in wider generality of optimization based control synthesis methods. An early paper, which suggested combining methods for diagnosis and control was (Nett et al., 1988). (Bokor and Keviczky, 1994) suggested to use $\mathcal{H}_\infty$ optimization to design fault diagnosis filters. The methods that used dedicated and specialized filter structures were presented in (Mangoubi, Appleby, and Farrell, 1992; Mangoubi et al., 1995; Mangoubi, 1998; Mangoubi and Edelmayer, 2000). Parametric faults are here of main interests as the real nature of many faults is in fact parametric. A fault diagnosis approach for systems with parametric faults has been used. Such an approach was presented in (Stoustrup and Niemann, 1999), (Stoustrup and Niemann, 2002), and (Niemann and Stoustrup, 2000). However, very few applications of this method has been reported (Soltani et al., 2008b).

In this paper, systems with parametric faults are studied in more details and extra notes are added such as introducing the fault model as a design factor to improve the performance of $\mathcal{H}_\infty$ optimization-based method and a practical algorithm for estimating the uncertain fault parameter. The main results of this paper are applied to the launch vehicle simulator.

A key element for the re-usability and maintainability of a space vehicle is provided by *health management system* (HMS) that is an integral part of the system design (Sommer and Belau, 2006). Part of the health management system's responsibility is to perform diagnosis on different parts of the launch vehicle's dynamic behavior, herein the engines. The HMS shall be able to diagnose faults of which the effect is hardly recognizable due to system uncertainties (unpredictable environmental conditions or system parameters). In addition, as the dynamics of the engines are highly nonlinear and varies depending on flight phases it is required that the corresponding diagnosis algorithms are sufficiently robust in order to avoid false-detection scenarios.

The paper is arranged as follows: In Section A.2, dynamics of the turbopumps of the engine is explained. In Section A.3, the employed method is discussed, the problem has been formulated into the standard set-up, and the fault detector for the system has been designed regarding the design factor. In section A.4, an algorithm to estimate the uncertainty is proposed and the fault estimation results of the obtained filter for the different designs are compared. Finally, section A.5 provides the conclusion of the paper.
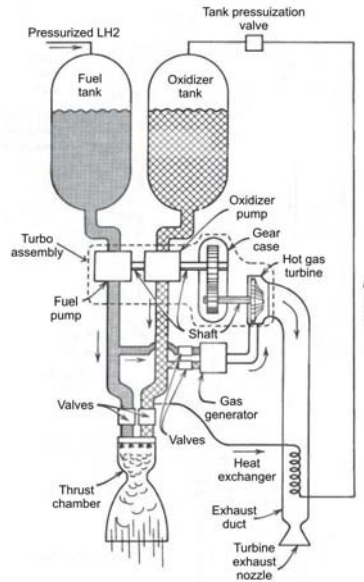
Tank pressuization valve

Pressurized LH2

Fuel tank

Oxidizer tank

Oxidizer pump

Gear case

Turbo assembly

Hot gas turbine

Fuel pump

Shaft

Valves

Gas generator

Valves

Heat exchanger

Thrust chamber

Exhaust duct

Turbine exhaust nozzle

Figure A.1: Simple diagram of liquid propellant engine containing turbopump feed system and gas generator (Sutton and Biblarz, 2001).

A.2 Problem Formulation

A.2.1 Turbopump Model

The assembly of a turbine with one or more pumps is called a turbopump. Its purpose is to raise the pressure of the following propellant. Its principal subsystems are a hot gas powered turbine and one or two propellant pumps. It is a high precision rotation machine, operating at high shaft speed with severe thermal gradients and large pressure changes, it usually is located next to a thrust chamber, which is a potential source of noise and vibration. The principal components of the engine with turbopump system is shown in the simplified diagram of figure A.1.

In the gas generator cycle, the turbine inlet gas comes from a separate gas generator. This cycle is relatively simple; the pressure in the liquid pipes and pumps are low but the pressure ratio across the turbine is relatively high; however, the turbine or gas generator flow is small compared to the closed cycle.

Cryogenic propellants use LOX-LH2 (Liquid Oxygen-Liquid hydrogen). Liquid hydrogen LH2 is sub-cooled below its normal boiling point to increase its density (propellant densification) and to reduce vapor pressure and correspondingly also tank pressure, tank

size, tank mass, and turbopumps power demand. For the same reasons liquid oxygen LOX is sub-cooled. The required pump flow is established by the design for a given thrust, effective exhaust velocity, propellant densities, and mixture ratios.

The dynamic model of LH2 turbopump includes three important elements: the pump speed R_h, the pump flow Q_h, and the mixture ratio R_{oh}. In a simplified way, the dynamics of LH2 turbopump is as follows

$$\dot{R}_h = \frac{a_h Q_h^2}{R_{oh}} + b_h Q_h R_h + c_h R_{oh} R_h^2 + b T_h, \tag{A.1}$$

where a_h, b, b_h, and c_h are constant coefficients depending on the design of the turbopump and T_h is the LH2 turbine torque. The same model can be used for LOX turbopump while to avoid repeating design procedure, we only continue with LH2 turbopump.

A.2.2 Fault Discussion

Efficiency loss (δ_h) has been considered as a parametric fault for LH2 turbopump. The more efficiency loss, the less change in speed. i.e., the dynamic equation is satisfied only for no fault case ($\delta_h = 0$). The fault augmented model is hence,

$$\dot{R}_h = (\frac{a_h Q_h^2}{R_{oh}} + b_h Q_h R_h + c_h R_{oh} R_h^2)(1 - \delta_h) + b T_h. \tag{A.2}$$

The linear representation of the LH2 pump dynamics is formulated as

$$\dot{R}_h = (-a R_h - c Q_h)(1 - \delta_h) + b T_h, \tag{A.3}$$

where a, b, and c are constant coefficients of the linear term of Taylor series about the operating point of the non-linear system.

A.3 Method

A.3.1 Robust Parametric FDI in A Standard Set-up

A general concept of parametric fault detection architecture in a robust standard set-up is proposed in (Stoustrup and Niemann, 2002). The approach is to model a potentially

faulty component as a nominal component in parallel with a (fictitious) error compo-
nent. The optimization procedure suggested here then tries to estimate the ingoing and
outgoing signals from the error component. This works only well in cases where the
component is reasonably well excited, but on the other hand, if the component is not
active at all, there is absolutely no way to detect whether it is faulty. The considered
plant is described by the model

$$\begin{cases} \dot{x} = A_\Delta x + B_u u \\ y = C_y x + D_{yu} u \end{cases} \tag{A.4}$$

where A_Δ is the deviated matrix from the nominal value (A) by a dependency to the
fault where the dependency can be nonlinear. The fault should not change B and C.
When this is the case (as in our plant and many other applications where sensor and
actuator faults are supposed to be detected), it is possible to model such faults in the
setup given by (A.4) with an input/output filter by introducing fast dynamics for the
filter such as

$$\dot{x}_u = -W x_u + W c Q_h. \tag{A.5}$$

The possibly nonlinear parameter dependency of A_Δ is approximated with a polyno-
mial. Therefore,

$$A_\Delta = A + p(\delta) A, \tag{A.6}$$

where p is a polynomial or rational function of the parameter δ satisfying $p(0) = 0$ (the
non-faulty operation mode).

Finally, the model (A.4) is written in linear fractional transformation form. As a result
we get a system of the form

$$\begin{bmatrix} \dot{x} \\ z \\ y \end{bmatrix} = \left[\begin{array}{c|cc} A & B_f & B_u \\ \hline C_f & D_{zf} & 0 \\ C_y & 0 & D_{yu} \end{array} \right] \begin{bmatrix} x \\ f \\ u \end{bmatrix} \tag{A.7}$$

where z is the external output, f is the fault input signal, the matrix D_{zf} is well-posed
(LFT's are normally used), and the connection between z and f is given by

$$
\begin{aligned}
f &= \Delta_{par} z \\
\Delta_{par} &= \delta I.
\end{aligned}
\tag{A.8}
$$
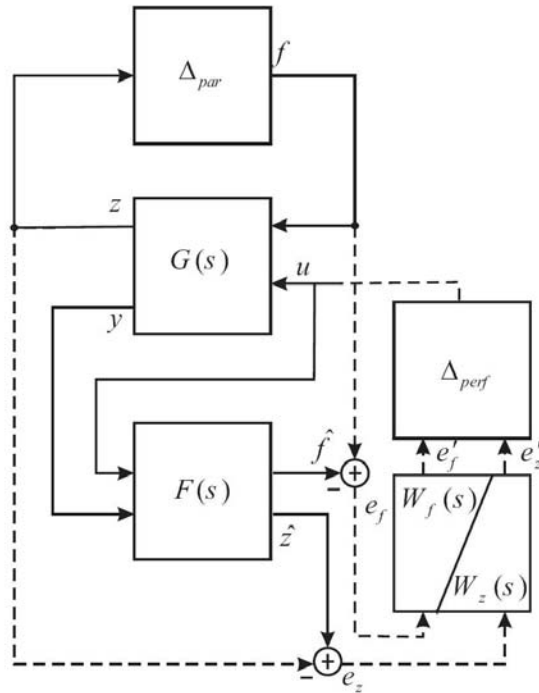
Figure A.2: Standard problem set-up for parametric fault detection combined with fictitious performance block (The dashed lines are the connections which are artificially assumed only for the design and they do not exist in implementation).

The next step in setting up the fault estimation problem as a standard problem is to introduce two fault estimation errors e_f ad e_z as

$$
\begin{cases}
e_f = f - \hat{f} \\
e_z = z - \hat{z}
\end{cases}
$$

where $\hat{f}$ and $\hat{z}$ are the estimation of f and z to be generated by the filter respectively.

Figure A.2 shows the setup for this approach. In order to design a filter F such that applying F to u and y provides the two desired estimates $\hat{f}$ and $\hat{z}$ one additional step is required, which is the introduction of a fictitious performance block Δ_{perf} ; suggesting that the input u was generated as a feedback Δ_{perf} from the outputs $\begin{bmatrix} e_f \\ e_z \end{bmatrix}$

$$u = \Delta_{perf} \begin{bmatrix} e_f \\ e_z \end{bmatrix}. \tag{A.9}$$

Therefore, two filters are introduced to make sure that the norm of $\frac{\|e_f\|}{\|f\|}$ is minimized in the frequency area of interest. (For incipient faults a low frequency filter is used.)

For instance,

$$\begin{aligned} \dot{x}_{ef} &= A_{ef}x_{ef} + B_{ef}e_f \\ \acute{e}_f &= C_{ef}x_{ef} + D_{ef}e_f \end{aligned} \tag{A.10}$$

so $\acute{e}_f = W_f(s)e_f$. The same procedure for e_z will be

$$\begin{aligned} \dot{x}_{ez} &= A_{ez}x_{ez} + B_{ez}e_z \\ \acute{e}_z &= C_{ez}x_{ez} + D_{ez}e_z \end{aligned} \tag{A.11}$$

i.e., $\acute{e}_z = W_z(s)e_z$. It should be noticed that these filters are only considered in the design phase, but they are not used in the implementation. In fact, we introduce these filters to handle the high excitation level of the inputs. Finally we introduce

$$\Delta = \begin{bmatrix} \Delta_{par} & 0 \\ 0 & \Delta_{perf} \end{bmatrix}. \tag{A.12}$$

The significance of the Δ_{perf} block is the following. According to the small gain theorem, the $\mathcal{H}_\infty$ norm of the transfer function from u to $\begin{bmatrix} \acute{e}_f \\ \acute{e}_z \end{bmatrix}$ is bounded by γ if and only if the system in figure A.2 is stable for all Δ_{perf}, $\| \Delta_{perf} \|_\infty < \gamma$. Hence, the problem of making the norm of the fault estimation error bounded by some quantity has been transformed to a stability problem. Eventually, the main result for FDI problem with parametric fault is provided by the following (Stoustrup and Niemann, 2002):

Theorem 1 *Let $F(s)$ be a linear filter applied to the system as in figure A.2 as $\begin{bmatrix} \hat{f} \\ \hat{z} \end{bmatrix} = F \begin{bmatrix} u \\ y \end{bmatrix}$, and assume that $F(s)$ satisfies:*

$$\| \mathcal{F}_l(G_{\tilde{z}\tilde{w}}, F) \|_\infty < \gamma, \tag{A.13}$$

where $\tilde{z} = \begin{bmatrix} z \\ \acute{e}_f \\ \acute{e}_z \end{bmatrix}$, $\tilde{w} = \begin{bmatrix} f \\ u \end{bmatrix}$, and $\mathcal{F}_l(.)$ is the lower Linear Matrix Transformation (LFT) representation of the two connected blocks (Zhou et al., 1996). Then the resulting fault estimation error is bounded by

$$\| \begin{bmatrix} \acute{e}_f \\ \acute{e}_z \end{bmatrix} \|_\infty < \gamma N \tag{A.14}$$

where N is the excitation level of the system i.e., $\| u \|_\infty = N$.

A.3.2   Design of The Fault Detector for Turbopump

The important fact which is emphasized in this paper is that the result we get from our design is fairly tunable by the model of the fault we consider in (A.6). This is the place we investigate in more details and finally perform the system (A.7). (For convenience, we avoid using the index h for δ_h and apply this to the end of the paper.)

Considering the fact that our uncertain parameter (as efficiency loss) in (A.2) changes from 0 to 1, it is obvious that the $\mathcal{H}_\infty$ design will be conservative because we only use half the range we considered in our design ($-1 < \delta < 1$). Thus, the basic assumptions are used for the fault model $p(\delta)$ are that it should satisfy the boundary conditions (in addition to $p(0) = 0$) as

$$p(-1) = 1$$

and

$$p(1) = 1.$$

A fast search for such functions is relatively easy by choosing polynomials as the structure of such function. To reduce the number of degrees of freedom and complexity of the system it is suggested to choose a low order polynomial. In the case of choosing

a second order polynomial, there is only one unique function satisfying the conditions $(p(\delta) = \delta^2)$ so we consider the third order case which has more generality and degree of freedom.

A third order polynomial $p(\delta) = \beta_3\delta^3 + \beta_2\delta^2 + \beta_1\delta + \beta_0$ which satisfies the mentioned conditions has the form

$$p(\delta) = \lambda\delta^3 + \delta^2 - \lambda\delta, \tag{A.15}$$

where we have one degree of freedom to tune our design when varying λ. The upper LFT of the polynomial should be composed into (A.7). The representation from robust control is

$$p(\delta) = \mathcal{F}_u(M, \delta I_3), \tag{A.16}$$

where $M = \begin{bmatrix} 0 & -\lambda & 1 & \lambda \\ 1 & 0 & 0 & 0 \\ 0 & 1 & 0 & 0 \\ 0 & 0 & 1 & 0 \end{bmatrix}$.

Finally, the system is formulated in a standard form as

$$
\begin{aligned}
\dot{x} &= -ax - x_u + bT_h + \lambda f_1 + f_2 - \lambda f_3 \\
\dot{x}_u &= -Wx_u + WcQ_h \\
\dot{x}_{ef} &= A_{ef}x_{ef} + B_{ef}(\lambda f_1 + f_2 - \lambda f_3 - \hat{f}) \\
\dot{x}_{ez} &= A_{ez}x_{ez} + B_{ez}(\lambda z_1 + z_2 - \lambda z_3 - \hat{z}) \\
z_1 &= ax + x_u \\
z_2 &= f_1 \\
z_3 &= f_2 \\
\acute{e}_f &= C_{ef}x_{ef} + D_{ef}e_f \\
\acute{e}_z &= C_{ez}x_{ez} + D_{ez}e_z \\
y_1 &= x \\
y_2 &= T_h \\
y_3 &= Q_h.
\end{aligned}
\tag{A.17}
$$

The standard model (with $D_{ef} = D_{ez} = 0$) becomes

$$
\begin{bmatrix}
\dot{x} \\
\dot{x}_u \\
\dot{x}_{ef} \\
\dot{x}_{ez} \\
\cdots \\
z_1 \\
z_2 \\
z_3 \\
\acute{e}_f \\
\acute{e}_z \\
\cdots \\
y_1 \\
y_2 \\
y_3
\end{bmatrix}
=
\begin{bmatrix}
A_1 & \vdots & B_1 & B_f & \vdots & B_2 \\
\cdots & & \cdots & \cdots & \cdots & \cdots \\
C_1 & \vdots & D_{11} & D_{1f} & \vdots & D_{12} \\
\cdots & & \cdots & \cdots & \cdots & \cdots \\
C_2 & \vdots & D_{21} & D_{2f} & \vdots & D_{22}
\end{bmatrix}
\begin{bmatrix}
x \\
x_u \\
x_{ef} \\
x_{ez} \\
\cdots \\
T_h \\
Q_h \\
f_1 \\
f_2 \\
f_3 \\
\cdots \\
\hat{z}_1 \\
\hat{f}_1
\end{bmatrix},
\qquad\text{(A.18)}
$$

where the matrix values are as bellow

$$
A_1 =
\begin{bmatrix}
-a & -1 & 0 & 0 \\
0 & -W & 0 & 0 \\
0 & 0 & A_{ef} & 0 \\
a\lambda B_{ez} & \lambda B_{ez} & 0 & A_{ez}
\end{bmatrix},
$$

$$
B_1 =
\begin{bmatrix}
T_h & 0 & 0 & 0 \\
0 & Wc & 0 & 0
\end{bmatrix}^T,
$$

$$
B_f =
\begin{bmatrix}
\lambda & 1 & -\lambda \\
0 & 0 & 0 \\
\lambda & 1 & -\lambda \\
0 & B_{ez} & -\lambda B_{ez}
\end{bmatrix},
$$

$$
B_2 =
\begin{bmatrix}
0 & 0 \\
0 & 0 \\
0 & -B_{ef} \\
-B_{ez} & 0
\end{bmatrix},
$$

$$
C_1 =
\begin{bmatrix}
a & 1 & 0 & 0 \\
0 & 0 & 0 & 0 \\
0 & 0 & 0 & 0 \\
0 & 0 & C_{ef} & 0 \\
0 & 0 & 0 & C_{ez}
\end{bmatrix},
$$

$$D_{11} = 0_{5 \times 2},$$

$$D_{1f} = \begin{bmatrix} 0 & 0 & 0 \\ 1 & 0 & 0 \\ 0 & 1 & 0 \\ 0 & 0 & 0 \\ 0 & 0 & 0 \end{bmatrix},$$

$$D_{12} = 0_{5 \times 2},$$

$$C_2 = \begin{bmatrix} 1 & 0 & 0 & 0 \\ 0 & 0 & 0 & 0 \\ 0 & 0 & 0 & 0 \end{bmatrix},$$

$$D_{21} = \begin{bmatrix} 0 & 0 \\ 1 & 0 \\ 0 & 1 \end{bmatrix},$$

$$D_{2f} = 0_{3 \times 3},$$

and $D_{22} = 0_{3 \times 2}$.

Finally, a $\mathcal{H}_\infty$ filter F, which estimates $\hat{f}$ and $\hat{z}$ and takes u and y as inputs, is designed using *hinfsyn* in **MATLAB**. This filter results in e_f and e_z vanishing to zero as time goes to infinity.

A.4   Results

The detector filters have been implemented in nonlinear Launch Simulator.

In order to obtain an estimation for δ, an algorithm has been employed as follows (See figure A.3).

1. A window has been located on the latest samples of $\hat{f}$ and $\hat{z}$. The length of the window is 5 samples and the sampling frequency is $67Hz$.

2. The second norm of the sampled data has been computed and multiplied by the sign of their mean values.
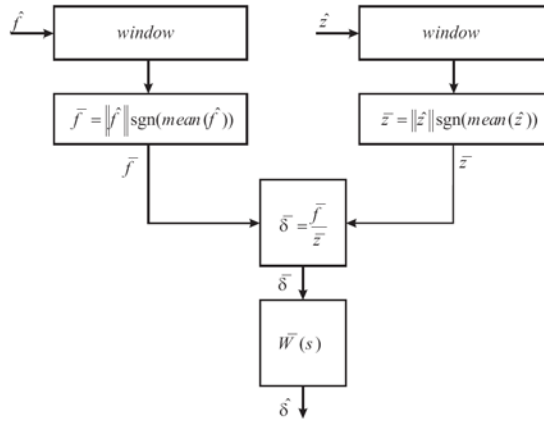
Figure A.3: Block diagram of the algorithm for the estimation of δ.

3. The results from the above blocks has been used to calculate $\bar{\bar{\delta}} = \frac{\|\bar{f}\|}{\|\bar{z}\|}$.

4. A low-pass filter $\bar{W}(s)$ is used to reduce the effect of the noise on the estimated fault.

Two series of comparison regarding the change in γ and λ values are considered here to show that the choice of the model plays an important role to improve the results. In these experiments, the injected parametric fault has been raised from 0 to 1 at $25s$.

In figure A.4 the comparison of estimation results among four different values of γ ranging from 0.005 to 0.1 for three constant values of λ is shown. In fact, it confirms that increasing γ is equivalent to pay less attention to the condition (A.13) and consequently changing the problem into a **Kalman Filter** optimization problem. This results in amplifying of the effect of the disturbances in the fault estimation and less robustness. On the other hand, decreasing γ reduces the effect of the disturbances and noise inputs to the estimation and increases the robustness. For example, in the case for $\lambda = 0.1$ we can see that the performance of the estimation with $\gamma = 0.005$ is better than those for $\gamma = 0.008$ and $\gamma = 0.01$.

In figure A.5 the comparison of estimation results among three different values of λ ranging from 0.01 to 1 for four constant values of γ is shown. Increasing the value of λ results in very weak estimation, however, decreasing λ does not mean that the estimation is perfect. Indeed, for $\lambda = 0.1$ the estimation of the δ is converging to 1 which corresponds to the injected value of δ. Therefore, one could say neither the increase of λ, nor the decrease of γ will give the best estimation results. In fact, there
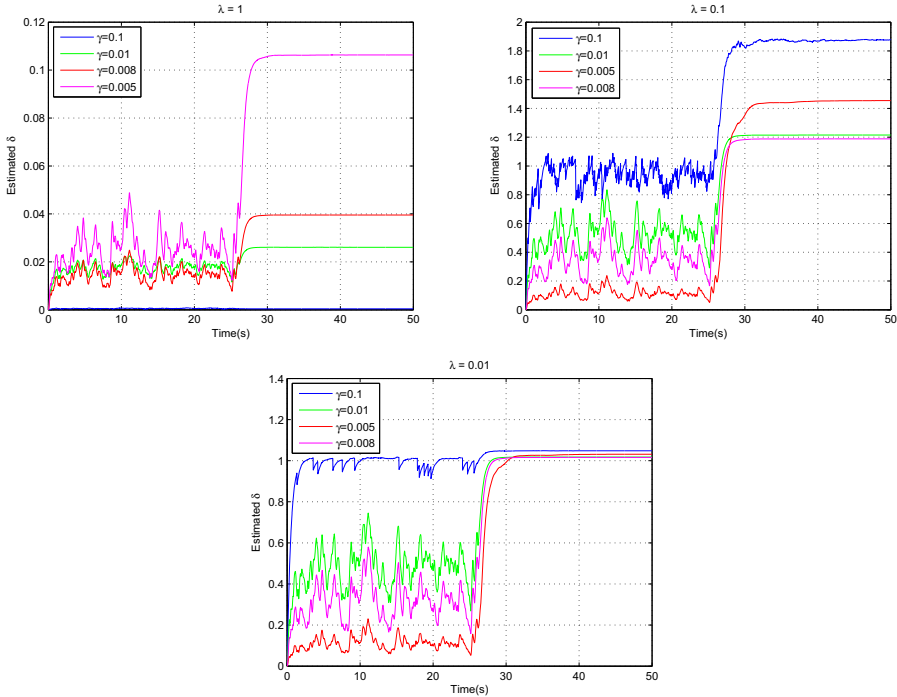
Figure A.4: Estimation of efficiency loss δ in LH2 pump for γ comparison while λ is constant.

is an optimal point λ which gives the best estimation, however, we did not consider a methodological way to obtain this optimal value but this example was a witness for existence of such point which can be considered in the future developments.

Eventually, any alternative optimization method could be considered to solve the problem e.g., numerical algorithms for μ optimization. However, by presenting this method and finding a significant model for the fault there is still the advantage of solving a convex optimization problem by $\mathcal{H}_\infty$ method compared to μ optimization.

A.5 Conclusions

The uncertainties/faults in turbopumps, a subsystem of the engine, have been modeled as parametric faults in this paper. This model has been formulated in a standard set-up which is compatible with $\mathcal{H}_\infty$ control design formulation. The designed $\mathcal{H}_\infty$ filter for
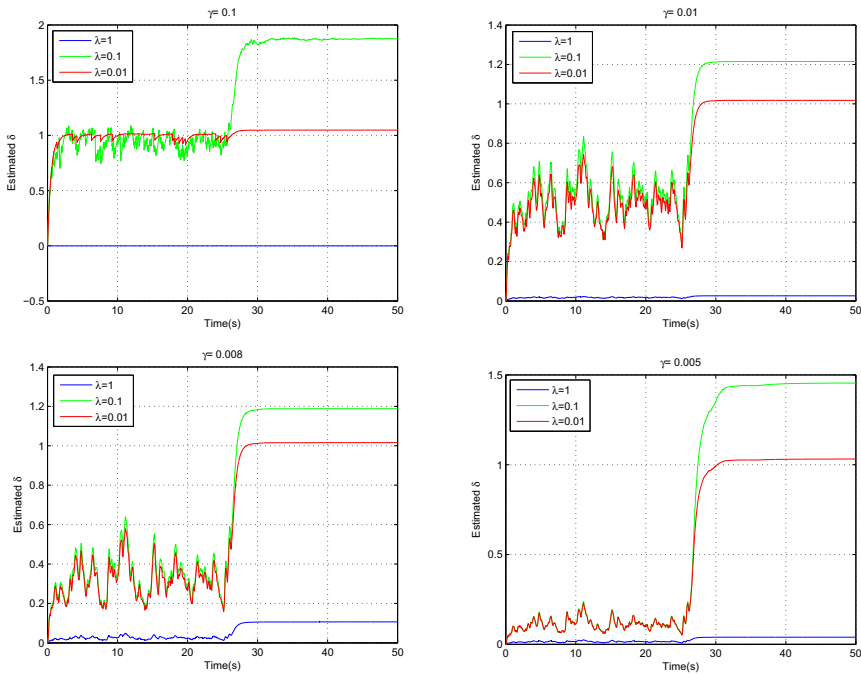
Figure A.5: Estimation of efficiency loss δ in LH2 pump for λ comparison while γ is constant.

different fault models are implemented to this system. The output of the filter processed in a way to produce the estimation of possible fault. Finally, the method has been verified in launch simulator and the results for different design factors have been compared then a trade off in the design has been demonstrated.

Appendix B

Boundary Conditions

In this appendix, it is shown under what conditions the motors are able to perform the demanded actuation.

Consider the figure B.1, we would like to show the relation between the angle θ and the maximum rate of angles φ and ψ.

Theorem 1 *Suppose S_1 and S_2 are two intersecting planes in three dimensional space. Assume that the plane S_3 is perpendicular to both S_1 and S_2 and intersecting at point o to both of them. Also, assume that two unit vectors r_1 and r_2 are with origin o in S_1 and S_2 respectively and make the angle θ with the intersection of S_3 with S_1 and S_2.. If the angle between S_1 and S_2 is ψ and the angle between r_1 and r_2 is φ, then θ, ψ, and φ have the following relation:*

$$1 - cos(\varphi) = (1 - cos(\psi))cos(\theta)^2. \tag{B.1}$$

Proof. The proof is strait-forward by the geometric calculation using figure B.1.

Now, considering the result of the theorem, the time derivation of the equation B.1 (with constant θ) is as follows

$$\dot{\varphi}sin(\varphi) = \dot{\psi}sin(\psi)cos(\theta)^2. \tag{B.2}$$

Therefore,

$$|\dot{\varphi}||sin(\varphi)| = cos(\theta)^2|\dot{\psi}||sin(\psi)| \leq cos(\theta)^2|\dot{\psi}_{max}|, \tag{B.3}$$

or

$$\frac{|\dot{\varphi}||sin(\varphi)|}{|\dot{\psi}_{max}|} \leq cos(\theta)^2. \tag{B.4}$$

Now, let's define a worst case problem as finding the maximum value of θ for maximum value (worst case) of the left side of inequality B.4. The result is clearly given by

$$\frac{|\dot{\varphi}_{max}|}{|\dot{\psi}_{max}|} \leq cos(\theta_{max-v})^2, \tag{B.5}$$

where in the antenna application, $|\dot{\varphi}_{max}|$ is considered as the maximum angular velocity of the ship motion and $|\dot{\psi}_{max}|$ is the maximum angular velocity that the motors can perform.
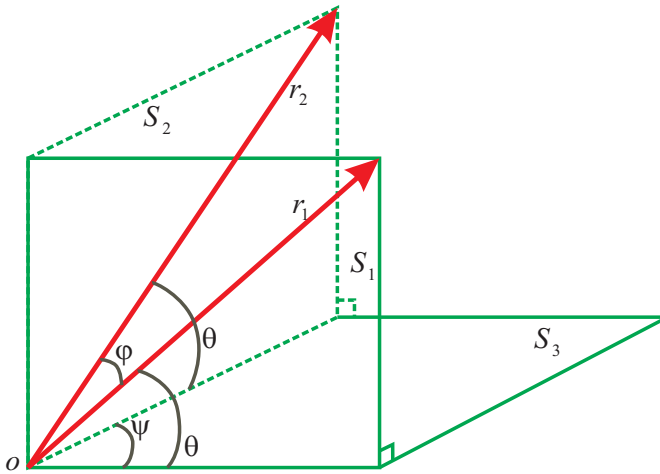

Figure B.1: Illustration of the angles and planes in theorem.

By the same procedure, if we differentiate the equation B.2 one more time and find the maximum θ again, it gives

$$\frac{|\dot{\varphi}_{max}^2| + |\ddot{\varphi}_{max}|}{|\dot{\psi}_{max}^2| + |\ddot{\psi}_{max}|} \leq cos(\theta_{max-a})^2, \tag{B.6}$$

where $|\ddot{\varphi}_{max}|$ is considered as the maximum angular acceleration of the ship motion and $|\ddot{\psi}_{max}|$ is the maximum angular acceleration that the motors can perform. Consequently, $\theta_{max} = max\{\theta_{max-a}, \theta_{max-v}\}$ is the maximum elevation angle which the 2-axis antenna is able to keep tracking for the worst case of the ship motions.

Appendix C

Kalman Filtering

The Extended Kalman Filter is used to correct the calculation of the rotation matrix when the data from the beam sensor is available. This appendix describes the EKF algorithm for the satellite tracking antenna.

Consider the discretized model of the antenna as

$$
\begin{aligned}
x_k &= f(x_{k-1}, u_k) + w_k \\
y_k &= h(x_k) + v_k,
\end{aligned}
\tag{C.1}
$$

where w_k is the process noise with zero mean and covariance Q_k, v_k is the observation noise with zero mean and covariance R_k. The state vector x is composed of two parts $x_k = (x^1_{k_{2\times 1}}, x^2_{k_{3\times 3}})$, where $x^1_{k_{2\times 1}}$ is the motor angle and $x^2_{k_{3\times 3}}$ is the rotation matrix R_{be} in Chapter 4, and the vector function $f(x_{k-1}, u_k) = \begin{pmatrix} f^1(x^1_{k-1}, u^1_k) \\ f^2(x^2_{k-1}, u^2_k) \end{pmatrix}$ is as following

$$
f^1(x^1_{k-1}, u^1_k) = x^1_{k-1} + t_s u^1_k,
\tag{C.2}
$$

and

$$
f^2(x^2_{k-1}, u^2_k) = x^2_{k-1} + t_s x^2_{k-1} Skew(u^2_k),
\tag{C.3}
$$

where t_s is the sampling time (0.005s here), $u^1_{k_{2\times 1}}$ is the actuation input, $u^2_{k_{3\times 1}}$ is the gyro measurement, and $Skew(.)$ is defined in Chapter 3.

The function h is

$$h(x_k) = \begin{pmatrix} x_k^1 \\[2em] tan^{-1}\big(\frac{-x_{k_{11}}^2 sin(x_{k_1}^1)cos(x_{k_2}^1)+x_{k_{21}}^2 cos(x_{k_1}^1)cos(x_{k_2}^1)}{x_{k_{11}}^2 cos(x_{k_1}^1)cos(x_{k_2}^1)+x_{k_{21}}^2 sin(x_{k_1}^1)cos(x_{k_2}^1)+x_{k_{31}}^2 sin(x_{k_2}^1)}\big) \\[2em] sin^{-1}\big(\frac{-x_{k_{11}}^2 cos(x_{k_1}^1)sin(x_{k_2}^1)-x_{k_{21}}^2 sin(x_{k_1}^1)sin(x_{k_2}^1)+x_{k_{31}}^2 cos(x_{k_2}^1)}{1}\big) \end{pmatrix}. \qquad \text{(C.4)}$$

The function f is used to compute the predicted state from the previous estimate and similarly the function h is used to compute the predicted measurement from the predicted state. However, f and h cannot be applied to the covariance directly. Instead a matrix of partial derivatives (Jacobian) is computed as

$F_k = \frac{\partial f}{\partial x}\big|_{\hat{x}_{k-1|k-1},u_k}$

and

$H_k = \frac{\partial h}{\partial x}\big|_{\hat{x}_{k|k-1}}$

At each time step the Jacobian is evaluated with current predicted states. These matrices can be used in the Kalman filter equations. This process essentially linearizes the nonlinear function around the current estimate.

This results in the following extended Kalman filter equations:

Prediction

$\hat{x}_{k|k-1} = f(\hat{x}_{k-1|k-1}, u_k)$

$P_{k|k-1} = F_k P_{k-1|k-1} F_k^T + Q_k$

Update

$\tilde{y}_k = y_k - h(\hat{x}_{k|k-1})$

$S_k = H_k P_{k|k-1} H_k^T + R_k$

$K_k = P_{k|k-1} H_k^T S_k^{-1}$

$\hat{x}_{k|k} = \hat{x}_{k|k-1} + K_k \tilde{y}_k$

$P_{k|k} = (I - K_k H_k) P_{k|k-1}$